U.PORTO

Universidade do Porto
FEUP Faculdade de Engenharia

Disc brake squeal

Mode coupling instability type

António José da Guia Rodrigues

Dissertation submitted to
Faculdade de Engenharia da Universidade do Porto
for the degree of:

Mestre em Engenharia Mecânica

Advisor:
Prof. José Dias Rodrigues
(Associate Professor)

Laboratório de Vibrações de Sistemas Mecânicos
Departamento de Engenharia Mecânica
Faculdade de Engenharia da Universidade do Porto

Porto, 2017

The work presented in this dissertation was performed at the
Laboratory of Vibrations of Mechanical Systems
Department of Mechanical Engineering
Faculty of Engineering
University of Porto
Porto, Portugal.

António J. Guia Rodrigues
E-mail: em10194@fe.up.pt

Faculdade de Engenharia da Universidade do Porto
Departamento de Engenharia Mecânica
Laboratório de Vibrações de Sistemas Mecânicos
Rua Dr. Roberto Frias s/n, Sala M206
4200-465 Porto
Portugal

Abstract

In the following, instability in disc brake systems, which leads to the emission of noise, caused by coupling of vibration modes is addressed.

Disc brake squeal has been an ongoing concern on the automotive industry and the subject of intense research over the years. It is caused by non-conservative friction forces at the contact interface of elastic bodies in relative sliding motion. The non-conservative work produced by friction forces may lead to unstable vibrations. The noise emitted by these undesirable vibrations leads to an increase in warranty costs since customers believe that it could be a symptom of the system malfunction.

It constitutes a very complex phenomena affected by many operational parameters. The random nature of the phenomena turns it particularly challenging to study. In fact, it was seen that a brake system may not always squeal given the same conditions.

It was seen that squeal events were related to the onset of instability, and the means by which the instability sets in are the squeal mechanisms. Several have been identified and it is generally accepted that the mode coupling of the doublet modes of the rotor is the main responsible mechanism for squealing brakes, although several others may induce the system into an unstable behaviour.

Experimental investigations that have been made regarding mode coupling will be presented. Test rigs are usually pin-on-disc systems and are very useful because they correlate the dynamic behaviour of the substructures with squeal occurrence.

To study mode coupling characteristics in friction-induced vibrations and to gain a deep understanding on the physical mechanisms underlying this type of instability, minimal models are used. Although they do not represent the actual brake system they provide a resourceful way to capture the properties of modal interaction in sliding friction events and see how modal interaction is influenced by system parameters. The damping and the friction law are of particular interest. Some relevant analytical models, namely the moving-load model and the single mode pair approximation, are also presented.

Finally, finite element models of a pin-on-disc system and a simplified brake system were developed in order to determine unstable modes by a complex eigenvalue analysis and to study the influence of systems parameters, namely the applied pressure and the friction coefficient in the behaviour of the complex eigenvalues.

Keywords: Disc Brake Squeal, Friction-induced vibrations, Dynamic instability, Squeal Mechanisms, Mode coupling

Resumo

No presente documento é abordado o acoplamento de modos de vibração, um dos fenómenos responsáveis pela instabilidade em sistemas de travões de disco que levam à emissão de ruído indesejável.

A emissão de ruído em sistemas de travagem constituí um problema de grande preocupação na indústria automotiva e tem sido o objecto de extensa investigação. É causado pela natureza não conservativa das forças de atrito que se geram na interface de contacto de corpos elásticos sujeitos a escorregamento relativo. O trabalho produzido pelas forças de atrito leva ao aparecimento de vibrações instáveis. O ruído emitido por estas vibrações indesejáveis leva a um aumento dos custos de garantia da indústria porque os clientes associam o ruído a um mau funcionamento do sistema.

A emissão do ruído neste tipo de sistemas consiste num fenómeno muito complexo. A natureza aleatória do fenómeno torna-o particularmente desafiante de o estudar. De facto, foi verificado que num determinado sistema de travagem nem sempre existe emissão de ruído para as mesmas condições operacionais.

Os eventos com emissão de ruído viriam a ser relacionados com o aparecimento de instabilidade no sistema, para os quais existem vários mecanismos. Dos vários mecanismos identificados, o acoplamento de modos de vibração é geralmente aceite como o principal responsável pela maioria dos eventos. No entanto, os restantes mecanismos podem induzir o sistema para um comportamento instável.

Existe também um vasto leque de trabalhos experimentais conduzidos para estudar este tipo de instabilidade. As bancas de teste apresentam-se com vários graus de complexidade, podendo ser apenas uma viga em contacto com um disco ou um sistema de travagem real. Este meio de investigação revela-se muito útil pois permite correlacionar o comportamento dinâmico das subestruturas do sistema de travagem com a emissão de ruído.

Para estudar as características do acoplamento modal e compreender os mecanismos físicos intrínsecos a este tipo de instabilidade vários modelos mínimos têm sido desenvolvidos. Apesar de não representarem um sistema de travagem real, permitem derivar algumas propriedades da interação modal e perceber como ela é influenciada pelos parâmetros operacionais, nomeadamente o amortecimento. São ainda apresentados alguns modelos analíticos entretanto desenvolvidos, em particular o modelo de carga em movimento.

Finalmente, um modelo de elementos finitos consistindo numa viga de secção quadrada em contacto com uma placa anular foi desenvolvido com o objectivo de determinar modos de vibração instáveis e de estudar o seu comportamento perante diferentes condições operacionais, nomeadamente a pressão aplicada, a velocidade de rotação do disco e o coeficiente de atrito entre as superfícies.

Palavras-chave: Ruído, Vibrações induzidas por atrito, Instabilidade dinâmica, Mecanismos de instabilidade, Acoplamento modal

To my niece Beatriz

'Failure is the fog from which we all glimpse triumph'

Aldrich Killian from Iron Man 3

Acknowledgements

Firstly, I would like to express my gratitude to my advisor, Professor José Dias Rodrigues, for all the support and availability, for the vast knowledge transmitted and for his patience during the past years.

To Faculdade de Engenharia da Universidade do Porto, a word of appreciation for the academic resources provided for the education of future engineers. We are fortunate to perform our studies in an environment of excelence.

To the friends I met during this journey, thank you. You personify the very known spiel; "Se quiseres ir rápido, vai sozinho. Se quiseres ir longe, vai acompanhado."

To my parents, António and Maria, for their invaluable support over the past years. You have always pushed me to do better, having provided me an excellent education, whose values and principles I will always take for the rest of my life and for that I am deeply grateful.

To my older brother Tiago, I made it! You are an inspiration and I am truly grateful for your unwearying support. I know that I always can count on you.

Contents

List of Figures

List of Tables

Chapter 1

Introduction

1.1 Motivation

Brake systems are one of the most important subsystems in an automobile. Since it has to dissipate the kinetic energy of the vehicle, to safely and successfully stop the vehicle, brake performance, in particular, breaking power and reliability have been the main focus of research and development. However, the effort to make vehicle acoustics more environment- and passenger-friendly, by improving other aspects of vehicle design, has increased brake noise contribution dramatically.

Several terminology can be found in the literature to describe brake noise, such as *squeal*, *groan*, *judder* and others. [Kinkaid et al., 2003] points out that *squeal* is probably the most prevalent one and, although there isn't a precise definition of brake squeal, it can be seen as a "sustained, high-frequency (> 1000 Hz) vibration of brake system components during a braking action resulting in noise audible to vehicle occupants or passers-by".

Brake noise causes discomfort for passengers, who may believe that it is symptomatic of malfunction of the brake system. In [Akay, 2002] it is stated that "warranty costs in North America for brake noise, vibration, and harshness reaches one billion dollars each year".

Brake squeal is not a classical problem of Mechanics, since it addresses a real, practical phenomena in the transportation industry, mostly the automotive one. It constitutes a very complex problem that is affected by many different factors on macro- and microscopic level. One characteristic that turns it particularly difficult to study is the random nature of brake squeal; that is, brake squeal can be non-repeatable, or, in other words, a brake system may not always squeal given the "same" conditions [Papinniemi et al., 2002].

1.2 Objectives

Recent research on automotive braking systems has taken two general paths. The first one, studies real brake systems and it is concerned in predicting and eliminating squeal occurrence at the design stage by a stability analysis. The second one has focused on identifying the sources for brake squeal, understanding by which mechanisms squeal is generated, and on providing ways to reduce it, since that there exists no general means for completely eliminate it [Akay, 2002].

The work presented in this document was developed with the following objectives:

- To study mode coupling characteristics in friction-induced vibrations and to gain a deep understanding on the physical mechanisms underlying this type of instability,

since it is generally recognized as the most significant one, leading to self-excited vibrations in relative sliding systems with friction [Nouby et al., 2014].

- To understand the mechanisms by which brake squeal occurs, since it is, in one hand a challenging task, and on the other, essential to be able to develop quieter brakes. In order to do so, simple mechanical models are used.
- To perform a complex eigenvalue analysis on finite element models of simplified systems in sliding friction in order to assess their stability and to evaluate the influence of system parameters, namely the applied braking pressure, on the stability of the system.

1.3 Layout of the document

Since the 1902 patented disc brake by a British engineer, brake noise phenomena has been the subject of research and investigation from at least 1930. A wealth of literature concerning brake squeal has been presented over the time and has been condensed in countless review papers. Regarding to the disc brake problem, chapter 2 presents a brief background on the problem. Disc brake configurations and vibrations modes are briefly presented, early reviews on the subject are referred and several squeal mechanisms, seen as the cause for dynamic instabilities, are briefly discussed. The chapter ends by providing some insight on the influence of system parameters in the stability of the system, such as mechanical properties of the components, or operational conditions, namely, applied braking pressure or disc rotational velocity.

In chapter 3, mode coupling, or mode lock-in, or even, binary flutter, is addressed. Several experimental and numerical papers regarding the features and characteristics of this type of instability are discussed. To be able to generate this instability phenomena, in order to understand the physical mechanisms regarding mode coupling, one only need models with two-degrees-of-freedom. In this line of thought, a variety of minimal models have been developed providing an increased knowledge on how the dynamical behaviour of the system is influenced by mode coupling. These models are presented in chapter 4.

However, minimal models do not represent the actual brake system dynamics, since the real system is much complex, either in geometry and contact interfaces. As it will be seen in chapter 5, brake squeal problem has also been addressed via analytical models with a variety of refinement. To approach experimental setups, analytical models of Pin-on-Disc, or Beam-on-Disc systems, have been proposed. One interesting analytical approach, that models the dynamics of brake systems as a moving-load problem, is also presented.

In chapter 6 finite element models of simple mechanical systems in sliding friction were develop and their dynamic stability was evaluated by a complex eigenvalue analysis. Results are presented also for various braking pressure values.

Chapter 2

State of the Art

2.1 Disc brake system configurations

A brake system is a mechanical device developed to decelerate a moving body in a control manner. In order to do so, kinetic energy of the moving car is dissipated at the friction interface of the braking system as thermal energy due to the friction between the brake components, namely the rotor and the pads. However, a small fraction of the energy is converted in vibrational energy that travels through the brake system's components.

There are several configurations for disc brake systems, such as *fixed-caliper* or *floating-caliper*. In this section, a brief overview of disc brake components and their function are presented.

A car disc brake system consists of steering knuckle assembly, wheel hub and the actual disc brake system assembly. In fig. 2.1a it is presented a simplified disc brake assembly, with a fixed-caliper configuration, where it can be seen a rotor, typically ventilated and made of grey cast iron, a caliper, the pistons, pads and backing plates.

The rotor is rigidly mounted on the axle, by screw connections, thus rotating with the vehicle's wheel. When brake pedal is pressed, hydraulic pressure is increased, the pistons move forward, and consequently brake pads, which contain frictional material, are pressed

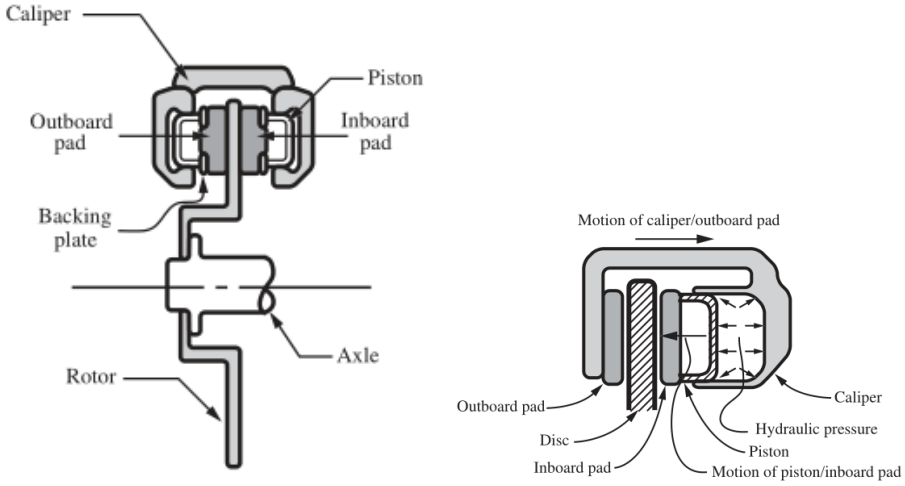

(a) Simplified disc brake assembly with fixed caliper from [Kinkaid et al., 2003]

(b) Simplified floating caliper design from [Kinkaid et al., 2003]

Figure 2.1: Disc brake system configurations

against the rotor in order to produce a frictional torque thus slowing the wheel's rotation. The increase in hydraulic pressure is due to the master's cylinder which is connected to the disc brake's caliper by brake lines and hoses.

The caliper houses the hydraulic pistons and is attached to the vehicle by a caliper mounting bracket. The attachment depends on the caliper configuration. In a floating-caliper configuration type (fig. 2.1b), the caliper is allowed to slide freely along two guided pins. When pressure is applied, the piston slides inside the caliper and presses the inner pad against the disc. Simultaneous, the outer pad is pushed forward by the caliper against the disc, thus creating a braking torque in both sides.

2.2 Disc vibration modes

To address friction-induced vibrations on disc brake systems, we provide in the following a brief insight on disc vibration modes. Generally, the disc is modelled as a circular or annular plate, where the transverse (out-of-plane) vibration is considered. Equation of motion for the transverse displacement can be written as,

$$D\nabla^4 w + \rho h \frac{\partial^2 w}{\partial t^2} = 0 \tag{2.1}$$

where

$$\nabla^4 = \nabla^2\nabla^2 = (\nabla^2)^2 = \left(\frac{\partial^2}{\partial r^2} + \frac{1}{r}\frac{\partial}{\partial r} + \frac{1}{r^2}\frac{\partial^2}{\partial \theta^2}\right)^2 \qquad D = \frac{Eh^2}{12(1-\nu^2)} \tag{2.2}$$

Transverse displacement is expressed in truncated modal expansion

$$w(r,\theta,t) = \sum_{n=0}^{\infty} R_n(r)\left[\cos(n\theta)\cdot q_{2n-1}(t) + \sin(n\theta)\cdot q_{2n}(t)\right] \tag{2.3}$$

where $R_n(r) = A_n J_n(\beta r) + B_n Y_n(\beta r) + C_n I_n(\beta r) + D_n K_n(\beta r)$. J_n and Y_n are Bessel functions of first and second order, I_n and K_n are modified Bessel functions of first and second order, A_n, B_n, C_n, D_n are constant coefficients to be determined from the boundary conditions.

Disc modes are characterized by n nodal circumferences and m nodal diameters. For example, the $(0,2)$ is the mode with only two nodal diameters (figure 2.2). Disc vibration modes characterized by nodal diameters are plotted in the set of figures (2.2)-(2.5).

Considering the axial symmetry of the disc, modes of the disc are pairs of doublet modes, the cosine and sine modes. Due to the contact, the disc looses symmetry and the doublet modes split [Francesco Massi, 2006].

2.3 Early reviews

A wealth of literature concerning brake squeal has been presented over the time and has been condensed in some review papers. [Kinkaid et al., 2003] is by far, the most comprehensive review concerning to disc brake squeal, since not only presents experimental studies and models developed at the time, but also discusses the main features of some theories for brake squeal, such as, stick-slip, sprag-slip, both combined or mode-coupling.

Some of these mechanisms were already subject of investigation several years ago, namely the coupling of vibration modes and the negative gradient of friction coefficient

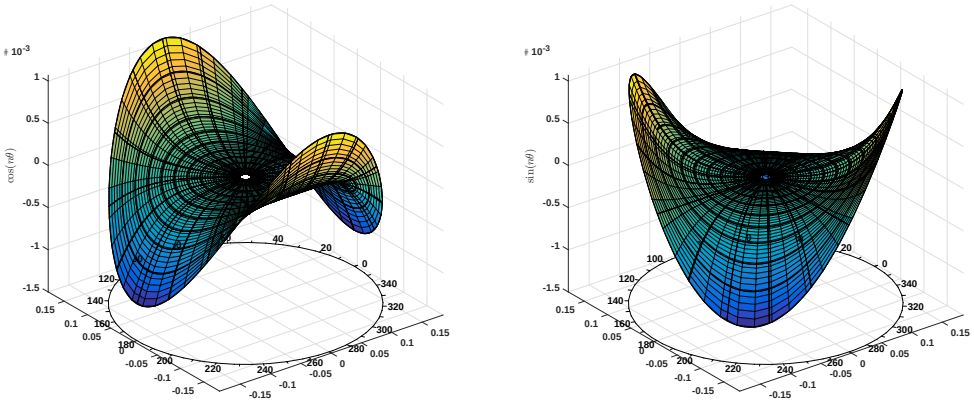

(a) Cosine mode (b) Sine mode

Figure 2.2: $(0, 2)$ Disc vibration mode

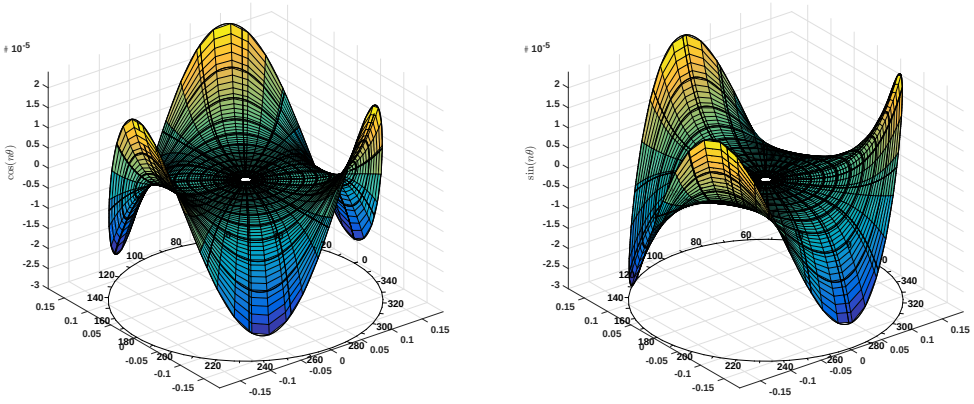

(a) Cosine mode (b) Sine mode

Figure 2.3: $(0, 3)$ Disc vibration mode

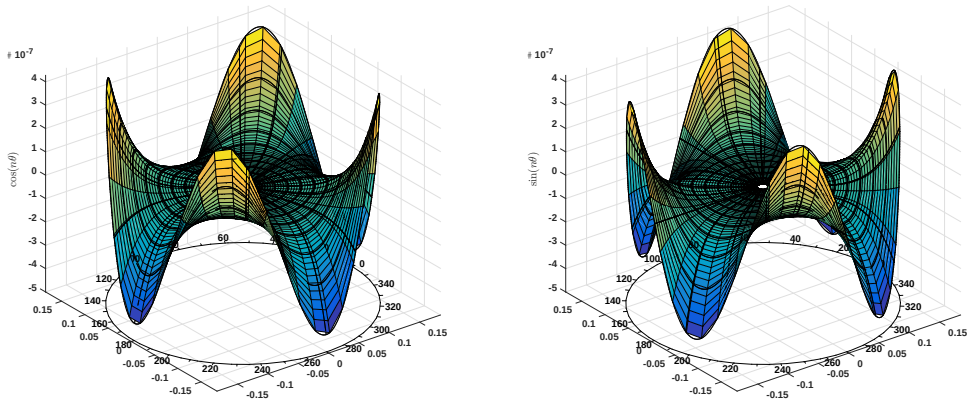

(a) Cosine mode (b) Sine mode

Figure 2.4: $(0, 4)$ Disc vibration mode

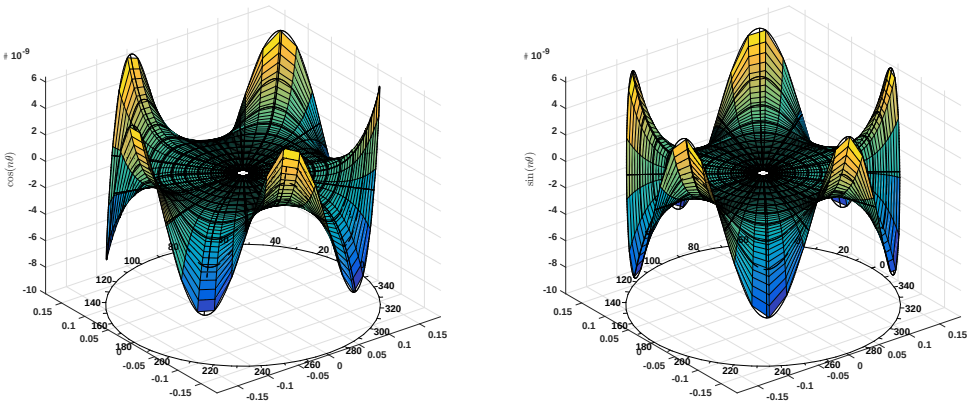

(a) Cosine mode (b) Sine mode

Figure 2.5: $(0, 5)$ Disc vibration mode

with respect to sliding velocity [Yang and Gibson, 1997]. Due to the difficulty in modelling boundary conditions, FEM was mostly used to modal analysis, and an experimental approach, by means of modal analysis and laser holography, was considered indispensable because one could measure both vibration and acoustic response simultaneously.

In his review on the acoustics of frictional contacts [Akay, 2002], Akay presents the mathematical model for pin-on-disc systems used to study brake squeal. An interesting feature presented at his review paper, was the formation of a basis for a feedback loop between the tribological and vibrational systems, since that in a sliding contact, the waves and oscillations alter the contact area, which in turn influences the contact forces. As pointed out in [Papinniemi et al., 2002], there was already an agreement that brake squeal was generated by the vibration of an unstable mode of the brake system. The appearance of this unstable mode was due to the asymmetric nature of the stiffness matrix as a result of the friction coupling forces at the friction interface.

The lack of a review on numerical methods to investigate disc brake squeal was the motivation for the work presented in [Ouyang et al., 2005], where the two main numerical approaches to address the problem, which are the Complex Eigenvalue Analysis (CEA) and the Dynamic Transient Analysis (DTA), are thoroughly discussed. CEA addresses the stability of the system, while DTA is useful to get an insight on the evolution of time response of vibrations. Both numerical methods were used to investigate the influence of contact regimes models, available on a commercial FE software, on the stability and dynamic behaviour of the FE model developed [AbuBakar and Ouyang, 2006]. Correlation between the methods was also addressed.

As seen in [G. Lallement, 1995], if the complex eigenvalue has a positive real part, the mode is characterized by an apparent negative damping, which means that the systems does not dissipate energy, rather absorbs it giving place to an exponentially growth of vibration amplitude. The great advantage of CEA is its computational efficiency. However is a limited numerical method since full effect of non linearities away from the steady sliding state are not accounted for. Another limitation is that the magnitude of the positive real part describes the growth rate and not necessarily the noise level. By other words, the stability analysis provides an insight into the tendency of divergence of the motion and not its actual amplitude. One final mark is related to the modes that CEA predicts. CEA is a conservative approach, since it predicts all unstable modes that may grow into a limit-cycle. However, depending on the triggering mechanism, not all modes will become unstable.

In their numerical review paper, Ouyang and others also address the influence of damping by stating that modal damping is still a difficult feature to model and it does not give a good representation of the energy dissipation of the system. The work by Hoffmann and Gaul on the influence of damping is also pointed out, since they found that viscous damping could promote mode-coupling instability.

One last, and recent, review is referred [Nouby et al., 2014], where the main squeal mechanisms, namely, stick-slip, sprag-slip, modal coupling and hammering are reviewed. The authors reinforce the already known idea that none of the studied mechanisms so far can alone explain all events related to squeal noise and that mode coupling is generally recognized as the most significant mechanism. They also point out that the mechanisms give an insight at which conditions squeal may occur but they don't explain how the squeal evolves and disappears.

2.4 Dynamic instabilities and squeal mechanisms

Squeal arises from self-excited vibrations, or friction-induced vibrations. Since friction is a merely dissipative feature, it is difficult to imagine how can friction cause a dynamic motion of increasing amplitude.

In frictional contacts, such as the contact between the rotor and the pads, solution of the steady state sliding may become unstable, thus constituting a dynamic instability. By the way this dynamic instability sets in, in disc brakes, is referred to a squeal mechanism.

2.4.1 Stick-slip

Stick-slip is an instability phenomena that occurs when the static friction coefficient is higher than the kinetic coefficient, often known as stiction. Pioneering work on drum brakes [Mills, 1938] lead to believe that squealing brakes were a result from the presence of decreasing kinetic friction coefficient with increasing sliding velocity. In this situation, systems may have apparent negative damping leading to unstable oscillations. Since Mills' work it was believed that the negative slope of the friction-speed curve would give rise to stick-slip motion. To better understand this unstable phenomena, a mass-damper-spring system is considered in contact with a belt that moves with constant velocity (fig. 2.6).

Initially, the mass moves with the belt, so the mass is stationary relatively to the belt. Since the spring force is smaller than the static friction force, deformation of the spring increases, until elastic force equals or is larger than the static friction force. Then, the mass begins to move relatively to the belt. As the mass slides, motion is ruled by the kinetic friction coefficient, which is smaller than the static coefficient. This leads to a decrease in the spring force causing the mass to gradually stop sliding. When the mass stops sliding, the process is repeated and a stick-slip limit-cycle is established.

If the friction coefficient is assumed to decrease linearly with sliding velocity such that

$$\mu = \mu_s - \alpha v_s \tag{2.4}$$

making use of eq. (2.4), equation of motion for the oscillator can be derived and it is expressed as

$$m\ddot{x} + c\dot{x} + kx = \mu F \tag{2.5}$$

$$m\ddot{x} + c\dot{x} + kx = F(\mu_s - \alpha(v - \dot{x})) \tag{2.6}$$

$$m\ddot{x} + (c - \alpha F)\dot{x} + kx = F(\mu_s - \alpha v) \tag{2.7}$$

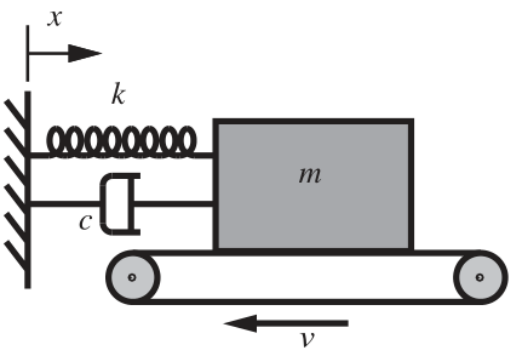

Figure 2.6: Single degree of freedom oscillator

where it can be seen that if $\alpha F > c$ then the system possesses negative damping leading to vibrations with increasing amplitude.

Although this may be true, later research demonstrated that this mechanism was insufficient to explain all squeal events [R. P. Jarvis and B. Mills, 1963]. In their work, they concluded that decreasing friction coefficient with increasing sliding velocity was not responsible for unstable behaviour and that instability was due to the motion coupling of the components.

2.4.2 Sprag-slip

Another squeal mechanism known as sprag-slip was proposed by Spurr in his theory of brake squeal. He analysed geometrical aspects of the brake systems and concluded that due to the geometry of the brake assembly, friction force is increased to unrealistic values. Due to the elasticity of the brake components, the structure would deform causing a slip and friction forces would reduce. The sprag-slip mechanism is also known as a geometrically-induced instability. To better understand this mechanism, fig. 2.7 is used, where a rigid structure inclined at an angle θ to a rubbing surface is presented.

Considering the force equilibrium and assuming Coulomb's friction law, friction forces are defined as

$$N = \frac{L}{1 - \mu \tan\theta} \qquad F_F = \frac{\mu L}{1 - \mu \tan\theta} \tag{2.8}$$

where, L is the load and μ is the friction coefficient. From eq. (2.8), it can be seen that as $\theta \to \tan^{-1}(1/\mu)$ or $\mu \to \cot\theta$, $F_F \to \infty$. So, *spragging* occurs when $\mu = \cot\theta$. In this situation, the structure locks and motion is impossible. Once again, due to the flexibility of the components, the structure releases itself by slipping through the rubbing surface and reaching its initial state.

This dynamic phenomena was later reexamined with the aim of developing a simple and intuitive method to predict whether the system would present sprag-slip oscillations or not [N. Hoffmann, 2004]. It was already known, by early investigations on the properties of rigid bodies subjected to the Coulomb-type sliding friction, that nonlinearity arising from the friction model could lead to the existence of multiple static solutions or to the loss of existent solutions, phenomena called Painléve paradox. By analysing a beam-on-disc setup, it was found that for a certain combination of parameters a steady state sliding does not exist and the system is dynamic by nature. In this situation, it was also found that

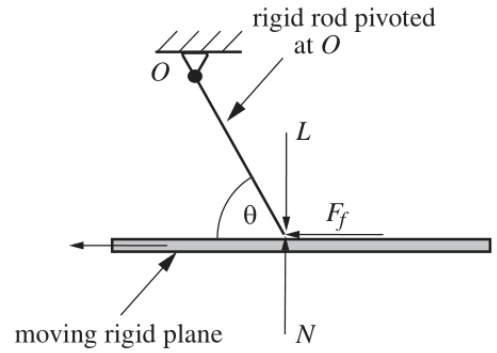

Figure 2.7: Mechanical structure used to explain the sprag-slip mechanism from [Kinkaid et al., 2003]

the system would inevitably show limit-cycle behaviour. So, to predict the appearance of sprag-slip oscillations, one must simply evaluate the existence of a steady state sliding and if it does not exist, then the system is intrinsically dynamic. One fundamental aspect that should also be mentioned is concerned with the measures that could be deployed to counteract this instability. Simply adding damping is not sufficient since the system does not possess a static solution. Quietening disc brakes that exhibit sprag-slip oscillations may, therefore, consist on finding an acceptable dynamical behaviour.

2.4.3 Follower forces

Pioneering work of North, regarding disc brake squeal, modelled friction force as a follower force [North and of Mechanical Engineers, 1977]. A follower force is a force that depends on displacements of the system but which cannot be derived from the potential energy associated whit those displacements [Kinkaid et al., 2003]. Follower force was then considered a squeal mechanism leading to self-excited vibrations where the friction forces that support the motion are fluctuating and controlled by the motion itself. Several analytical models inspired in this theory for brake squeal were developed, where the disc brake problem was considered as a moving-load problem and contact forces were introduced producing a friction couple [Ouyang, 2003], [Ouyang and Mottershead, 2004].

To provide an experimental evidence that flutter instability (a blowing-up vibrational motion of increasing amplitude) and divergence instability (an exponentially growing motion) could be induced by dry friction, a two degree-of-freedom system, known as *Ziegler column*, was studied [Bigoni and Noselli, 2011]. The two-degree-of-freedom structure, whose free body diagram is presented in fig. 2.8, is composed by two rigid rods, AB and BC, connected by two rotational springs k_1 and k_2. By mounting a wheel of negligible mass, free of rotating at its axis, at the top of the structure and constrained to slide against a frictional plane, friction force was introduced as a follower load, coaxial to rod BC. Load is applied by means of a lever in the experimental setup.

Assuming that the follower load P is given by Coulomb friction law with stiction and applying the principle of virtual works, two nonlinear differential equations of motion were derived. By assuming that the plate/wheel sliding condition is always verified, the authors developed a linearized version of equations of motion. The linearized analysis correctly predicts the onset of instability but does not provide information about how nonlinearities affect the development of instability. They found out that when nonlinearities are considered, flutter instability develops in a way that oscillation reaches a steady state and maximum amplitudes of displacement depend on the initial relative velocity.

As stated before, mode coupling instability type, also known as mode lock-in or binary flutter, is generally recognized as the most significant squeal mechanism. In this case, two vibration modes of brake components coincide and energy is feed into the vibrational

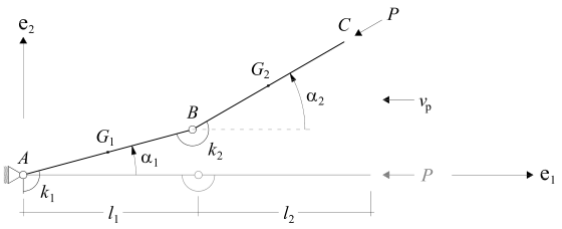

Figure 2.8: Free body diagram of Ziegler column subject to a follower force **P**, from [Bigoni and Noselli, 2011]

system. Later chapters will describe in detail this type of instability.

2.5 Influence of system parameters

As reported by many authors, it is still difficult to express the squeal phenomena since it is influenced by many design variables and operational conditions. A common approach adopted by the automotive industry consists on assessing the stability of the system by a complex eigenvalue analysis, thus evaluating the design of the brake system. In this line of work, several parametric studies have been performed on real brake systems by FE models, experimental approaches or the both combined.

A simplified brake model, containing only the disc and a pair of brake pads, was used to investigate the effects of system parameters on squeal propensity by finite element modelling [Liu et al., 2007]. Parameters included, hydraulic pressure, rotational velocity of the disc, friction coefficient and stiffness of both the disc and the back plates of the brake pads. Regarding the friction coefficient it was found that by increasing it, dynamic instability was increased and vice-versa. However, reducing the friction coefficient as a countermeasure to reduce squeal propensity would affect braking performance which is undesirable. Applied hydraulic pressure and rotational velocity were found to have little significance on squeal propensity. Effect of the stiffness of the disc on squeal propensity was studied by changing its Young's modulus and its thickness. On both cases, it was shown that a larger Young's modulus or larger thickness lead to an increase on disc stiffness and a reduction on squeal propensity. Lastly, stiffness of the brake pads was investigated and it was found that stiffer pads lead to higher squeal propensity.

The same parameters were investigated later [Nouby and Srinivasan, 2009]. Although the parameter range differs, similar qualitative results were achieved. However, in this later paper, numerical simulation showed that by increasing braking pressure, unstable frequency increases linearly. Both papers point out the pad bending vibration as the responsible for the squealing brake and suggest the use of softer materials for the back plates of the brake pads or the inclusion of viscoelastic damping, since out-of-plane magnitude vibration of the brake pads was significant.

In order to predict optimal pad design, through various geometrical construction factors, a combined approach of CEA and design of experiments (DOE) was performed [Nouby et al., 2009]. Those constructions factors included Young's modulus, back plates thickness, chamfer size and slots configurations on the pads. With that aim an "input-output" relationship between squeal propensity, namely the damping ratio, and brake pad geometry was built. Their strategy comprehended two phases. In the first phase, the most influential variables on the negative damping ratio were identified by means of fractional factorial design (FFD) of experiments. In the second phase, central composite design (CCD) based response surface methodology (RSM) was deployed to develop the non-linear model of prediction. From the first phase it was observed that the four most influential factors were Young's modulus of the back plate, chamfer of the pad, slot angle and distance between two slots. In the second phase a significance test was performed to evaluate the effects of the factors stated above and their interactions on the negative damping ratio. It was found that, in the authors' words, squeal propensity decreases with higher back plate Young' modulus, higher distance between slots and higher chamfer in both sides of friction material. Their model was proven to show good agreement with actual simulation results. This means that, in the authors' words, by applying this methodology, while designing brake systems, corrective and iterative design steps can be initiated and implemented for betterment of component design.

Evaluation of rotor structural modifications, in order to reduce squeal propensity, was also addressed [Nouby et al., 2011] by a combined numerical and experimental approach. Firstly, dynamic behaviour of the brake system was known. Natural frequencies obtained from both approaches were compared and was seen good agreement between the models thus validating the FE model. Then, dynamic behaviour of the brake assembly under applied pressure was investigated. Although predicted and measured results showed good agreement, from the seven unstable modes predicted, by CEA, only four exhibited squealing behaviour, identified by the measurement of sound pressure level at a 500 mm distance from the brake assembly. Then, with the aim of altering modal characteristics of the brake assembly, several modifications on the rotor design were proposed. These included changing neck thickness, neck height, top hat thickness and changing hat asymmetry. Some of these had already been proposed by other authors such as [J.D. Fieldhouse and Siddiqui, 2004]. It was seen that from the twelve proposed modifications, only four prevented/reduced disc brake squeal, namely, the increased neck thickness, the created disc asymmetry, by adding mass in the top-hat section, the reduced neck height and reduced number of cooling vanes. They also observed that creating the disc asymmetry was the most effective way in reducing squeal noise, since it eliminate 6 of the unstable modes and concluded that squeal was not completely eliminated since it does not depend on the rotor structure alone.

A lumped parameter model, representing a fixed caliper disc brake system and containing 10 degrees of freedom, was developed to asses the influence of system parameters on the stability of the system [Ahmed, 2011], by an eigenvalue analysis. Obtaining the real and imaginary parts of the complex eigenvalues λ, a squeal index σ was defined as

$$\sigma = \sqrt{\alpha^2 + \omega^2} \sin \frac{\delta}{2} \tag{2.9}$$

where, α, ω are the real and imaginary parts of the eigenvalues, respectively, and δ is the phase angle, expressed as $\delta = \tan^{-1} \frac{\Im[\lambda]}{\Re[\lambda]}$. The squeal index is used to evaluate the propensity, or tendency, of brake squeal. It was seen that, Young's modulus of both the disc and the friction material, and caliper weight influence squeal propensity, but Young's modulus of the rotor was the most influencing one.

Damping is a fundamental feature that was subject of several experimental and numerical analysis. [Francesco Massi, 2006], [Cantone and Massi, 2011], are papers that will later be discussed. In those works, mode coupling was considered as the squeal mechanism. Since this is the main subject of this project, the conclusions drawn from there will be presented later.

2.6 Summary and outlook

Kinetic energy of moving vehicles is dissipated through the brake system at the contact interface between the rotor and the pads. The components, which are subjected to sliding friction, a complex and nonlinear phenomena, experience friction-induced vibrations leading to emission of audible noise that may be uncomfortable for passengers.

A wealth of literature addressing this problem has been presented over the years. Research conducted regarding disc brake squeal has taken two general paths. The first deals with squealing brake systems whose design is finished and evaluates measures to reduce it, usually by a stability analysis. To this end, complex eigenvalue analysis is performed and if any of the eigenvalues has a positive real part, then the system may become unstable. The second approach to study disc brake squeal is concerned with

investigating the mechanisms by which the brake system may turn unstable.

Several mechanisms have been identified, such as, *stick-slip*, *sprag-slip*, instability due to follower forces or mode-coupling. In early days, it was thought that a decreasing friction coefficient with increasing sliding velocity would be the mechanism responsible for squealing brakes since it lead to stick-slip motions. It was seen later that even assuming a constant friction coefficient, disc brakes could be present squeal. It was proved that instability could be induced by geometric features. Sprag-slip was then identified. According to this theory, for a certain geometric configuration, the structure locks and due to the elasticity of the system slip occurs. This theory was later reexamined and it was seen that, for a certain parameter combination, non-existence of a steady state sliding would be the case for instability, in a way that the system is dynamic by nature. Other line of research as incorporated the friction forces as follower forces, which are forces that depend on the displacement of the system but which can not be derived from the potential energy of the system. It was proven experimentally that friction forces modelled as follower forces could be the cause for flutter instability, which is a blowing-up vibrational motion, or divergence, a motion of exponential amplitude growth.

It is recognized by the majority of the authors that mode coupling is the responsible for most of the squealing events. If two components of the disc brake system have similar vibration modes, these modes may lock establishing a energy flow between and leading to dynamic motions of increasing amplitude. This is the topic to be addressed in later chapters.

Finally, the influence of several parameters on squeal propensity was discussed. Several ways to define squeal propensity do exist. For simplicity, one can evaluate squeal propensity by examining the real parts of the complex eigenvalues, as stated before. It was seen that squeal behaviour of the brake system is mostly affected by the stiffness of the rotor, the pads and the back plates. These parameters may be modified by selecting softer or stiffer materials and by changing the design of the components.

Chapter 3

Mode coupling instability

Although there are several mechanisms that could lead to squeal, regarded as a consequence of dynamic instability, it is generally accepted that mode-coupling, leading to the appearance of an unstable mode, is the responsible for the majority of the events.

According to this line of though, in disc brake systems, if two substructures have close range natural frequencies, then their dynamical motions may couple geometrically (same wavelength), establishing a energy flow between them, thus leading to an increase in vibration amplitudes.

[Akay, 2002], in his acoustics of friction review, pointed out distinct types of mode lock-in. There is the *classical lock-in*, in which modes of the components are almost equal in frequency and lock-in occurs at that frequency. The second one, the *intermediate mode lock-in* in which the system locks into a frequency that lies between the eigenfrequencies of the components. At last, the *multiple lock-in*, where the squeal spectrum contains not only a dominant frequency and its harmonics, but also side bands.

Insight on this type of instability has been gained, mostly, by a combined numerical and experimental approach. A variety of experimental setups have been developed and some of them are discussed in this chapter. To model the disc brake system analytically, almost relevant papers make use of pin-on-disc or beam-on-disc systems, which will also be addressed.

From the experimental work reviewed, that shall be presented in the following sections, a variety of approaches was noticed regarding the way mode coupling is studied. We notice studies on the influence of friction models in mode coupling phenomena and, in particular, the friction coefficient, seen as a control parameter [Massi et al., 2013], [Allgaier et al., 1999]. Other approaches combine experimental modal analysis and power spectral density of the acceleration of the components to achieve a correlation between squeal noise occurrence and mode lock-in instability type.

Making use of experimental setups with well known dynamics, the influence of damping is investigated. It will be seen how does the damping affects the merging scenario.

3.1 Squeal phenomena and mode coupling

[Allgaier et al., 1999] performed an experimental analysis on a pin-disc set-up and generated a FE model to investigate the mode lock-in phenomena aiming at the determination of which friction model and which modelling details would be necessary and sufficient to simulate it.

The experimental set up consisted in a pin with adjustable length on rotating disc system. The arrangement allowed to, not only adjust the length of the beam, thus modifying

its natural frequencies, but also to vary the angle of attack between the vector normal to the disc and the neutral axis of the pin. First, they tried to generate friction-induced vibrations, so 2nd mode frequency of the pin was trimmed (2100 Hz) to the same value of 3rd mode frequency of the disc (2250 Hz). An example of a "classical" lock-in occurred at a frequency 2215 Hz, slightly lower than the 3rd mode frequency of the disc. Secondly, they increased the pin's length so that the new 2nd mode frequency of the pin were 1500 Hz. Dynamic behaviour was completely different. Although both components vibrated at the same frequency (1445 Hz), dominant frequency was determined by the 2nd mode of the pin. Amplitudes of the disc harmonics and pin harmonics were completely different. The measured sound spectrum showed that not only the disc radiates sound but also the pin.

Pin-on-disc system was also used to investigate general squeal characteristics [Tuchinda et al., 2001], [Tuchinda, 2003]. In their work they found that instability could occur when one of the natural frequencies of the pin approaches one of the natural frequencies of the disc. The friction coefficient value at which lock-in sets in is the critical friction coefficient. A second critical value was found at which the unstable mode splits into two stable modes. To this behaviour, that has never been seen before, the authors called locking-out.

The beam and the disc were considered flexible thus allowing that the vibration of one component locked onto different modes of the other. For a frequency band 10-16 kHz it was found that the natural frequency of the 8 nodal diameter mode combined with the natural frequency of the 4^{th} transverse mode of the beam, when $\mu = 0.51$. Lock-in phenomena, already known by the time, was observed. However, lock-in frequency predicted by their model changed significantly with the friction coefficient. For that case a *Locus plot* was plotted giving an helpful insight on the onset of instability. When $\mu = 0$, eigenvalues of the modes in play (8 nodal diameter mode of the disc and 4^{th} transverse mode of the beam) were purely imaginary. They stated that by increasing the friction coefficient, the two eigenvalues approach each other along the imaginary axis until a critical point μ_c is achieved. In that point the eigenvalues coincide and instability first occurs. For $\mu > \mu_c$ the two purely imaginary eigenvalues turn into two complex eigenvalues, resulting into one stable mode (negative real part) and one unstable mode (positive real part). The same procedure was conducted in a different frequency range [500-4000] Hz. Lock-in between the 2^{nd} transverse mode of the pin and the 3 nodal diameter mode of the disc was observed. Lock-in occurred for $\mu = 0.27$. An interesting feature regarding this case, that by the time hadn't been identified, was that when μ reached a higher value lock-in separated into two stable modes ("lock-out"). So, a second critical point (μ value) is identified.

They tried to explain lock-in and lock-out phenomenon by analysing the phase difference between the frictional force and the response. It was stated that for stable modes without lock-in, the phase difference between frictional force and the response are either 0^o or 180^o which meant that there were no net energy transferred between the pin and the disc in one complete cycle. For unstable modes, the response leads the frictional force by 90^o. In this case the frictional force provides net energy input into the pin and the disc. If the response lags the frictional force, then it will dissipate vibrational energy and hence lead to a damped response.

An experimental setup named TriboBrake was used to investigate brake squeal as a dynamic instability [Francesco Massi, 2006]. Their setup consisted of three substructures, the disc, the pad and the support/thin plates assembly, whose dynamics were known and could be changed by varying a few parameters, namely the normal load applied on the top of the support, the dimension of the pad or the stiffness of the thin plates. Dynamic behaviour was monitored by measuring acceleration of the pad and obtaining FRF for the

disc and support. Pad and support modes were characterized by tangential vibrations and disc modes by bending vibrations.

Their work showed that squeal events can arise either from the coupling dynamics of the disc and the pad or from the coupling between the disc and the support. They found that squeal happens when a mode, characterized by a large tangential displacement of either the pad or the support, couples with a mode characterized by large bending vibration of the disc. In order to this coupling take place, a tuning between two components' modes must exist, or, in other words, natural frequencies of the substructures must be close in range. They end by concluding that since squeal is triggered by tuning between two modes, modal distribution of the system must be accounted in order to eliminate this tuning without creating a new one.

Making use of a beam-on-disc system, a numerical model was developed in order to reproduce experimental results regarding mode lock-in characteristics in the presence of damping [Cantone and Massi, 2011]. In their previous experimental work [Francesco Massi, 2008], the beam length was chosen so that the natural frequency of its second bending mode was just over the natural frequency of the (0,4+) mode of the disc (4 diametral nodes). By adding a lumped mass at one side of the beam they could vary the natural frequencies of the beam modes and thus modifying the system dynamics. The added mass was included in the numerical model by changing the density of the elements. So, added mass was taken as a control parameter and it was seen that increasing the mass, the beam natural frequency decreases and approaches the disc frequency until both modes coalesce. In this point, the "lock-in point", the real part of one of the eigenvalues becomes positive giving rise to vibrations of increasing amplitude and squeal noise. Numerical results also confirmed the roots behaviour in the complex plane. Since their model accounted for structural damping, initially the eigenvalues are not purely imaginary. They move towards each other along a straight line representing the structural damping. At the "lock-in point", eigenvalues move in the opposite direction. One towards the negative real half-plane and the other towards the positive. By further increasing the mass, "lock-out" was also observed.

Structural damping was then modified to investigate its influence on the system dynamics and their findings will be discussed in the following section.

A different mechanical system, constituted by an elastic cylinder (polycarbonate) that rotates around a rigid cylindrical surface (steel) with friction, was used to investigate dynamic instabilities produced by sliding contact [Massi et al., 2013]. Both stability analysis and transient analysis were conducted. From the CEA it was observed that when μ was increased, real part of each couple of modes diverged from initial values, and while one shifted towards negative values, the other moved towards positive values, thus becoming unstable.

From the time history response of a node of the disc, provided by the transient simulation, it was observed that in the pre load phase the amplitude of response increased (due to the first contact between the discs) and were quickly damped (by the material damping of the polycarbonate disc). Then the response amplitude increased exponentially (due to apparent negative damping provided by friction contribution) until a limit-cycle was reached.

3.2 Influence of damping

Finally, the influence of damping on the stability of the disc brake system is discussed. Many experimental and numerical investigations have been reported. Damping effect was investigated using an experimental setup named TriboBrake [Francesco Massi, 2006]. Their

TriboBrake considered three main substructures namely, the disc, the pad and the caliper (represented by thin plates and a support). The test rig allowed to measure and adjust dynamic behaviour quite easily, so in the first part of their work, different approaches were put forward to shift natural frequencies of the system and find dynamic instabilities. Their findings on this matter have already been reported in the previous section. In the second part of their investigation, the influence of modal damping on squeal instability was addressed and it was seen that it could have two different opposite roles. Their experiments showed that a higher modal damping could either lead to a rise of squeal or to a reduction of instability amplitude. On one hand, addition of layers of rubber between the support and the thin plates prevented the coupling between the disc and the support, but could not prevent the mode coupling of the disc and the pads.

This means that, as the authors state, introducing solutions to avoid squeal caused by the coupling between modes of two substructures can be useless to prevent squeal caused by the coupling of two others substructures, and that dynamics of all brake components should be taken into account.

The reproduction of experimental results obtained by Massi and others, via a numerical approach, was the motivation for a later follow-up paper [Cantone and Massi, 2011], where the effect of damping distribution was studied. Though it had already been seen experimentally, the numerical results allowed to conclude that an homogeneous modal distribution of damping reduced the squeal propensity, and, on the opposite, non-homogeneous distribution lead to an increase in the coupling of the eigenvalues, thus leading to an increase in squeal propensity.

3.3 Summary and outlook

In the following, several aspects regarding mode coupling instability and its general characteristics are summarized. When two structures in sliding friction, have close range natural frequencies, their dynamic motions may couple geometrically.

Taking the friction coefficient as a control parameter, it was seen that by increasing it, mode frequencies approach each other until they merge. This is the ”lock-in” phenomena. At this point, two complex conjugate eigenvalues appear. The one whose real part is positive consists on an unstable mode, since it leads to an apparent negative damping.

In some cases, by further increasing the friction coefficient, the modes split. This behaviour is known as ”lock-out”. So, two critical friction coefficients may exist; one that defines the ”lock-in” phenomena and other that may induce the ”lock-out”.

It was seen that when two modes couple, an energy flow is established and its direction is defined by the phase between the frictional force and the displacement in a manner that if the response leads the frictional force, the last provides net energy input into the pin and the disc. If the response lags the frictional force, then it will dissipate vibrational energy and hence lead to a damped response.

Damping modal distribution is a key feature regarding the dynamic behaviour of systems with sliding friction, particularly, in the way that affects mode coupling. When modal damping was included with an homogeneous distribution, real parts of the eigenvalues merely lowered, meaning that mode merging was delayed. In other words, mode coupling occurred for higher friction coefficient values. On the other hand, introducing damping with a non-homogeneous distribution may increase squeal propensity or be useless to prevent it.

Chapter 4

Minimal models to study mode-coupling instability

In order to analyse and understand vibration phenomena and modal interaction in friction-induced vibrations, several authors used models with a minimal number of degrees of freedom, usually 2, to represent in-plane and out-plane oscillations. Although these do not represent geometrically the real brake systems, they are very useful to capture mode-coupling characteristics and the influence of system parameters in this squeal mechanism. In an attempt to produce a minimal model to be easily associated to disc brake systems, a wobbling disc model was presented [von Wagner et al., 2007]. This article is useful because it also presents a review of minimal models developed in the meantime, such as the model presented in [Shin et al., 2002], that was developed to investigate self-excited vibrations assuming a negative slope friction/velocity characteristic. But, since dynamic instability was proven to exist even with a constant friction coefficient, our attention is driven to minimal models developed to investigate modal interaction in sliding friction contacts as a mechanism for the onset of instability.

In the following sections, a global and yet detailed perspective on the characteristics and properties of the modal interaction with frictional coupling is given. From the minimal models reviewed it will be seen the merging scenario, which numerically is associated with the loose of symmetry of the stiffness matrix, and it is affected by structural parameters. Insight has been gained on how several parameters affect this merging scenario. It has been seen before, how mechanical properties and geometry modifications could eliminate some unstable frequencies. To further extend our comprehension on mode lock-in, other mechanical effects such as the gyroscopic effect, are also presented.

4.1 Properties of Mode lock-in and conditions for its onset

In order to capture and investigate all the essential properties of the mode-coupling instability type, a minimal 2 dof (in-plane and out-of-plane displacements) model was presented *in* [Hoffmann et al., 2002], where both structural and frictional coupling coexisted (fig. 4.1). After conducting a brief review on the generation of vibrational energy it was concluded that the cyclic growth of vibrational energy is due to the simultaneous presence of force oscillations and out of phase relative tangential displacements. Equations of motion in the matrix form for the minimal model presented are

$$\begin{bmatrix} m & 0 \\ 0 & m \end{bmatrix} \begin{Bmatrix} \ddot{x} \\ \ddot{y} \end{Bmatrix} + \begin{bmatrix} k_{11} & k_{12} \\ k_{21} & k_{22} \end{bmatrix} \begin{Bmatrix} x \\ y \end{Bmatrix} = \begin{Bmatrix} F_F \\ F_N \end{Bmatrix} \tag{4.1}$$

Assuming that the friction force can be approximated in terms of the contact spring deformation, such as $F_F = \mu k_3 y$, the equations of motion are rewritten as a homogeneous

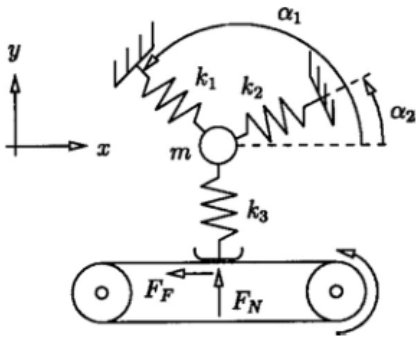

Figure 4.1: 2-dof minimal model of Hoffmann and co-workers

system with non-symmetric stiffness matrix as

$$\begin{bmatrix} m & 0 \\ 0 & m \end{bmatrix} \begin{Bmatrix} \ddot{x} \\ \ddot{y} \end{Bmatrix} + \begin{bmatrix} k_{11} & k_{12} - \mu k_3 \\ k_{21} & k_{22} \end{bmatrix} \begin{Bmatrix} x \\ y \end{Bmatrix} = \{0\} \tag{4.2}$$

System parameters were defined conducting to special case of

$$\begin{bmatrix} 1 & 0 \\ 0 & 1 \end{bmatrix} \begin{Bmatrix} \ddot{x} \\ \ddot{y} \end{Bmatrix} + \begin{bmatrix} 2 & 1 - \Delta \\ 1 & 2 \end{bmatrix} \begin{Bmatrix} x \\ y \end{Bmatrix} = \{0\} \tag{4.3}$$

and a complex eigenvalue analysis was performed. Also, the variation of mode frequencies and growth rates with respect to the friction coefficient, assuming $\Delta = \mu k_3$, was plotted. This analysis showed a well know feature for the mode-coupling instability (figure 4.2). It was shown that at a critical friction coefficient, corresponding to $\Delta = 1.0$, instability set in, resulting in the merging of real vibration modes. When these real vibration modes merged, two complex conjugate modes appeared, where one of them exhibited a positive real part (*negative apparent damping*), thus turning into an unstable mode and leading to a cyclic increase of the amplitude vibrations.

Rewriting the equations of motion, with the inertial forces on the left-hand side and the stiffness forces on the right-hand side, allowed to get a further insight in the nature of mode-coupling.

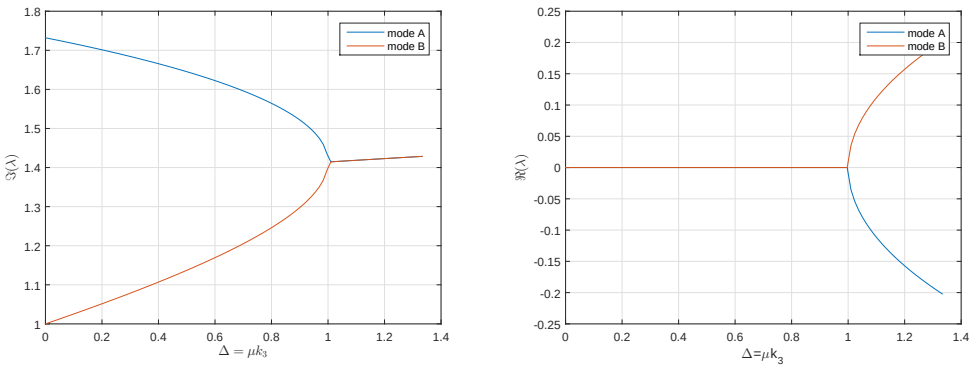

(a) $\Im(\lambda)$ (b) $\Re(\lambda)$

Figure 4.2: Merging scenario

$$\ddot{x} = -2x - (1-\Delta)y \tag{4.4}$$
$$\ddot{y} = -x - 2y \tag{4.5}$$

By plotting the left-hand side as a restoring force vector-field for *subcritical*, *marginally critical* and *supercritical*, it was seen that "for subcritical configurations, two directions of displacements may be found for which the restoring forces are inversely proportional to the direction of displacement" (figure 4.3). The vector-field is increasingly distorted as the friction becomes substantial and the directions come closer and closer until they merged at the marginal point $\Delta = 1.0$ (figure 4.4). For supercritical configurations $\Delta > 1.0$, already in the unstable regime, the vector-field has achieved such a degree of distortion that no directions of displacements are found where the restoring forces could lead the point mass to equilibrium. The resulting motion exhibits a spiral behaviour corresponding to the formal appearance of complex modes (figure 4.5b).

Time history of in-plane and out-plane motion for the three friction configurations shown that for subcritical configuration, motion consisted of a periodical exchange of energy between in- and out-plane motion and the appearance of phase shifts between them was also observed. For supercritical configurations, energy is generated continuously and motions of increasing amplitude happen.

In summary, they concluded that the source of vibrational energy was due to the non-conservative nature of the frictional forces. By hinting at an equilibrium between friction-induced and structural cross-coupling forces as a source of instability, they suggested that, from a physical point of view, simultaneous in- and out-of-plane oscillations which are out of phase are necessary for a cyclic increase in vibrational energy. Also, that friction forces link the in- and out-of-plane motion and that the phase shifts between them dictates the energy flow between the vibrational and frictional system.

A follow-up study on the effect of damping in mode lock-in was conducted later [Hoffmann and Gaul, 2003]. Mode-coupling instability was studied in the presence of structural damping, considered linear viscous, by means of an eigenvalue analysis.

According to the model presented in fig. 4.6, equations of motion were written in the matrix form as

$$\begin{bmatrix} m & 0 \\ 0 & m \end{bmatrix} \begin{Bmatrix} \ddot{x} \\ \ddot{z} \end{Bmatrix} + \begin{bmatrix} c_x & 0 \\ 0 & c_z \end{bmatrix} \begin{Bmatrix} \dot{x} \\ \dot{z} \end{Bmatrix} + \begin{bmatrix} k_x + \frac{1}{2}k & -\frac{1}{2}k + \mu k_z \\ -\frac{1}{2}k & k_z + \frac{1}{2}k \end{bmatrix} \begin{Bmatrix} x \\ z \end{Bmatrix} = \{0\} \tag{4.6}$$

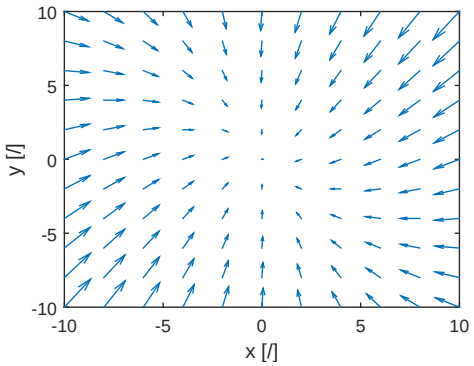

Figure 4.3: Restoring force field for subcritical configuration

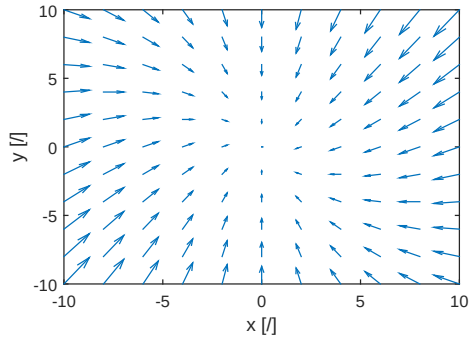

Figure 4.4: Restoring force field for marginally critical configuration

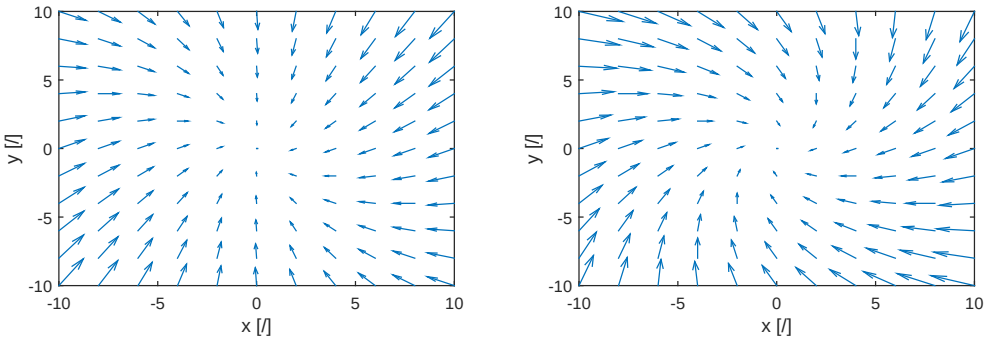

(a) $\Delta = 1.1$ (b) $\Delta = 2.0$

Figure 4.5: Restoring force field for supercritical configuration

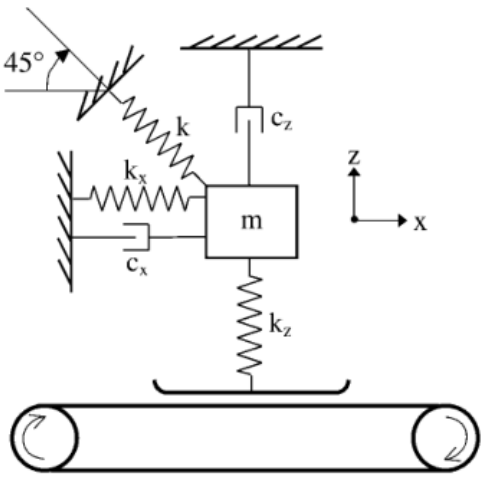

Figure 4.6: Minimal model with damping included

Using relative damping coefficients $D_i = c_i/(2\omega_i m)$ with $\omega_i^2 = (k_i + k/2)/m$ $(i = x, z)$, eq. (4.6) can be re-written as

$$\begin{bmatrix} 1 & 0 \\ 0 & 1 \end{bmatrix} \begin{Bmatrix} \ddot{x} \\ \ddot{z} \end{Bmatrix} + \begin{bmatrix} 2D_x\omega_x & 0 \\ 0 & 2D_z\omega_z \end{bmatrix} \begin{Bmatrix} \dot{x} \\ \dot{z} \end{Bmatrix} + \begin{bmatrix} \omega_x^2 & -\frac{k}{2m} + \mu(\omega_z^2 - k/2m) \\ -\frac{k}{2m} & \omega_z^2 \end{bmatrix} \begin{Bmatrix} x \\ z \end{Bmatrix} = \{0\} \quad (4.7)$$

After conducting an eigenvalue analysis to investigate the influence of damping in the mode merging, stability considerations were established by analysing FRF's, thus without solving the characteristic equation. Considering the above equation, the system is governed by a system of two equations,

$$\ddot{x} + 2D_x\omega_x\dot{x} + \omega_x^2 = (k/2m - \mu(\omega_z^2 - k/2m))z \quad (4.8)$$

$$\ddot{z} + 2D_z\omega_z\dot{z} + \omega_z^2 = (k/2m)x \quad (4.9)$$

where the first may be considered the in-plane equation and the second the out-of-plane equation. From equations ((4.8)) and ((4.9)) it can be seen that an out-of-plane displacement leads to excitation in the in-plane equation and vice-versa, so a feedback loop can be established between x and z. It should also be noted that in the in-plane equation, both structural and frictional quantities play a role in the forcing term which does not happen in the out-of-plane equation. Considering $x(t) = \hat{x}\exp(i\omega t)$ and $z(t) = \hat{z}\exp(i\omega t)$, frequency response functions F_x and F_z are defined as

$$\hat{x} = F_x(\omega) \cdot \hat{z} = \frac{\frac{k}{2m} - \mu(\omega_z^2 - \frac{k}{2m})}{(\omega_x^2 - \omega^2) + 2i\omega D_x\omega_x}\hat{z} \quad (4.10)$$

$$\hat{z} = F_z(\omega) \cdot \hat{x} = \frac{\frac{k}{2m}}{(\omega_z^2 - \omega^2) + 2i\omega D_z\omega_z}\hat{x} \quad (4.11)$$

and feedback arguments can be developed. It is supposed that a small x-displacement will induce an out-of-plane-displacement due to structural coupling, that in turn will induce an in-plane displacement, due to both structural and frictional coupling. It can be seen that

$$z(t) = \hat{z}\exp(i\omega t) = F_z(\omega)\hat{x}\exp(i\omega t) \quad (4.12)$$

$$\tilde{x}(t) = \tilde{\hat{x}}\exp(i\omega t) = F_x(\omega)\hat{z}\exp(i\omega t) = F_x(\omega)F_z(\omega)\hat{x}\exp(i\omega t) \quad (4.13)$$

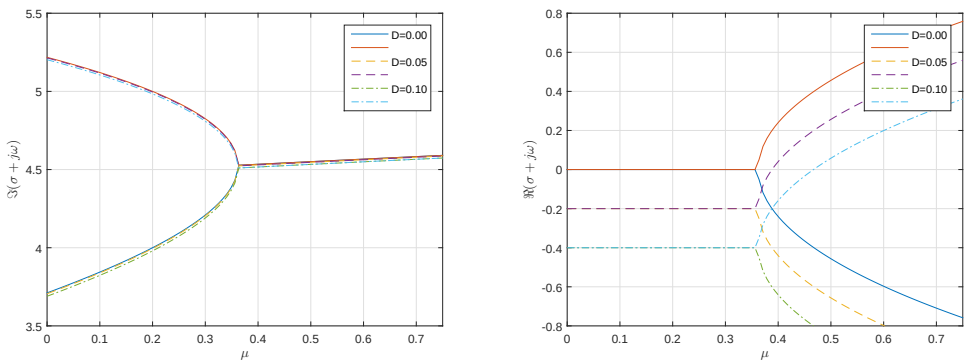

(a) $\Im(\lambda)$ (b) $\Re(\lambda)$

Figure 4.7: Merging scenario in the presence of proportional damping

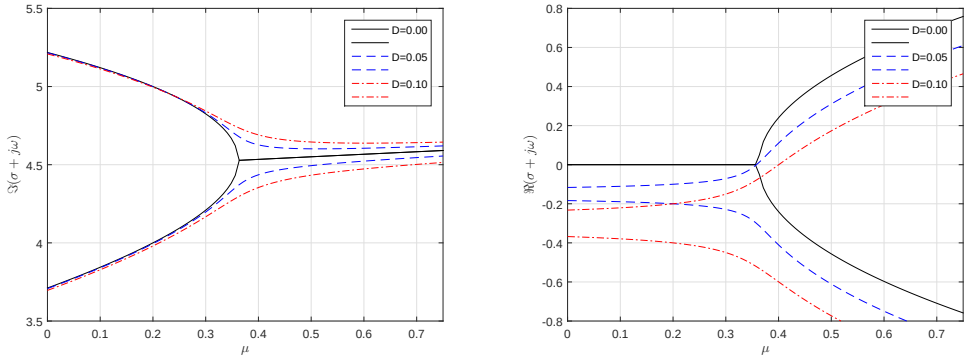

(a) $\Im(\lambda)$ (b) $\Re(\lambda)$

Figure 4.8: Merging scenario in the presence of non proportional damping

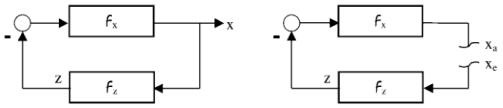

Figure 4.9: Feedback loop established showing the closed and open loop

A closed loop is established, and transfer functions are defined via the open loop (fig. 4.9). From the open loop system, transfer functions are expressed as

$$F_z = \frac{z}{x_e} = F_z \tag{4.14}$$

$$F_x = -\frac{x_a}{z} = -F_x \tag{4.15}$$

Having $x_a = -F_x F_z x_e$ the closed loop is obtained by enforcing $x_a = x_e$ and represented by

$$1 + F = 0 \tag{4.16}$$

where $F = -F_x F_z = \frac{x_a}{x_e}$ is the open loop transfer function. Eq. 4.16 is the characteristic equation that provides the eigenvalues of the closed loop system and they are analysed by the Nyquist criterion. In short, Nyquist criterion states that if the open loop is stable, the closed loop is only stable if the critical point $(-1, i0)$ is not allowed to be surrounded by $F(i\omega)$.

If the critical point is surrounded, then there is a frequency ω_{ZPSF} at which the response is in phase with the input and if amplitude amplification results so that $|F| > 1$, the closed loop system passes from stable to unstable.

Bearing this formulism in mind, friction coefficient influence was studied with proportional damping, and then an investigation on the role of damping was conducted.

Confirming the results of the previous work, it was seen that by increasing μ, oscillation frequencies came closer and closer until they merged. At that point of coalescence a stable and an unstable mode evolve from two original undamped modes. Also, that addition of proportional damping didn't alter the merge of the modes, when compared with the undamped case (figure 4.7a). Adding proportional damping merely lowered the growth rates by a certain amount determined, according to the authors, by the inherent structural damping (figure 4.7b). By lowering the growth rate curves, which constitutes a stabilizing

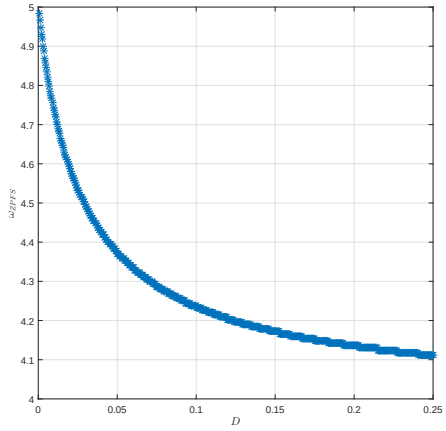

Figure 4.10: Zero phase shift frequency with respect to damping coefficient D_z

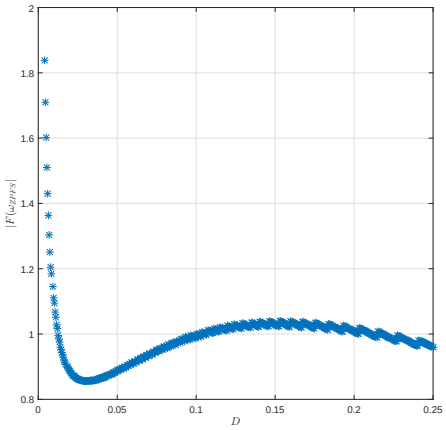

Figure 4.11: Magnitude of the closed loop transfer function evaluated at ω_{ZPSF} with respect to damping coefficient D_z

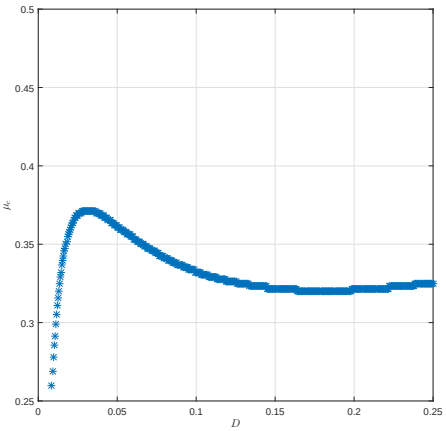

Figure 4.12: Critical friction coefficients with respect to damping coefficient D_z

effect, the mode becomes unstable for higher μ-values , i.e, the critical friction coefficient increases.

Non-proportional damping was then studied (figure 4.8). It was seen that with the introduction of non-proportional damping no clear merging occurred. The modes merely approach each other in terms of frequency but coalescence of the frequencies does not occur and the less damped mode goes continuously into the regime of instability. This effect was identified by the authors as a imperfect merging.

Numerical example showed that in the undamped case, typical behaviour of mode-coupling instability is recovered. Also, that increase of damping merely lowers the damping rates, and the merging is not altered. By plotting the critical friction coefficient versus the damping, it was shown that increasing the damping increases the μ_c-values monotonically.

4.2 Damping effect on mode coupling behaviour

Insight on how structural damping affects the stability of the system has already been gained on the previous chapter. In the following, investigation about the optimal values of structural damping that would reduce mode-coupling instability is presented, where a linear and non-linear 2-dof minimal model were developed [Sinou and Jézéquel, 2007] and a robust damping factor was introduced [J-J. Sinou, 2007]. This minimal model was introduced earlier in [Hultén, 1993] and is composed by a single-mass held in contact with a moving band by the mechanical elements displayed in fig. 4.13. The contact is modelled by two plates supported by two springs assuming that there is no separation between the plates and the band, that moves with constant velocity. Structural damping is included by introducing two dampers.

Friction forces are included using Coulomb's friction law, such that $F_T = \mu F_N$, and assuming that the normal contact forces are related to the displacement of the mass normal to the contact surface. Following, equations of motion can be written in matrix form as,

$$[M]\{\ddot{X}\} + [C]\{\dot{X}\} + [K]\{X\} + \{F_{NL}(X)\} = \{0\} \tag{4.17}$$

where, $[M]$ is the mass matrix, $[C]$ is the damping matrix, $[K]$ is the non-symmetric stiffness matrix. $\{X\} = \{X_1, X_2\}^T$, $\{\dot{X}\}$ and $\{\ddot{X}\}$ are the displacement, velocity and acceleration vectors, respectively. $\{F_{NL}(X)\}$ is the non-linear term, that depends on the cubic of displacement.

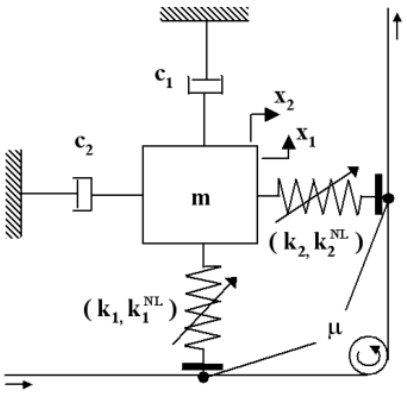

Figure 4.13: Non-linear mechanical minimal model investigated

$$[M] = \begin{bmatrix} m & 0 \\ 0 & m \end{bmatrix} \tag{4.18}$$

$$[C] = \begin{bmatrix} c_1 & 0 \\ 0 & c_2 \end{bmatrix} \tag{4.19}$$

$$[K] = \begin{bmatrix} k_1 & -\mu k_2 \\ \mu k_1 & k_2 \end{bmatrix} \tag{4.20}$$

$$\{F_{NL}(X)\} = \begin{Bmatrix} k_1^{NL} X_1^3 - \mu k_2^{NL} X_2^3 \\ \mu k_1^{NL} X_1^3 + k_2^{NL} X_2^3 \end{Bmatrix} \tag{4.21}$$

Considering relative damping coefficients $\eta_i = c_i/\sqrt{m_i k_i}$ and natural frequencies $\omega_i = \sqrt{k_i/m_i}$ $(i = 1, 2)$, dividing eq. (4.17) by m, equations of motion can be re-written in the form

$$\begin{bmatrix} 1 & 0 \\ 0 & 1 \end{bmatrix} \begin{Bmatrix} \ddot{X}_1 \\ \ddot{X}_2 \end{Bmatrix} + \begin{bmatrix} \eta_1\omega_1 & 0 \\ 0 & \eta_2\omega_2 \end{bmatrix} \begin{Bmatrix} \dot{X}_1 \\ \dot{X}_2 \end{Bmatrix} + \begin{bmatrix} \omega_1^2 & -\mu\omega_2^2 \\ \mu\omega_1^2 & \omega_2^2 \end{bmatrix} \begin{Bmatrix} X_1 \\ X_2 \end{Bmatrix} = \begin{Bmatrix} -\varphi_1^{NL} X_1^3 + \mu\varphi_2^{NL} X_2^3 \\ -\mu\varphi_1^{NL} X_1^3 - \varphi_2^{NL} X_2^3 \end{Bmatrix} \tag{4.22}$$

where, $\varphi_i = \omega_i^2$.

The eigenvalues of the system are found by solving the characteristic equation

$$\det(\lambda^2[M] + \lambda[C] + [K]) = 0 \tag{4.23}$$

Due to the non-symmetric nature of stiffness matrix, some λ eigenvalues may have a positive real part. When at least one of eigenvalues has a positive real part, the static solution is unstable. Friction coefficient was also taken as the control parameter in their stability analysis, and same merging scenario presented in figures 4.7 and 4.8 was achieved.

It was seen that damping ratio may have an optimal value that not only maximizes the critical friction coefficient, but also influences the dynamical behaviour of the unstable mode.

To verify the stability of a dynamical system, an approach by the Routh-Hurwitz criterion was also undertaken. This method verifies if all the roots of the polynomial characteristic equation have negative real parts. So, developing the characteristic determinant, eq. (4.23)

$$\det(\lambda^2[M] + \lambda[C] + [K]) = \begin{vmatrix} \lambda^2 + \eta_1\omega_1\lambda + \omega_1^2 & -\mu\omega_2^2 \\ \mu\omega_1^2 & \lambda^2 + \eta_2\omega_2\lambda + \omega_2^2 \end{vmatrix} \tag{4.24}$$

a four-order polynomial is obtained $(\lambda^4 + a_1\lambda^3 + a_2\lambda^2 + a_3\lambda + a_4 = 0)$, where

$$a_1 = \eta_1\omega_1 + \eta_2\omega_2 \tag{4.25}$$

$$a_2 = \eta_1\eta_2\omega_1\omega_2 + \omega_1^2 + \omega_2^2 \tag{4.26}$$

$$a_3 = \eta_1\omega_1\omega_2^2 + \eta_2\omega_2\omega_1^2 \tag{4.27}$$

$$a_4 = \omega_1^2\omega_2^2(1 - \mu^{\,2}) \tag{4.28}$$

From the application of the stability criterion mentioned above, the following four coefficients were obtained,

$$H_1 = a_1 \tag{4.29}$$
$$H_2 = a_1 a_2 - a_3 \tag{4.30}$$
$$H_3 = a_1 a_2 a_3 - a_3^2 - a_4 a_1^2 \tag{4.31}$$
$$H_4 = a_1 a_2 a_3 a_4 \tag{4.32}$$

and, if they all are positive, then the solution is stable. It was seen that the stability was only ruled by the coefficient H_3. Introducing frequency ratio and damping ratio defined as

$$\alpha_\omega = \frac{\omega_1}{\omega_2}$$

and

$$\alpha_\eta = \frac{\eta_1}{\eta_2}$$

respectively, boundary between stable and unstable regions may be determined by making H_3 equal to zero.

$$H_3 = 0 = \omega_2^3 \eta_2^2 \alpha_\omega (\eta_2^2 \sqrt{\alpha_\omega} \alpha_\eta (\sqrt{\alpha_\omega}\alpha_\eta + 1)(\alpha_\eta + \sqrt{\alpha_\omega}) + \alpha_\eta (\alpha_\omega - 1)^2 - \mu^2 \sqrt{\alpha_\omega}(\sqrt{\alpha_\omega}\alpha_\eta + 1)^2) \tag{4.33}$$

and the critical friction coefficient is found by solving eq. (4.33) in order to μ. By doing so, one gets

$$\mu_{cr}^2 = \frac{\eta_2^2 \sqrt{\alpha_\omega} \alpha_\eta (\sqrt{\alpha_\omega}\alpha_\eta + 1)(\alpha_\eta + \sqrt{\alpha_\omega}) + \alpha_\eta (\alpha_\omega - 1)^2}{\sqrt{\alpha_\omega}(\sqrt{\alpha_\omega}\alpha_\eta + 1)^2} \tag{4.34}$$

From the above equation, the authors performed several parametric studies to demonstrate the influence of the friction coefficient, structural damping, damping ratio and frequency ratio on the stability of the mechanical system. It was concluded that an optimal damping ratio could exist, and in that case, increasing either one or both damping coefficients would conduct to an increase in the stable region.

Having studied the influence of structural damping on the evolution of limit-cycle amplitudes, further insight on the role of damping on mechanical systems was gained by investigating the evolution of the stable and unstable modes as a function of the damping ratio $\frac{\eta_1}{\eta_2}$ between them [J-J. Sinou, 2007].

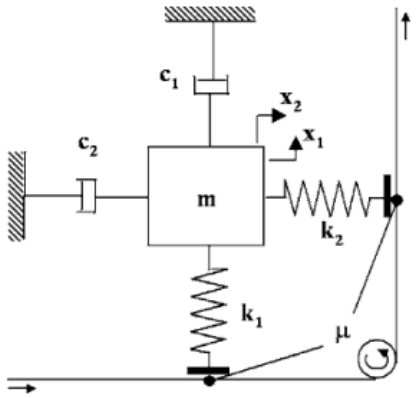

Figure 4.14: Minimal model proposed by Hulten

Making use of the mechanical system presented in fig. 4.14, evolution of both the real parts and frequencies, of the stable and unstable modes, was observed with respect to the damping ratio for two values of η_2. In the first case, $\eta_2 = 0.02$ and in the second case $\eta_2 = 0.1$. They found that by modifying the damping ratio the merging scenario is altered and there is a value for which the modes reverse.In other words, the unstable mode becomes stable and vice-versa. The value of damping ratio for this situation is given by

$$\frac{\eta_1}{\eta_2} \approx \frac{\omega_2}{\omega_1} \tag{4.35}$$

By observing these evolutions, it was found that for the first case, the optimal damping ratio, which leads to a more stable system, corresponded to the modification of the merging scenario. Thus, its value is given by equation 4.35. In the second case, for higher damping values, it was seen that an increase on damping ratio always conducted to a more stable system, even when merging scenario modification is present for the damping ratio given by equation 4.35.

To provide a further insight on the role of the structural damping ratio on the stability of mechanical systems, evolution of real parts was observed with respect to damping and frequency ratio for given values of friction coefficient and η_2. Two remarks are made. Firstly, for a given value of damping coefficient η_2 increasing the friction coefficient increases the unstable area, and, secondly, for a given value of damping ratio, increasing η_2 increases the stable area.

This constitutes an evidence that structural damping is not only a key feature on the stability of the system, but also influences the merging scenario and the origin of the unstable mode.

After conducting this parametric study on the damping ratio effect, the authors were intrigued if there were an optimal damping ratio that would lead to the more stable system.

They found that this optimal damping ratio as defined by equation 4.35, could be a good compromise solution, since it included, on one hand, the best solution for a certain combination of parameters and on the other, a better solution than nonproportional damping or no damping at all.

As stated by the authors, to this solution corresponds the case when the difference between the real parts of the modes is zero. This value is defined by

$$\Delta R = \left|\Re(\lambda_{unstable}) - \Re(\lambda_{stable})\right| \tag{4.36}$$

and the associated difference ΔF of the two imaginary parts as

$$\Delta F = \left|\Im(\lambda_{unstable}) - \Im(\lambda_{stable})\right| \tag{4.37}$$

Variability of this amounts with respect to the friction coefficient, damping ratio and frequency ratio was studied and it was seen that the minimum of ΔR corresponded to $\eta_1/\eta_2 \approx \omega_2/\omega_1$, the merging scenario discussed previously, and the minimum of ΔF is obtained when the system is unstable and the merging scenario occurs.

So, the robust damping factor to be developed would be defined by the lesser difference between the real parts of the merging modes, which is zero when the modes reverse, and would correspond to the greater difference between the two frequencies. Bearing this in mind, the criterion of the robust damping factor was defined by the authors as

$$\begin{aligned} RD - factor &= -\max[\Re(\lambda)] \log\left(\frac{\Delta F}{\Delta R + 1} + 1\right) \qquad if \Re(\lambda) \leq 0 \\ RD - factor &= 0 \qquad if \Re(\lambda) > 0 \end{aligned} \tag{4.38}$$

Variability of the RD-factor was again studied with respect to the damping and frequency ratio for given values of the friction coefficient. It was observed the following:

- for a given value of the friction coefficient, the RD-factor is greater when equation 4.35 is verified;
- for a given value of the damping ratio, an increase in damping increases the RD-factor;
- for a given value of the friction coefficient, the RD-factor indicates the same zone for the damping ratio, even when η_1 varies.

With these observations, they concluded that the RD-factor, which is a function of the real and imaginary parts of the eigenvalues, is a good indicator to the most suitable damping ratio that leads to a more stable system.

4.3 Reduced-order model

In their dynamic instability study [Kang et al., 2008], an analytical approach was used to derive a reduced-order model containing a single doublet mode pair. Same as previous works, in order to get a deep understanding of modal instability, a new minimal model, mathematically equivalent to the reduced-order model, was proposed (fig. 4.15).

In the development of the analytical problem, it was considered the steady state sliding between a thin stationary annular plate and two annular sector plates in frictional contact. To develop the analytical model, rotational and follower force effects were neglected. Boundary conditions are set, so the disc is clamped at the inner radius and free at the outer edge.

Since this chapter is concerned with the minimal model itself, the analytical formulism is presented at chapter 5. As it shall be seen later, equations of motion are derived from the assumed modes method and are, in the matrix form

$$\ddot{q} + [\omega^2]q + [A]q + \eta[B_\theta]q = \{0\} \tag{4.39}$$

where $[A] = [A]^T$ is the contact stiffness matrix and $[B] \neq [B]^T$ is the non-symmetric non-conservative work matrix produced by friction forces. In the minimal model, the matrixes have the form

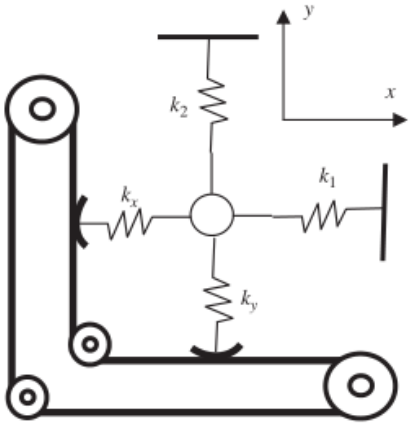

Figure 4.15: Minimal model proposed in [Kang et al., 2008]

$$[\omega^2] = \begin{bmatrix} k_1 & 0 \\ 0 & k_2 \end{bmatrix} \tag{4.40}$$

$$[A] = \begin{bmatrix} k_x & 0 \\ 0 & k_y \end{bmatrix} \tag{4.41}$$

$$[B] = \begin{bmatrix} 0 & -k_y \\ k_x & 0 \end{bmatrix} \tag{4.42}$$

where, in order to be mathematically equivalent to the reduced-order model, the system parameters are defined as

$$k_1 = \omega_{2n-1}^2, \qquad k_2 = \omega_{2n}^2, \tag{4.43}$$

$$k_x = \frac{k_c \theta_c \tilde{R}_n^z}{2} \left(1 + \frac{\sin(n\theta_c)}{n\theta_c}\right) \tag{4.44}$$

$$k_y = \frac{k_c \theta_c \tilde{R}_n^z}{2} \left(1 - \frac{\sin(n\theta_c)}{n\theta_c}\right) \tag{4.45}$$

$$\eta = \mu n \frac{\tilde{R}_n^\theta}{\tilde{R}_n^z} \tag{4.46}$$

The authors also state that from the eigensolutions of eq. (4.39), it is possible to derive an expression for the critical friction factor η.

$$\eta_{cr} = \frac{|(\omega_{2n-1}^2 - \omega_{2n}^2) + (k_x - k_y)|}{2\sqrt{k_x k_y}} \tag{4.47}$$

It can be seen from eq. (4.47) that the dynamic instability, represented by the critical friction factor, is expressed by a component frequency separation $(\omega_{2n-1}^2 - \omega_{2n}^2)$ and a contact stiffness separation $(k_x - k_y)$, and as they get smaller, modal instability increases, because the critical friction factor becomes smaller. It will be seen in a later chapter that contact stiffness terms k_x and k_y are determined from the contact span angle θ_c and are equivalent to the modal contact strain energies from the disc sine and cosine modes. So, contact stiffness separation in the single-mass model represents the difference between modal contact strain energies of a doublet mode pair. If two modes in a doublet pair have identical modal contact strain energies, the propensity of the modal instability due to the interaction of doublet modes reaches to the maximum level.

From a design point of view, it is crucial to know the values of the contact span angle that minimize the critical friction coefficient. Numerical results presented by the authors showed that for doublet mode pairs with zero frequency separation ($\omega_{2n-1} = \omega_{2n}$), critical contact span angles have periodic values as opposed to those with non-zero frequency separation ($\omega_{2n-1} \neq \omega_{2n}$). Variation of the ratio of contact stiffness with respect to variation of contact span angle was also presented. Knowing that as $\frac{k_y}{k_x}$ approaches unit, squeal propensity increases, it could be seen that critical contact span angles correspond to $\frac{k_y}{k_x} = 1$ and that different doublet modes could have one or more critical θ_c-values.

4.4 Reduced-order model and gyroscopic effect on binary flutter

The concept of a minimal model mathematically equivalent to the reduced-order model, constituted only by a doublet mode pair, was used to perform a comprehensive stability

analysis regarding disc brake squeal [Kang et al., 2009a].

Disc brake squeal occurs for low rotational velocities, where gyroscopic and circulatory effects are negligible, and so, most investigations do not address these mechanical effects.

In an attempt to investigate how mode coupling behaviour is affected when these are considered, the reduced-order model previously presented was adapted to include gyroscopic and negative friction slope mechanisms, thus providing a comprehensive stability analysis.

From the discretization of Lagrange equations by modal coordinates, topic that will be addressed in the following chapter, equations of motion were derived. In matrix form, equation of motion is

$$\{\ddot{a}\} + ([G] + [D])\{\dot{a}\} + ([K_s] + [K_{ns}])\{a\} = \{0\} \tag{4.48}$$

where,

$$[D] = [C] + [R_d] + [N_s] \tag{4.49}$$

$$[K_s] = diag(\omega_n^2) + [A] + [P] \tag{4.50}$$

$$[K_{ns}] = [B] + [F] \tag{4.51}$$

and, $[G] = -[G]^T$, $[C] = 2\xi_n \cdot diag(\omega_n)$, $[R_d] = [R_d]^T$ and $[N_s] = [N_s]^T$ are respectively, the gyroscopic, the structural modal damping, the radial dissipative and friction slope matrices. $[A] = [A]^T$ and $[P] = [P]^T$ are the contact stiffness and pre-load stiffness matrices, in the symmetric stiffness matrix, and $[B] \neq [B]^T$ and $[F] \neq [F]^T$ are the non-symmetric, non-conservative work matrices produced by friction couple and follower forces, respectively.

So, the model comprehends a wide range of effects that by the time had not been included and whose contribution was not completely understood. Their main objective was not only to study the stability of the system, but also to investigate analytically the contribution of such effects on the onset of instability. To this end, the reduced-order model containing a single doublet pair was used. The matrices in equation 4.48 have the form:

$$G = \begin{bmatrix} 0 & 2n\Omega \\ -2n\Omega & 0 \end{bmatrix} \tag{4.52}$$

$$C = 2\xi_n\omega_n \begin{bmatrix} 1 & 0 \\ 0 & 1 \end{bmatrix} \tag{4.53}$$

$$R_d = \begin{bmatrix} R_{d1} & 0 \\ 0 & R_{d2} \end{bmatrix} \tag{4.54}$$

$$N_s = \begin{bmatrix} N_{s1} & 0 \\ 0 & N_{s2} \end{bmatrix} \tag{4.55}$$

$$K_s = \begin{bmatrix} \Omega_1^2 & 0 \\ 0 & \Omega_2^2 \end{bmatrix} \tag{4.56}$$

$$K_n s = \begin{bmatrix} 0 & b_1 \\ b_2 & 0 \end{bmatrix} \tag{4.57}$$

From the matrices defined above, focus is given, not only on the non-symmetric stiffness elements b_1 and b_2, that reflect the frictional coupling terms and comprehend the non-conservative work produced by the friction couple and the follower forces, but also on the coupling terms of the gyroscopic matrix. To consult the analytical expressions

for the several terms presented in the matrices above, [Kang et al., 2009b] is referred. Characteristic equation may be developed in the form

$$\lambda^4 + c_1\lambda^3 + c_2\lambda^2 + c_3\lambda + c_4 = 0 \tag{4.58}$$

Same as previous authors, Routh-Hurwitz criterion was applied, to address the stability of the system. To face this approach, it was assumed that D_1 and D_2 are positive values and b_1 and b_2 were defined in a way that the first is positive and the second is negative. Two necessary and sufficient conditions for the stability of the system were developed,

$$c_1c_2 - c_3 > 0 \tag{4.59}$$

$$(c_1c_2 - c_3)c_3 - c_1^2c_4 > 0 \tag{4.60}$$

where,

$$c_1 = D_1 + D_2 \tag{4.61}$$

where $D_i = 2\xi_n\omega_n + R_{di} + N_{si}$, for $i = 1, 2$, and

$$c_2 = \Omega_1^2 + \Omega_2^2 + D_1D_2 + (2n\Omega)^2 \tag{4.62}$$

$$c_3 = D_2\Omega_1^2 + D_1\Omega_2^2 - (b_2 - b_1)(2n\Omega)^2 \tag{4.63}$$

$$c_4 = \Omega_1^2\Omega_2^2 - (b_1b_2) \tag{4.64}$$

Developing the set of equations (4.59)-(4.60), and making them equal to zero gives

$$0 = \{D_1\Omega_1^2 + D_2\Omega_2^2 + (D_1 + D_2)(D_1D_2 + (2n\Omega)^2)\} - (b_2 - b_1)(2n\Omega)^2 \tag{4.65}$$

and

$$\begin{aligned} 0 =& \{D_1\Omega_1^2 + D_2\Omega_2^2 + (D_1 + D_2)(D_1D_2 + (2n\Omega)^2)\} \\ & \cdot (D_2\Omega_1^2 + D_1\Omega_2^2) + (D_1 + D_2)^2 \cdot (\Omega_1^2\Omega_2^2 - b_1b_2) \\ & + \{D_1\Omega_1^2 + D_2\Omega_2^2 + (D_1 + D_2)(D_1D_2 + (2n\Omega)^2)\} \\ & \cdot (b_2 - b_1)(2n\Omega) - (D_2\Omega_1^2 + D_1\Omega_2^2) \cdot (b_2 - b_1)(2n\Omega) - (b_1 - b_2)^2(2n\Omega)^2 \end{aligned} \tag{4.66}$$

From the equation 4.65, it is evident that without damping ($D_1 = D_2 = 0$), the system is unstable, thus indicating that gyroscopic term has a destabilizing effect.

Influence of damping was evaluated by the perturbation method. The following parameters were defined

$$\varepsilon_o = D_1 \qquad \varepsilon_d = D_2 - D_1 \tag{4.67}$$

It was found that for $\varepsilon_d = 0$ (equal damping) ε_o has a stabilizing effect. This formulism is in a good agreement regarding the influence of damping until now discussed. It was already seen that by adding damping in equal manner, growth rates, with respect to the friction coefficient, are lowered and the unstable mode occurs for higher critical values.

For the stationary disc, they expressed the condition for instability as

$$(\Omega_1^2 - \Omega_2^2)^2 + 4b_1b_2 < 0 \tag{4.68}$$

By considering D_1 much smaller than D_2, such that $\varepsilon_o \to 0$ and $\varepsilon_d > 0$, then instability sets in when

$$b_1 b_2 \varepsilon_d^2 < 0 \tag{4.69}$$

Reminding that $b_1 > 0$ and $b_2 < 0$, the product $b_1 b_2$ is negative and non-zero ε_d implies instability, which the authors refer to "smoothing effect".

Having the above exposition in mind, two destabilizing situations were identified; the first related to the term $(b_1 - b_2)(2n\Omega)$, to which the authors refer to gyroscopic frictional mode-coupling, and the second, the product $b_1 b_2$, the stationary frictional mode coupling.

To further comprehend the effects in play, solutions of equation (4.58) were examined for three proposed cases: equal damping with no gyroscopic effect, gyroscopic effect without damping and general disc operation which included both effects and no equal damping such that $D_1 \neq D_2$.

For the first case, assuming that $D^2 \ll 2(\Omega_1^2 + \Omega_2^2)$, solution has the form

$$\lambda \cong -\frac{D}{2} \pm \frac{1}{2}\sqrt{-2(\Omega_1^2 + \Omega_2^2) \pm 2\sqrt{(\Omega_1^2 - \Omega_2^2)^2 + 4b_1 b_2}} \tag{4.70}$$

For non-zero frequencies, second term on the right-hand side of equation (4.70) has positive real parts only when equation (4.68) is verified. This also evidences the influence of the product $b_1 b_2$, that is always negative, on the onset of instability. The first term confirms the stabilizing behaviour of equal damping since it shifts the eigenvalues negatively.

For the second case, setting $D_1 = D_2 = 0$ and $2n\Omega \neq 0$, the characteristic equation is expressed as

$$\lambda^4 + (\Omega_1^2 + \Omega_2^2 + (2n\Omega)^2)\lambda^2 + 2n\Omega(b_1 - b_2)\lambda + (\Omega_1^2 \cdot \Omega_2^2 - b_1 b_2) = 0 \tag{4.71}$$

To solve equation (4.71) a perturbation parameter was introduced such that

$$2n\Omega = g = \varepsilon g_o \tag{4.72}$$

$$\lambda = \lambda_0 + \varepsilon\lambda_1 + O(\varepsilon^2) \tag{4.73}$$

They substitute equations (4.72) and (4.73) on equation (4.71), resulting in

$$\lambda_0 = \pm\frac{1}{2}\sqrt{-2(\Omega_1^2 + \Omega_2^2) \pm 2\sqrt{(\Omega_1^2 - \Omega_2^2)^2 + 4b_1 b_2}} \tag{4.74}$$

$$\lambda_1 = \pm\frac{g_o(b_1 - b_2)}{\sqrt{(\Omega_1^2 - \Omega_2^2)^2 + 4b_1 b_2}} \tag{4.75}$$

where λ_0 is identical to the second term of equation (4.70) and λ_1 was identified as the correction factor for the reduced-order model subject to gyroscopic loading.

As contrary to λ_0, real parts of λ_1 have both a positive and negative branch when $(\Omega_1^2 - \Omega_2^2)^2 + 4b_1 b_2 > 0$ and coalesce when $(\Omega_1^2 - \Omega_2^2)^2 + 4b_1 b_2 < 0$.

By the perturbation method they found that, for $\Re(\lambda_0) = 0$ gyroscopical friction mode coupling term $(2n\Omega(b_1 - b_2))$ contributed to the real positive part of λ_1, in the order of ε^1. These formulism allowed to conclude that both stationary frictional and gyroscopic frictional mode-coupling terms, respectively, $b_1 b_2$ and $2n\Omega(b_1 - b_2)$, have a destabilizing, smoothing-like, effect.

The final case included both the presence of damping, in a non equal manner, and the consideration of gyroscopic effects. For this operational scheme, both a smoothing and a tilting effect was observed.

The smoothing effect was already explained and is similar to the idea of imperfect merging. The tilting effect consists on the rotation of the entire locus plot around the pivot point ($\mu = 0$). The authors point out the radial dissipative terms ($R_{d1}$and R_{d2}), which are proportional to the friction coefficient, as the cause for this effect. Since radial dissipative terms are inversely proportional to disc velocity, they were also found effective at low speeds.

So real parts of the eigenvalues possess a negative and a positive branch that may undergo a smoothing and tilting modification caused by the gyroscopic and radial dissipative mechanisms, respectively.

Both effects are opposite regarding their influence on real parts. On one hand, gyroscopic effects increases $\Re(\lambda)$, on the other, radial dissipative decreases $\Re(\lambda)$. Since, the first is proportional to Ω and the second to $1/\Omega$, there is a speed that the effects cancel out.

At that speed, rotation effects are neglected, and mode-coupling behaviour is described by frictional coupling and structural damping ratio. So, two models were compared, namely the rotating disc model and the rotating-free. They found that at low speeds, the rotating-free disc is a good and valid approximation to the rotating the disc since it predicts almost the same stability boundaries. At higher velocities, rotation effects were seemed to be insignificant, and so the main responsible for the mode-splitting would be the frictional coupling. At very low speeds, rotation effects, in particular, the radial dissipative, stabilizes the system, so one must use the rotating disc model to analyse the overall stability of the system, since the rotating-free is not a good approximation.

Lastly, they address the effect of a negative-friction slope. The negative slope depends on the disc rotation speed and it seems that this effect could appear as rotation effect.

4.5 Summary and outlook

In order to study, specifically, mode-coupling instability type, a minimal model incorporating both structural and friction coupling was developed [Hoffmann et al., 2002], and later, with the inclusion of damping [Hoffmann and Gaul, 2003]. In their work, they showed that modal interaction may lead to energy transfer from the frictional system to the vibrational one, and clarify it from a phase shifts point of view. In the later work, they were curious about the qualitative and quantitative behaviour of mode-coupling instability in the presence of structural damping. Eigenvalue analysis and FRF analysis allowed not only to get a very good insight into the physical aspects of mode lock-in, but also to derive necessary and sufficient conditions for the onset of instability.

Later, a similar study on the effect of structural damping on the coupling of doublet modes was conducted [Sinou and Jézéquel, 2007] making use of a non-linear minimal model. The model, that had been proposed earlier in [Hultén, 1993], allowed for a stability analysis by the Routh-Hurwitz criterion, meaning that, analytical expressions could be calculated for the stable/unstable boundary regions without, actually, solving the characteristic equation. It was also demonstrated that variation of structural damping affects the dynamic behaviour of the coupling modes.

In their dynamic instability study, [Kang et al., 2008] investigated the mode-coupling squeal mechanism. The authors modified the mechanical model presented in [Hoffmann et al., 2002] in order to create a simplified, mathematically equivalent model to the one-doublet mode model. Their analytical formulism for the development of the single mode-pair will be introduced in the following chapter. From their minimal model, frequency separation of the disc mode pair and consequent modal stability boundary was investigated

with respect to the contact stiffness variation. The authors found that the contact span angle of the pads have a key role on squeal propensity and should be taken into account in a design stage of a braking system.

By recreating numerically the work presented in [Hoffmann et al., 2002] and [Hoffmann and Gaul, 2003], it became evident that the use of minimal models are very useful to investigate modal interaction. Their work provides a very accurate description of mode-coupling behaviour in the presence of friction as a mechanism for the onset of instability. By considering both structural and frictional coupling their conclusions are enhanced in the following:

- A look at the restoring force vector fields for various friction configurations allowed to conclude that as the friction coefficient increases, the vector field becomes increasingly distorted and, at supercritical configuration, where the friction coefficient is higher than the critical one, no path to restore equilibrium exists because the vector field presents a spiral behaviour.

- Energy can be transferred from the frictional to the vibrational system due to normal force oscillations that lead to oscillations of the tangential frictional force

Their follow-up investigation also allowed to see how damping would affect the merging behaviour. Regarding the merging scenario, we can sum up the influence of damping on the following:

- The merging scenario is not altered by adding proportional damping, but, by doing so, growth rates are lowered and the system becomes unstable for higher friction coefficients. This constitutes a stabilizing effect.

- If non-proportional damping is added, merging scenario is altered. The modes do not actually merge. As the friction coefficient increases, the modes approach each other but coalescence of the frequencies does not occur. This phenomena is called by the authors "imperfect merging".

- It was seen that, in a non-proportional damping scheme, for small values of damping, the critical friction coefficient decreases, which constitutes a destabilizing effect.

Approaching the system as a closed loop whose transfer function is the product of the FRF, two conditions were developed for the onset of instability. First, there would be a frequency ω' at which the displacements would be out of phase and, second, at the frequency ω', the magnitude of the transfer function would exceed a value of one. This is understood as an amplification of amplitude, evidencing that their formulism suits well in a self-excited system frame. Their investigation also allowed to see how damping would affect the merging behaviour, and it was seen that as damping increases the frequency ω' would shift and tend asymptotically to the less damped natural frequency.

Their stability investigation, by the simplified Nyquist criterion, on the effect of damping would be later confirmed in [Sinou and Jézéquel, 2007] and [J-J. Sinou, 2007], where they address the influence of structural damping on mode lock-in, by another stability criterion, namely, the Routh-Hurwizt criterion. Without solving the characteristic equation, an expression defining the critical friction coefficient, as a function of the damping and frequency ratio, was developed. The expression derived also defined the boundary between the stable and unstable region. By performing several parametric studies it was concluded that, for a certain combination of parameters, an optimal damping ratio between the stable and unstable modes, which decreases the unstable region, could exist.

To avoid design errors, they introduced the robust damping factor as an indication of the most stable mechanical system for a given damping ratio.

Reminding that a minimal model to study modal interaction requires only two degrees of freedom, we enhance the analytical and numerical results achieved by Kang and others. Regarding mode-coupling as a squeal mechanism, in order to study the stability of the transverse modes, they approached the problem as an annular plate in sliding friction with two sector plates over a finite contact area.

Using a single mode pair, composed by the cosine and sine modes, they studied a wide range of parameter effects on mode coupling behaviour.

By defining the critical friction coefficient they found that frequency separation of the doublet mode pair influences squeal propensity. By assuming a finite contact area, they also found that there are specific contact span angles that increases squeal propensity, assuming a zero frequency separation.

Not only did they studied this design parameter, but they also derived a minimal model containing the doublet modes of a single pair, to investigate deeper on the properties of mode lock-in. They found that the contact strain energy, which depends on the contact span angle, is related to squeal propensity.

Later they developed again a reduced-order model, but containing rotation, negative friction slope and follower force effects. In their approach, frictional coupling arose from both the friction couple, which is the moment generated at the disc midplane by the circumferential component of the friction force, and also from the frictional follower force, generated by the change of direction of the friction force, caused by the disc deformation.

By means of the perturbation method they showed that the frictional coupling could be either stationary friction couple, providing the well known merging scenario, or gyroscopic frictional coupling. It was seen that gyroscopic effect also has a smoothing effect of the growth rate curves, contributing to the onset of instability. They also found that, at low speeds radial slip dissipative terms have a stabilizing effect, and with increase in velocity, this effect is diminished, and the stationary and gyroscopic frictional coupling mechanisms dominate.

Chapter 5

Analytical modelling of the brake system

Minimal models are useful to capture underlying characteristics of mode coupling instability type, but they do not represent the actual brake system. Although the aim of this project is to study mode-coupling instability, as a squeal mechanism, we notice the development of several analytical models for the brake system. Early analytical models developed to analyse disc brake squeal consisted on pin-on-disc or beam-on disc systems. Several experimental setups consisted of this type of system, so there is a wide range of papers that deal with the disc brake as a beam-on-disc system such as [Allgaier et al., 1999], [Akay, 2002], [Tuchinda et al., 2001] or [Tuchinda, 2003].

Several other models have been based on a moving-load concept. In [Ouyang, 2003], not only a review on the vibrations due to moving loads is presented, but also modeling issues regarding the contact interface and friction law are discussed. These works have focused on studying dynamic instability of a spinning disc past stationary loads or stationary discs excited by moving-loads. One of them is presented in [Ouyang and Mottershead, 2004], where the disc brake is modeled as a thin circular disc excited by two moving loads acting on both sides.

Having seen the properties of mode-coupling and how the merging scenario is affected by the system parameters, in the following we focus the attention on some analytical models developed to investigate disc brake squeal.

Some have been developed to deeply investigate the system stability with respect to a determined instability mechanism, such as the effect of negative friction slope or gyroscopic effects. Regarding how friction is included, it will be seen that follower forces are usually neglected but may have some importance on the system stability, and friction is usually modelled as producing a friction coupling.

5.1 Pin-on-disc systems

A variety of studies using pin-on-disc or beam-on-disc systems, to study disc brake squeal, can be found in the literature, and some of them were already pointed out. To what modeling is concerned, it is a general approach to model the transverse vibration of the disc by the plate theory and the axial and transverse vibration of the beam by the Euler-Bernoulli theory. Then, a coupling condition is established. Here, the model proposed in [Tuchinda et al., 2001], is pointed out.

The model was developed to study mode coupling characteristics (chapter 3) and comprehends on one hand a pin with a square cross-sectional area, fully clamped at one end and in contact with the disc at the other. The pin is allowed to vibrate on the axial and transverse directions. On the other hand, the disc is clamped at the inner bore and free

at the outer rim and can only vibrate in the out-of-plane direction. The pin is placed so that the tangential friction force (in-plane force) can excite only one of the transverse directions of the pin.

From the classical plate theory, equation of motion for the out-of-plane vibration of the disc is established, since it is assumed that the rotational speed is very small.

$$D\nabla^4 w + \rho h \frac{\partial^2 w}{\partial t^2} = f_w(r,\theta,t) \tag{5.1}$$

Solution of equation (5.1) is assumed to be a sum of normal modes having the form

$$w(r,\theta,t) = \sum_{n=0}^{\infty}\sum_{m=0}^{\infty} {}_c\phi^d_{nm}(r,\theta)\,{}_cq_{nm}(t) + \sum_{n=0}^{\infty}\sum_{m=0}^{\infty} {}_s\phi^d_{nm}(r,\theta)\,{}_sq_{nm}(t) \tag{5.2}$$

where, ${}_c\phi^d_{nm}(r,\theta)$ is the cosine mode shape of the disc given by ${}_c\phi^d_{nm}(r,\theta) = [A_nJ_n(kr) + B_nY_n(kr) + C_nI_n(kr) + D_nK_n(kr)]\cos(n\theta)$, and ${}_s\phi^d_{nm}(r,\theta)$ is the sine mode shape of the disc given by ${}_s\phi^d_{nm}(r,\theta) = [A'_nJ_n(kr) + B'_nY_n(kr) + C'_nI_n(kr) + D'_nK_n(kr)]\sin(n\theta)$.

Equations of motion for the axial and transverse vibration of the pin are, respectively, expressed as

$$\rho A\frac{\partial^2 u}{\partial t^2} - EA\frac{\partial^2 u}{\partial x^2} = f_u(x,t) \tag{5.3}$$

and

$$\rho A\frac{\partial^2 v}{\partial t^2} + EI\frac{\partial^4 v}{\partial x^4} = f_v(x,t) \tag{5.4}$$

Solutions for equations (5.3) and (5.4), are written as

$$u(x,t) = \sum_{j=0}^{\infty}\phi^a_j(x)g_j(t) \tag{5.5}$$

and

$$v(x,t) = \sum_{j=0}^{\infty}\phi^t_j(x)p_j(t) \tag{5.6}$$

where ϕ^a_j is the axial mode shape given by $\phi^a_j = A_j\sin\left(\frac{\omega_j x}{c}\right) + B_j\cos\left(\frac{\omega_j x}{c}\right)$, with $c = \sqrt{E/\rho}$ and ϕ^t_j is the transverse mode shape given by $\phi^t_j = A'_j\sin(\lambda_j x) + B'_j\cos(\lambda_j x) + C'_j\sinh(\lambda_j x) + D'_j\cosh(\lambda_j x)$, with $\lambda^4 = \frac{\rho A\omega_j^2}{EI}$.

Substituting the general solutions (5.2), (5.5) and (5.6) in equations (5.1), (5.3) and (5.4), and using modal procedures, equations of motion were expressed as

$${}_c\ddot{q}_{nm} +_c \omega^2_{nm} \cdot_c q_{nm} = \int_b^a\int_0^{2\pi} f_w(r,\theta,t)\,{}_c\phi^d_{nm}(r,\theta)\,r\,dr\,d\theta \tag{5.7}$$

$${}_s\ddot{q}_{nm} +_s \omega^2_{nm} \cdot_s q_{nm} = \int_b^a\int_0^{2\pi} f_w(r,\theta,t)\,{}_s\phi^d_{nm}(r,\theta)\,r\,dr\,d\theta \tag{5.8}$$

$$\ddot{g_j} + \omega_j^2 \cdot g_j = \int_0^l f_u(x,t)\phi^a_j(x)dx \tag{5.9}$$

$$\ddot{p_j} + \omega_j^2 \cdot p_j = \int_0^l f_v(x,t)\phi^t_j(x)dx \tag{5.10}$$

Considering that the pin is placed in contact with the disc, so that its axis makes an angle α with the normal of the disc surface, friction forces expressed in the equations above have the form

$$f_w(r,\theta,t) = -P \tag{5.11}$$
$$f_u(x,t) = P(\mu \sin\alpha - \cos\alpha) \tag{5.12}$$
$$f_v(x,t) = P(\mu \cos\alpha + \sin\alpha) \tag{5.13}$$

In the point of contact, (r_0, θ_0) for the disc and $(x = l)$ for the pin, it is assumed that the two bodies are always in contact. This implies a continuity of displacements at the point of contact as

$$-w(r_0,\theta_0,t) = u(l,t)\cos\alpha - v(l,t)\sin\alpha \tag{5.14}$$

These formulism gives rise to the equation of motion of the combined system in the form

$$[M]\ddot{z} + [K]z = 0 \tag{5.15}$$

where $[K]$ is non symmetric. Assuming that $z = Z\exp^{\lambda t}$, where Z is the complex eigenvector and λ the complex eigenvalue, the authors would, then, study the stability of the pin-on-disc system by investigating the real part of λ.

5.2 Brake squeal as a moving-load problem

One interesting approach to tackle disc brake squeal problem is by the moving-load concept. This concept has been used to address systems where a stationary disc is excited by a rotating load, such as in computer discs. In the following, we present some theoretical developments to investigate dynamic instability of circular plates subjected to moving-loads.

In a disc brake system, the disc rotates past the stationary pads and, as a result, the pads make contact with different areas of the disc as it rotates and vibrates. Since, generally, squeal occurs at low speeds, the relative motion is usually neglected. However, on one hand, we have already seen that rotation effects influence the stability of the system. The parametric studies performed using the moving-load concept confirmed the importance of the relative motion between the disc and the pads on the stability of the system.

For a tutorial on vibrations due to moving loads, [Ouyang, 2003] and [Ouyang, 2011] are referred.

In order to investigate parametric resonances in disc brakes, by a multiple scales analysis, an elastic system that was rotated around an annular disc with friction was developed [Ouyang et al., 1998]. The system consisted in a point mass, a stationary annular disc and two spring-dashpots (one in the in-plane or circumferential direction and one in the transverse direction). The in-plane spring-damper system drives the m-k-c system around the disc at a radius r_0 with friction having a negative slope with velocity (fig. 5.1). It is assumed that the point mass always remains in contact with the disc and constant velocity is applied at one end of the in-plane spring-damper system as shown in the fig. 5.1.

It is a well known fact that when a mass is driven across a dry surface and if the velocity is very low, stick-slip motion may occur. To eliminate non-linearities related to

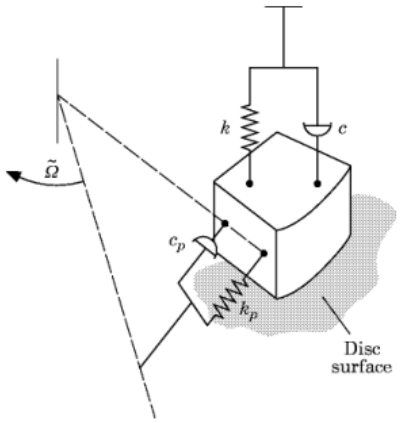

Figure 5.1: Lumped system driven by a spring-damper system in frictional contact with a stationary disc

stick-slip motion, it is assumed a high enough speed, so that no sticking phase occurs. Friction force is modeled as

$$F_\theta = \tilde{F}_\theta \left[1 - \alpha(\dot{\phi} + \tilde{\Omega})\right] \tag{5.16}$$

where, $\tilde{\Omega}$ is the angular velocity at the driven end of the in-plane spring-damper system, $\dot{\phi}$ is the velocity of the mass relative to the driving speed, $\tilde{F}_\theta$ is the product of normal force with static coefficient of friction, α defines the slope of friction-velocity characteristic. So the velocity of the mass is $(\dot{\phi} + \tilde{\Omega})$. F_θ is considered to act as a follower force, thus there is a coupling of the transverse an in-plane motions.

Equations of motion for the in-plane and transverse vibration of the system are defined by the authors, respectively, as

$$r_0(m\ddot{\phi} + c_p\dot{\phi} + k_p\phi) = -F_\theta = -\tilde{F}_\theta \left[1 - \alpha(\dot{\phi} + \tilde{\Omega})\right] \tag{5.17}$$

and

$$\begin{aligned} \rho h\frac{\partial^2 w}{\partial t^2} + D^*\nabla^4\frac{\partial w}{\partial t}/ + D\nabla^4 w = &-\frac{1}{r}\delta(r - r_0)\delta(\theta - \phi - \tilde{\Omega}t) \\ &\times m\left[\ddot{\phi}\frac{\partial w}{\partial t} + (\dot{\phi} + \tilde{\Omega})^2\frac{\partial^2 w}{\partial t^2} + 2(\dot{\phi} + \tilde{\Omega})\partial^2 w/\partial\theta\partial t + \partial^2 w/\partial t^2\right] \\ &+ c\left[(\dot{\phi} + \tilde{\Omega})\frac{\partial w}{\partial\theta} + \frac{\partial w}{\partial t}\right] + kw - \tilde{F}_\theta\left[1 - \alpha(\dot{\phi} + \tilde{\Omega})\right]\frac{\partial w}{r\partial\theta} \end{aligned} \tag{5.18}$$

where, ρ, h, D and D^* are the density, thickness, flexural rigidity and flexural damping of the disc, respectively. Displacement w of the disc is identically the transverse displacement of the mass at the point indicated by the Dirac delta functions. Equations (5.17) and (5.18) show that there is a "one-way" coupling between the in-plane and transverse motions.

A similar study was conducted one year later [Ouyang et al., 1999], but considering stick-slip motion. The most interesting work in modeling the brake system as a moving-load problem appears in [Ouyang and Mottershead, 2004], where the instability of the transverse vibration of a disc under two co-rotating sliders, modelled as a mass-spring-damper systems, was investigated (fig. 5.3).

The sliders are treated as moving loads and friction forces acting on both sides of disc, at the contact interface, produce a bending couple in the circumferential direction.

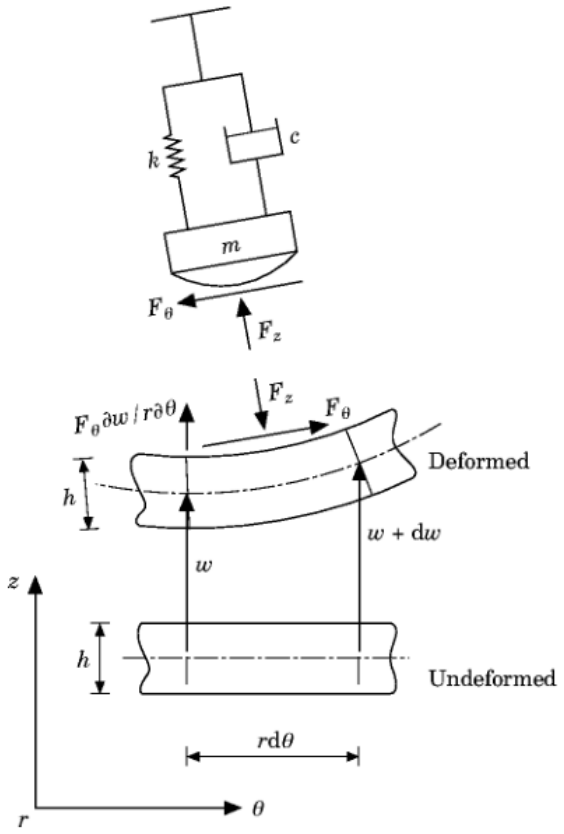

Figure 5.2: Friction forces at contact interface are included as follower forces and as a friction couple. From [Ouyang et al., 1998]

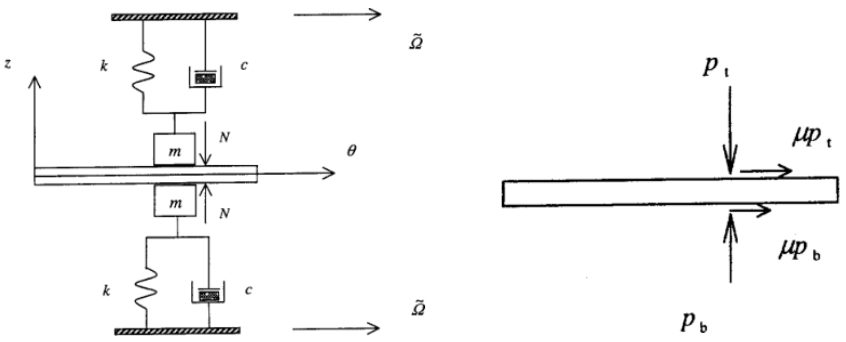

(a) Moving load mechanical model (b) Friction couple

Figure 5.3: Disc brake model investigated in [Ouyang and Mottershead, 2004]

By considering the transverse vibration of the disc, normal forces vary with time, and consequently, so does the bending couple too (fig. 5.3b).

Assuming that the disc and the two sliders are always in contact, as the disc vibrates, the sliders move in the transverse direction. Normal forces acting on the disc are

$$p_t = N + m\ddot{u} + c\dot{u} + ku \tag{5.19}$$

$$p_b = N - m\ddot{u} - c\dot{u} - ku \tag{5.20}$$

and considering Coulomb's friction law, tangential forces are defined as

$$f_t = \mu p_t = \mu(N + m\ddot{u} + c\dot{u} + ku) \tag{5.21}$$

$$f_b = \mu p_b = \mu(N - m\ddot{u} - c\dot{u} - ku) \tag{5.22}$$

As stated before, initially, the tangential forces expressed by the equations (5.21) and (5.22) are equal in magnitude, but as disc transverse vibration initiates, they fluctuate, thus becoming uneven, and consequently, they produce a bending couple at the mid-plane of the disc. From fig. 5.3b, the bending moment is

$$M = \frac{h(f_t - f_b)}{2} = \frac{\mu h(p_t - p_b)}{2} = \mu h(m\ddot{u} + c\dot{u} + ku) \tag{5.23}$$

From figure 5.2, considering the deformed shape of the disc as it vibrates, tangential friction force is included as a follower forces. Equation of motion, describing a circular thin plate excited by concentrated moving loads at location defined by the Dirac δ functions, are presented by the authors as

$$\begin{aligned}
\rho h\frac{\partial^2 w}{\partial t^2} + D^*\frac{\partial w}{\partial t} + D\nabla^4 w = \frac{1}{r}\Bigg\{&\left[p_b - p_t + \mu(p_b + p_t)\frac{\partial w}{r\partial\theta}\right]\delta(r - r_0)\delta(\theta - \tilde{\Omega}t) \\
&+ \frac{\partial}{r\partial\theta}[M(t)\delta(\theta - \tilde{\Omega}t)]\delta(r - r_0)\Bigg\} \\
= \frac{1}{r}\Bigg\{&\left[p_b - p_t + 2\mu N\frac{\partial w}{r\partial\theta}\right]\delta(r - r_0)\delta(\theta - \tilde{\Omega}t) \\
&+ \frac{\partial}{r\partial\theta}[M(t)\delta(\theta - \tilde{\Omega}t)]\delta(r - r_0)\Bigg\}
\end{aligned} \tag{5.24}$$

It is pointed out the term $2\mu N\frac{\partial w}{r\partial\theta}$ in eq. 5.24 represents the in-plane friction as a follower force. The displacement of the disc is expressed as the sum of its vibration modes as

$$w(r, \theta, t) = \sum_{m=0}^{\infty}\sum_{n=-\infty}^{\infty}\psi_{mn}(r, \theta)q_{mn}(t) \tag{5.25}$$

where $\psi_{mn}(r, \theta)$ are the mode shapes, not necessarily described by the Bessel functions, but that satisfy the ortho-normality properties. The authors further development allowed to derive the equation of motion in modal coordinates. Non dimensional variables and a scaling parameter were then introduced and the equation of motion was solved numerically by the state-space method.

A parametric study to predict regions of instability, was then conducted involving 5 variables, related to the mass, stiffness, damping, velocity and friction coefficient. One of

the interesting results they achieved was that the inclusion of friction as a follower force, in the model presented, was able to produce speed-dependent instabilities over a wide range of parameter values. Because of that, the authors claim that disc brake vibration should be modeled as a moving-load problem.

Based on a moving-load problem, a combined analytical and numerical approach was adopted to perform a linear eigenvalue analysis to address the stability of the disc brake system [Cao et al., 2004]. The disc was modelled as a thin annular plate with axial symmetry and the stationary components were modelled by FE. They were interested on addressing the problem at the low frequency squeal, the first in-plane squeal frequency of the disc brake system. By focusing on the range between 1 kHz to the low frequency squeal, in-plane motion was omitted from the analysis. Friction forces were included so that their action in the top and bottom surfaces of the disc would produce a bending friction couple in mid-plane of the disc.

To construct the assembled dynamic model, displacement continuity at the contact interface nodes of the stationary components were imposed to be equal to the transverse displacements of the plate. Stability analysis by means of CEA was performed and noise index, defined as $\alpha = \frac{\sigma}{\sqrt{\sigma^2+\omega^2}}$, was calculated and plotted for the unstable frequencies. Ultimately they found that unstable frequencies and noise indices are speed-dependent confirming that moving-loads consideration affects the degree of instability.

5.3 Analytical approach for development of a reduced-order model

As reported in the section 4.3, an analytical approach was used to derive a reduced-order model containing a single doublet mode pair [Kang et al., 2008]. Later, a detailed analysis on the stability of disc brake vibrations, by the Routh-Hurwitz criterion was reported [Kang et al., 2009b], in which the model accounted for gyroscopic and negative friction

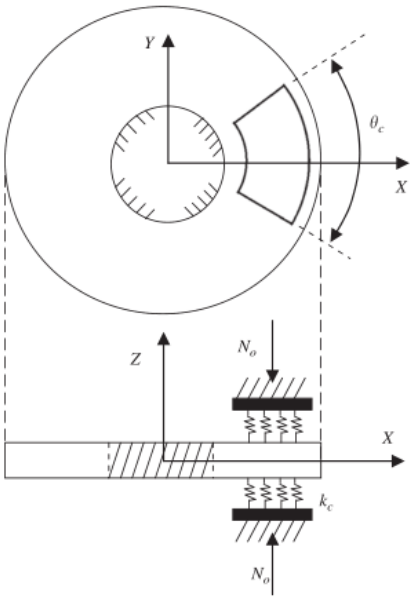

Figure 5.4: Analytical model for the frictional contact between an annular plate and two annular sector plates

slope effects. Mode-coupling behaviour was then studied by using the reduced-order model.

In their first study they developed a simplified mathematical model based on a physical disc brake system studied before in [Vanderlugt, 2004].

For the model development, it was considered an annular plate in frictional contact over a finite contact area with two annular sector plates in steady sliding conditions (fig. 5.4). It will be seen that the contact area has influence on squeal propensity.

It was assumed that the rotation speed is near the critical speed, (gyroscopic destabilizing effects and radial dissipative effect cancel out), so rotational effects were not considered. Also assuming that the contact stiffness term is much larger than pre-stress term, the effect of frictional follower force was also neglected.

Equation of motion for the transverse displacement is then written as,

$$D\nabla^4 w + \rho h \frac{\partial^2 w}{\partial t^2} = 0 \tag{5.26}$$

where

$$\nabla^4 = \nabla^2\nabla^2 = (\nabla^2)^2 = \left(\frac{\partial^2}{\partial r^2} + \frac{1}{r}\frac{\partial}{\partial r} + \frac{1}{r^2}\frac{\partial^2}{\partial \theta^2}\right)^2 \qquad D = \frac{Eh^2}{12(1-\nu^2)} \tag{5.27}$$

Transverse displacement is expressed in truncated modal expansion

$$w(r,\theta,t) \cong \sum_{n=1}^{N/2} R_n(r)\cos(n\theta)q_{2n-1}(t) + \sin(n\theta)q_{2n}(t) \tag{5.28}$$

$$\equiv \sum_{j=1}^{N} \phi_j(r,\theta)q_j(t) \tag{5.29}$$

where $R_n(r) = A_n J_n(\beta r) + B_n Y_n(\beta r) + C_n I_n(\beta r) + D_n K_n(\beta r)$. J_n and Y_n are Bessel functions of first and second order, I_n and K_n are modified Bessel functions of first and second order, A_n, B_n, C_n, D_n are constant coefficients to be determined from the boundary conditions.

The disc is modelled as an annular plate, clamped at the inner radius (r_i) and free at the outer radius (r_o), thus meaning, that at r_i the deflection and the slope of deflection must be equal to zero and, at r_o, the moment and shear force must be zero. From [Ouyang et al., 2000] the four boundary conditions are imposed. At $r = r_i$

$$W(r,\theta) = 0 \qquad \frac{\partial W(r,\theta)}{\partial r} = 0 \tag{5.30}$$

and at $r = r_o$

$$M_r = -D\left[\frac{\partial^2 w}{\partial r^2} + \nu(\frac{1}{r}\frac{\partial w}{\partial r} + \frac{1}{r^2}\frac{\partial^2 w}{\partial \theta^2})\right] = 0 \qquad V_r = Q_r + \frac{1}{r}\frac{\partial M_{r\theta}}{\partial \theta} = 0 \tag{5.31}$$

gives place to a set of algebraic equations with constant coefficients whose determinant, that must equal zero, constitutes the characteristic equation for the determination of natural frequencies.

$$\begin{bmatrix} J_n(\beta r_i) & Y_n(\beta r_i) & I_n(\beta r_i) & K_n(\beta r_i) \\ (p_n J_n - J_{n+1})(\beta r_i) & (p_n Y_n - Y_{n+1})(\beta r_i) & (p_n I_n + I_{n+1})(\beta r_i) & (p_n K_n - K_{n+1})(\beta r_i) \\ (t_n+1)J_n + s_n J_{n+1}(\beta r_o) & (t_n+1)Y_n + s_n Y_{n+1}(\beta r_o) & (t_n+1)I_n - s_n I_{n+1}(\beta r_o) & (t_n+1)K_n + s_n K_{n+1}(\beta r_o) \\ p_n(t_n+1)J_n - (np_n s_n - 1)J_{n+1}(\beta r_o) & p_n(t_n+1)Y_n - (np_n s_n - 1)Y_{n+1}(\beta r_o) & p_n(t_n-1)I_n + (np_n s_n - 1)I_{n+1}(\beta r_o) & p_n(t_n-1)K_n - (np_n s_n - 1)K_{n+1}(\beta r_o) \end{bmatrix} \begin{Bmatrix} A_n \\ B_n \\ C_n \\ D_n \end{Bmatrix} = \begin{Bmatrix} 0 \\ 0 \\ 0 \\ 0 \end{Bmatrix} \tag{5.32}$$

where

$$p_n(\beta r) = \frac{n}{\beta r} \tag{5.33}$$

$$s_n(\beta r) = \frac{1-\nu}{\beta r} \tag{5.34}$$

$$t_n(\beta r) = \frac{n(n-1)(1-\nu)}{(\beta r)^2} \tag{5.35}$$

and β is defined according to [Leissa, 1969], that for an annular plate with boundary conditions similar to the problem in hands is

$$\beta^2 = \omega r_o^2 \sqrt{\rho/D} \tag{5.36}$$

Hydraulic brake pressure is applied on both sides of the disc depending on the brake system configuration. If the subsystem comprehends double-sided pistons, then brake pressure is applied symmetrically on both sides, but if it is considered a floating-caliper configuration, then the caliper moves from side to side as the pressure is applied.

In their work, it was assumed that brake pressure applied at the bottom and top of the disc is identical and uniformly distributed over the contact area. Forces applied at the disc in the contact interface are presented in fig. 5.5 and are defined as

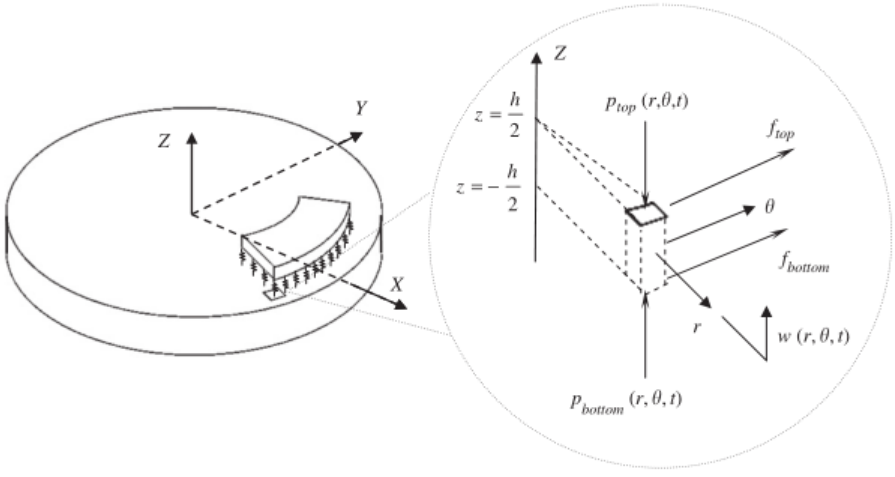

Figure 5.5: Applied forces at contact interface, from [Kang et al., 2008]

$$
\begin{aligned}
p_{top}(r,\theta,t) &= p_0 - k_c w(r,\theta,t) && (5.37)\\
p_{bottom}(r,\theta,t) &= p_0 - k_c w(r,\theta,t) && (5.38)\\
f_{top}(r,\theta,t) &= \mu p_{top} && (5.39)\\
f_{bottom}(r,\theta,t) &= \mu p_{bottom} && (5.40)
\end{aligned}
$$

where $p_0 = N_0/A_C$ is the pre-stress acting on both pads, N_0 is the pre-load and A_C is the contact area. k_c is the contact stiffness and μ is the friction coefficient, assumed to be constant over the contact area. p_{top} and p_{bottom} act on the transverse direction ($u_z = w$) of the disc and f_{top} and f_{bottom} act on the circumferential direction ($u_\theta = -h/2(\partial w/r\partial\theta)$).

Having the friction forces defined, the non-conservative virtual frictional work over the contact area was expressed as

$$
\begin{aligned}
\delta W_{Ac} = &\int_{-\theta_c}^{\theta_c}\int_{r_i}^{r_o}[-(p_0 + k_c w)\delta w - f_{top}\delta u_\theta]rdrd\theta \\
&+ \int_{-\theta_c}^{\theta_c}\int_{r_i}^{r_o}[-(p_0 - k_c w)\delta w - f_{bottom}(-\delta u_\theta)]rdrd\theta
\end{aligned} \tag{5.41}
$$

Equations of motion are then derived from the Assumed Modes Method. Making use of eq. (2.3) and Lagrange equation

$$
\frac{d}{dt}\left[\frac{\partial T}{\partial \dot{q}_i}\right] + \frac{\partial U}{\partial q_i} = \sum_{j=1}^{N} Q_{ij}(q_j) \tag{5.42}
$$

kinetic energy is defined as

$$
T = \frac{\rho h}{2}\int_0^{2\pi}\int_a^b \left[\frac{\partial w(r,\theta,t)}{\partial t}\right]^2 rdrd\theta \tag{5.43}
$$

Substituting equation (5.29) in the above equation with mass normalization, the kinetic energy is decomposed into each coordinate. By doing so, potential energy gives arise to the square of natural frequencies. Equation of motion of the system was then obtained in the matrix form

$$
\ddot{q} + ([\omega^2] + [A])q + [B]q = 0 \tag{5.44}
$$

where $[\omega^2]$ is the natural frequency matrix, $[A] = [A]^T$ is the stiffness contact matrix and $[B] \neq [B]^T$ is the non-symmetric non-conservative work matrix.

A reduced-order model based on the presented analytical approach was then developed. The model, that comprehends a single doublet mode, would later be used to derive a minimal model that has already been presented at chapter 4.

In a general way, for the nth doublet pair, linearized equations of motion have the form of eq. 5.44 where,

$$q = \{q_{2n-1}, q_{2n}\}^T \tag{5.45}$$

$$[\omega^2] = \begin{bmatrix} \omega_{2n-1}^2 & 0 \\ 0 & \omega_{2n}^2 \end{bmatrix} \tag{5.46}$$

$$[A] = k_c \tilde{R}_n^z \int_{-\theta_c}^{\theta_c} \begin{bmatrix} \cos^2(n\theta) & 0 \\ 0 & \sin^2(n\theta) \end{bmatrix} d\theta \tag{5.47}$$

$$[B] = \mu k_c n \tilde{R}_n^\theta \int_{-\theta_c}^{\theta_c} \begin{bmatrix} 0 & -\sin^2(n\theta) \\ \cos^2(n\theta) & 0 \end{bmatrix} d\theta \tag{5.48}$$

$$\tilde{R}_n^z = 2 \int_{r_i}^{r_0} R_n^2(r) r dr \tag{5.49}$$

$$\tilde{R}_n^\theta = -2 \int_{r_i}^{r_0} \frac{h}{2} R_n^2(r) r dr \tag{5.50}$$

Assuming a solution of the form $\{q(t)\} = \{C\} \exp^{\lambda t}$, and having $[H] = [\omega^2] + [A] + [B]$, the characteristic equation for the system is

$$|H + \lambda^2 I| = 0 \tag{5.51}$$

where λ are the eigenvalues. Due to the non-conservative nature of frictional force, eigenvalues may present a positive real part thus indicating an unstable equilibrium.

From eq. (5.51), an analytical expression was derived for the onset of instability having the friction coefficient as a control parameter.

$$\mu > \mu_{cr} = \frac{|\Omega_{2n-1}^2 - \Omega_{2n}^2|}{k_c |\tilde{R}_n^\theta| \sqrt{(n\theta_c)^2 - \sin^2(n\theta_c)}} \tag{5.52}$$

where Ω_{2n-1} and Ω_{2n} are the stiffness-coupled natural frequencies obtained from $[\omega^2]$ and $[A]$. It can be seen from eq. (5.52), that as the numerator (frequency separation) becomes smaller, μ_{cr} becomes smaller, thus increasing squeal propensity. Insight about the relation between the critical friction coefficient and frequency separation reported in previous works was then explained analytically.

The mathematical model was developed for a rotation speed assumed to be near the critical one, so that gyroscopic and radial dissipative effects would cancel out. In the later study, the same approach was employed but, this time, considering the rotation effects [Kang et al., 2009a].

To develop the model including rotation effect, contact kinematics were defined and a linearized contact model was applied. Friction was included such that friction-speed had the following relationship

$$\mu = \mu_k + (\mu_s - \mu_k) \cdot \exp^{-\alpha |V_{a'} - V_{c'}|} \tag{5.53}$$

where μ_k and μ_s are the kinetic and static friction coefficient, $V_{a'}$ and $V_{c'}$ are the velocity vectors of the disc at a' and of the stationary pad at c', respectively.

After defining friction forces, virtual work over the top and bottom contact areas was expressed as

$$\delta W_t op = \int_{\frac{\theta_c}{2}}^{\frac{\theta_c}{2}} \int_{r_i}^{r_o} \{(-N_1 - F_1) \cdot \delta u_{c'} + (N_1 + F_1) \cdot \delta u_{a'}\} \cdot r dr d\theta \tag{5.54}$$

where, $u_{a'}$ and $u_{c'}$ are the displacement vectors of the disc at point a' and of the pad at point c'. Contact strain energy was derived as

$$U_{c,top} = \int_{\frac{\theta_c}{2}}^{\frac{\theta_c}{2}} \int_{r_i}^{r_o} (u_{b'} \cdot e_z - u_{c'} \cdot e_z)^2 \cdot r dr d\theta \tag{5.55}$$

and the total virtual work and strain energy is obtained as

$$\delta W = \delta W_{top} + \delta W_{bottom} \tag{5.56}$$
$$U_c = U_{c,top} + U_{c,bottom} \tag{5.57}$$

The total kinetic energy of the system is the sum of the kinetic energies of the disc and both pads.

$$T = T_{top} + T_{disc} + T_{bottom} \tag{5.58}$$

where

$$T_{disc} = \frac{1}{2}\rho h \int_0^{2\pi} \int_{a_i}^{a_o} \left[\frac{\partial w(r,\theta,t)}{\partial t} + \Omega \frac{\partial w(r,\theta,t)}{\partial \theta}\right]^2 \cdot r dr d\theta \tag{5.59}$$
$$T_{top} = \frac{1}{2}\rho_p h_p \int_{\frac{\theta_c}{2}}^{\frac{\theta_c}{2}} \int_{r_i}^{r_o} \left[\frac{\partial w^{pt}(r,\theta,t)}{\partial t}\right]^2 \cdot r dr d\theta \tag{5.60}$$
$$T_{bottom} = \frac{1}{2}\rho_p h_p \int_{\frac{\theta_c}{2}}^{\frac{\theta_c}{2}} \int_{r_i}^{r_o} \left[\frac{\partial w^{pb}(r,\theta,t)}{\partial t}\right]^2 \cdot r dr d\theta \tag{5.61}$$

where, a_i and a_o denote the inner and outer radius of the disc, r_i and r_o the inner and outer radius of the pads and w^{pt} and w^{bt} are, respectively, the transverse displacements of the top and bottom pad which are found by the Rayleigh-Ritz method.

As a result, transverse displacements are written in modal expansion as

$$w(r,\theta,t) = \sum_{n=1}^{N_d} R_n(r)\{\cos(n\theta) \cdot q_{2n-1}(t) + \sin(n\theta) \cdot q_{2n}(t)\} \tag{5.62}$$
$$w^{tp}(r,\theta,t) = \sum_{k=1}^{N_p} W_k(r,\theta) \cdot q_k^{tp}(t) \tag{5.63}$$
$$w^{bp}(r,\theta,t) = \sum_{k=1}^{N_p} W_k(r,\theta) \cdot q_k^{bp}(t) \tag{5.64}$$

Substituting the set of equations (5.62)-(5.64) in equations (5.59)-(5.61), and taking in consideration the normalization relations, equation of motion is derived (4.48).

5.4 Summary and outlook

To investigate mode coupling instability, minimal models are useful, because in a concise and intuitive way, fundamental properties of modal interaction can be observed. However, in real brake systems several other destabilizing mechanisms can arise or play a simultaneous role.

There are several approaches to model disc brake squeal. To approach experimental investigations on pin-on-disc test rigs, analytical models have been provided for this kind of systems. To study theoretically squeal characteristics this seems to be the better approach, since is not time consuming like a FE model, with many degrees of freedom, but still is refined enough to give an insight on the multi-natural frequency nature of flexible components which is not possible from discrete models.

The analytical formulism for the beam-on-disc system used to study squeal characteristics was reported in [Tuchinda et al., 2001] and reproduced here. By computing the complex eigenvalues of the assembled modal model and presenting the locus plot, trajectory of the eigenvalues, with respect to the friction coefficient, was observed. They provided a good picture on two squeal characteristics, the mode lock-in and mode lock-out. By considering the vibration modes of the elastic bodies in contact, they showed how closed range frequencies could merge in the presence of friction. Numerically, they saw the merging of the 8^{th} nodal diameter mode of the disc with the 4^{th} transverse mode of the pin as the friction coefficient was increased. At a critical value, the two modes, which initially are purely imaginary, merge given birth to a pair of complex conjugate modes in which one is unstable.

For a distinct range of frequencies, the mode lock-out phenomena became evident. The modal interaction between the 2^{nd} transverse mode of the pin and the 3^{rd} nodal diameter mode was observed and it was seen that increasing the friction coefficient the modes approach each other until they merge at the first critical value. By further increasing the friction coefficient a second critical point was identified, at which the modes separated and instability stopped.

In the context of friction-induced vibrations, disc brake squeal has also been addressed by considering elastic systems rotating around stationary discs, which fits into the moving-load frame (a tutorial is provided in [Ouyang, 2011]) and introduces friction forces as a friction couple and frictional follower forces.

With this approach, they first studied stick-slip phenomena and effect of negative friction slope [Ouyang et al., 1997], [Ouyang et al., 1998]. They found that at very low speeds, the in-plane flexibility of the pad, which is modelled as an elastic system, leads to stick-slip vibrations that would couple with the transverse vibrations of the disc.

By considering the in-plane system (the elastic system that rotates around the surface of the disc in sliding friction), negative friction-velocity slope effects were deeply studied by a parametric study. It was seen that by introducing this feature, for same values of friction coefficients, existent resonances were modified and additional ones appeared. For the existent resonances, regions of instability reduced. The resonances initiated would occur for lower speeds.

The findings shown above were found assuming such a speed, that the stick phase would not occur. The same elastic system and disc arrangement was later used in which the static friction coefficient was assumed higher than the kinetic one, thus allowing for stick-slip motion [Ouyang et al., 1999]. The in-plane vibration of the slider system induces transverse vibration which change the normal forces on the disc, which, in turn, affect the in-plane oscillation of the slider. This fits into the feedback formulism presented in [Hoffmann and Gaul, 2003], where in-plane and out-of-plane equations were defined and it was seen that an out-of-plane displacement would lead to excitation on the in-plane equation and vice-versa.

Coupled equations of motion were written for both the sticking and the slipping phase and were numerically solved. They found that for higher values of normal pressure and rotating speed the vibrations become larger and unstable. Also, that including damping in

the transverse direction reduces the magnitude of the vibrations and has a stabilizing effect. Damping in the in-plane direction, although it would reduce the vibration amplitude, turned to be ineffective to stabilize unstable modes. Lastly, they found that the stiffness in the in-plane direction can have two sided effects, and has a critical value at which the system becomes unstable.

Later, modelling disc brake squeal problem by the moving-load concept, the transverse vibration of stationary disc excited by two co-rotating sliders was investigated [Ouyang and Mottershead, 2004]. Friction was included such that friction forces produce a bending couple at the midplane of the disc and follower force effects are included. Friction coefficient was assumed to be a linear function of the relative speed with a negative gradient. Their objective was to achieve regions of instability by parametrical analysis. They found that the size and location of the stability regions were dependent of the specific parameters of the system. Increasing damping of the sliders would contract regions of instability, for low damping values, instability may exist for a wide range of stiffness values. Lastly, they found that including friction as a friction couple and follower forces and assuming a negative friction slope, instability of the disc vibration would be speed-dependent, pointing out that disc rotational velocity should be considered and disc brake squeal should be modelled as a moving-load problem.

To determine and investigate the dynamic instability of the transverse vibration of annular plates, a simplified mathematical model inspired in a real, physical brake system was developed, assuming a finite contact area [Kang et al., 2008]. Assuming a solution for the vibration of the annular plate as a sum of vibration modes, equations of motion were developed in the modal basis. From the overall system, a single pair of doublet modes is extracted to create a reduced-order model allowing to study their modal interaction influenced by system parameters. They found that squeal propensity would be affected by the frequency separation of the doublet modes and by the modal contact strain energies and, that the contact span angle, that defines the contact area is parameter of increased importance. For zero frequency separation, it was seen that higher squeal propensity would occur for specific values of the contact span angle and for non-zero frequency separation, critical values were a function of the contact stiffness and frequency separation.

In their follow-up study, the reduced-order model was extended to comprehend gyroscopic and negative friction slope effects [Kang et al., 2009a]. The brake system included a disc clamped at the inner radius and subjected to a rotation with constant velocity and free at the outer edge. The disc, modelled as an annular plate, was assumed in contact with two annular sector plates over a finite contact area defined by a contact span angle and friction material was modelled by a linear contact stiffness parameter. After defining the contact kinematics of the system, by making use of a linearized contact model, equations of motion were derived by the Lagrange equations. Energies were defined, where the displacement of the disc and the pads were given by modal expansion. For the calculation of flexible modes of the pads, the Rayleigh-Ritz method was employed.

Equations of motion derived accounted for gyroscopic, radial dissipative and friction-slope damping terms, contact and pre-load stiffness terms (symmetric) and friction couple and follower force terms which would give rise to a non-symmetric stiffness matrix.

By the single-doublet model, using the Routh-Hurwitz criterion, they found how the gyroscopic effects influences the merging behaviour. This has already been discussed in the previous chapter.

So, various models of the disc brake squeal problem, based either on the moving-load concept or in physical disc brakes, have been presented and their qualitative results (regions of instability) are very similar. The main contribution provided in [Ouyang et al., 1998]

and [Ouyang et al., 1999] is that the in-plane vibration of the elastic system in contact with the disc, where negative friction slope effects and stick-slip motion are proeminent, should not be neglected because it can excite the transverse vibration of the disc.

We find that this conclusions fits well in the feedback frame provided earlier. By modelling the problem as a moving load, motion in the in-plane direction (stick-slip), would excite the transverse vibration and eventually the two motions would couple, establishing an energy flow between them and leading to self-excited vibrations.

The analytical formulism provided in [Kang et al., 2009b] allowed to incorporate a wide range of effects, however, we note that contrary to the investigations of Ouyang and others, stick-slip phenomena was not included which gives rise to further development. The single-doublet model approximation allowed to investigate the stability of the system in terms of binary-flutter and see how the mode merging scenario would be affected by these phenomena. The qualitative aspects of their conclusions were already discussed.

Chapter 6

Finite element analysis

To address disc brake squeal and, particularly, mode coupling instability type, the numerical work presented in [Hoffmann et al., 2002] and [Hoffmann and Gaul, 2003] was recreated and a finite element analysis approach using a commercial FE software was undertaken. To this end, finite element models of a pin-on-disc system and a simplified brake system were developed.

6.1 Methodologies

It has been seen that minimal models are useful to study mode coupling characteristics. In previous chapters, by reproducing previous work on the subject, the archetypic merging scenario, either considering or not the damping, in a proportional or non-proportional scheme, was reproduced. The distortion of the force vector field and the feedback formulism were also numerically reproduced.

By making use of the minimal model presented in [Hoffmann and Gaul, 2003] another picture of the merging scenario was produced. In their work, they make use of the Nyquist simplified criterion to derive necessary conditions for the onset of instability. However, the Nyquist plots are not presented in their work, so they are reproduced here.

To complement our investigation on the subject, several finite element analysis were carried out to find unstable vibration modes of the brake system. To model the brake system, two models were developed. The first constitutes the well known pin-on-disc system and the second represents a real, simplified brake system.

The main goal is to identify unstable vibration modes for the two models by examining the damping ratio of each mode, which is directly related to the real part of the complex eigenvalue. In order to do so, the components are firstly examined separately and their natural vibration modes are obtained. Then, the components are assembled, contact properties are defined and the operational conditions, namely, the applied pressure and rotational velocity of the disc are set. By the complex eigenvalue analysis, the complex modes are obtained and stability considerations can be derived.

To engage in such work we took [Nouby et al., 2009], [AbuBakar and Ouyang, 2006] and [Liu et al., 2007] as reference articles. In those papers, it is well described the problem formulation and the main steps necessary to perform the complex eigenvalue analysis in ABAQUS. According to articles mentioned above those are:

- nonlinear static analysis to apply the brake pressure;
- nonlinear static analysis to impose the rotational speed of the brake disc;
- natural frequency extraction;

- complex eigenvalue analysis.

The first two steps are required to create a sliding friction condition in the system. Since the complex eigenvalues are solved using the subspace projection method, natural modes are required to be calculated previously in order to determine the projection subspace. Governing equations of the system are given as

$$\mathbf{M}\ddot{x} + \mathbf{C}\dot{x} + \mathbf{K}x = 0 \tag{6.1}$$

where M is the mass matrix, C is the damping matrix which besides including material damping effects may also contemplate friction-induced contributions and K is the stiffness matrix, which is asymmetric due to friction effects. Equation 6.1 may be re-written in the form

$$(\lambda^2\mathbf{M} + \lambda\mathbf{C} + \mathbf{K})\Phi = 0 \tag{6.2}$$

where λ is the eigenvalue, Φ is the eigenvector and both may be complex. It has been already stated that complex eigenvalue extraction uses the subspace projection method, which means that eigenmodes of the undamped system with a symmetrized stiffness matrix may be first determined. Having the eigenvectors determined, mass, damping and stiffness matrixes are projected as

$$\hat{\mathbf{M}} = [\phi_1, ..., \phi_N]^T\mathbf{M}[\phi_1, ..., \phi_N] \tag{6.3}$$

$$\hat{\mathbf{C}} = [\phi_1, ..., \phi_N]^T\mathbf{C}[\phi_1, ..., \phi_N] \tag{6.4}$$

$$\hat{\mathbf{K}} = [\phi_1, ..., \phi_N]^T\mathbf{K}[\phi_1, ..., \phi_N] \tag{6.5}$$

By doing so, the eigenvalue problem is then expressed as

$$(\mu^2\hat{\mathbf{M}} + \mu\hat{\mathbf{C}} + \hat{\mathbf{K}})\Phi^* = 0 \tag{6.6}$$

The complex eigenvalue μ is expressed as $\mu = \alpha \pm \imath\omega$, where $\alpha = \Re(\mu)$ is the damping coefficient and $\omega = \Im(\mu)$ is the damped natural frequency. The damping ratio is then defined as $\xi = \frac{-2\alpha}{|\omega|}$. Having this in mind, if a determined eigenvalue possesses a positive real part ($\alpha > 0$), then the damping ratio is negative ($\xi < 0$), which is interpreted as an absorption of energy instead of its dissipation. This means that the vibration mode is unstable.

Bearing this, we took the damping ratio as an indicator of stability and performed a systematic analysis to evaluate the influence of the operational parameters on squeal propensity, namely the applied brake pressure and the friction coefficient.

For the pin-on-disc system, the components were first examined separately. Natural vibration modes of the disc were compared with the set of analytical results presented in [Leissa, 1969]. For the annular plate clamped at the inner radius and free at the outer edge those results are presented in table 6.1, where n is the diametral nodes and the solutions are expressed in the form

$$\lambda^2 = \omega r_o^2\sqrt{\rho/D} \tag{6.7}$$

where, $D = \frac{Eh^3}{12(1-\nu^2)}$. For comparison we took the radii ratio of 0.2.

Having the pin-on-disc model assembled the analysis was performed for several values of operational parameters. Regarding mode coupling, it was seen in previous chapters that the friction coefficient plays an important role, since it was identified two critical points that induce the mode lock-in and mode lock-out. Bearing this, friction coefficient values used were 0.4, 0.5 and 0.9, because, as it will be seen later, the finite element model comprehends a steel on steel contact. Besides varying the friction coefficient, the influence of the applied pressure in the damping ratio was also investigated. For this purpose, reference values of several papers were used and are 0.5 MPa, 0.9 MPa and 1.3 MPa. Rotational velocity was set to π rad/s.

Table 6.1: Analytical solutions of the eigenvalue problem for the free, clamped annular plate

n	m	$\frac{r_i}{r_o} = 0.2$
0	0	5.244
1	0	4.814
2	0	6.345

6.2 Finite Element Models

6.2.1 Pin-on-disc system

The pin-on-disc model proposed comprehends a beam clamped at one side, but free to move on the direction normal to the disc surface, and in contact with the disc at the other. The disc is clamped at its inner radius and free at the outer edge. The mechanical properties used to model the system are presented in table 6.3. These were used for both the pin and the disc. Geometrical parameters of the system are presented at table 6.2.

There are several approaches in ABAQUS to define the contact interaction between bodies. To this system a general contact interaction was used and it is defined by specifying the surfaces that interact with one another and the mechanical contact property model which includes the frictional behaviour between the components. The Coulomb friction model was used with friction coefficient values mentioned previously with a Lagrange multiplier method.

According to ABAQUS user's guide, general contact always uses the finite-sliding, as the contact tracking approach, and surface-to-surface contact discretization.

The FE mesh is generated using three-dimensional hexahedral elements for the pin (C3D20R) and three-dimensional tetrahedron elements for the disc (C3D10).

The model obtained is presented in figure 6.1.

6.2.2 Simplified brake system

Although modelling the disc brake as a flat annular plate provides a simple manner to approach the problem analytically, real brake systems are not flat. Since that there is heat

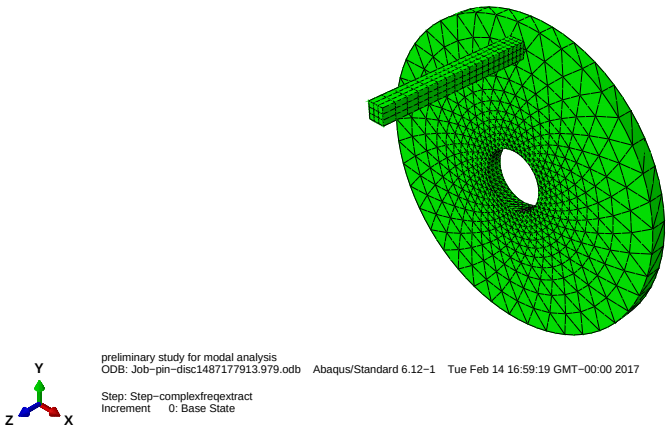

Figure 6.1: FE model of the pin-on-disc system

Table 6.2: Geometrical parameters for the pin-on-disc model

Parameter	Symbol	Value	Units
Inner radius of the disc	r_i	20	$[mm]$
Outer radius of the disc	r_o	100	$[mm]$
Thickness of the disc	h_d	10	$[mm]$
Length of the pin	l	100	$[mm]$
Cross section area of the pin	A	10×10	$[mm^2]$

Table 6.3: Mechanical properties of the pin-on-disc model

Parameter	Symbol	Value	Units
Young's moduli	E	210	$[GPa]$
Poisson coefficient	ν	0.3	$[/]$
Density	ρ	7800	$[kg/m^3]$

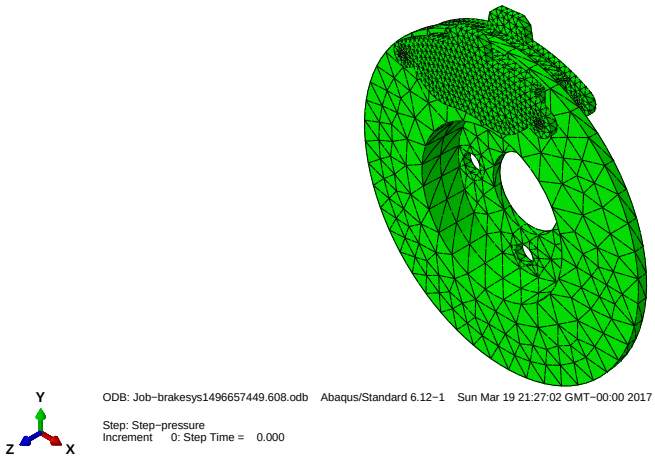

Figure 6.2: Simplified model of a real brake system

generation at the friction interface, real disc brakes have a top hat to set apart the friction interface from the wheel shaft thus avoiding its heating.

A simplified model of a real brake system, consisting of only the disc and the brake pads, was also investigated. For simplicity, both components were modelled as steel, although the friction material of the brake pads has an anisotropic behaviour. Mechanical properties used are the same of those presented in table 6.3. A side view of the disc is presented in fig. 6.3. The brake pads are allowed to move only in the normal direction to the disc surface and are subject to the brake pressure of 1 *MPa*. Although the pressure is applied in a circumferential area, owing to the shape of the brake piston, in the model, the area is extended to the entire exterior surface of the brake pads, for simplicity of the analysis.

The brake rotor is constrained at the bolt holes and rotates about its axis at π *rad/s*. In order to define the contact model, general contact type was used and already discussed in the previous section. Two surface pairs were selected. The contact property model used comprehended Coulomb's friction law with a friction coefficient of 0.375. Contact formulation used consisted on surface-to-surface in a finite-sliding scheme.

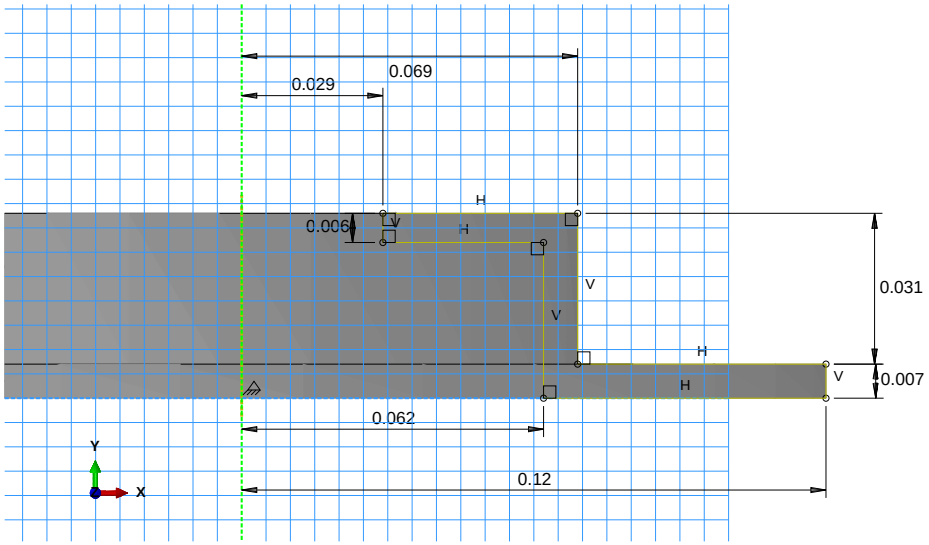

Figure 6.3: Side view of the rotor designed in ABAQUS (*units in meters*)

The FE mesh was generated using tetrahedron elements (C3D10) for all the components. The simplified FE model, that consists on a three-dimensional top hat disc and two brake pads, is presented in figure 6.2.

6.3 Numerical analysis

Besides reproducing numerically the results presented in [Hoffmann and Gaul, 2003], the Nyquist diagrams to infer about the stability of the system by the Nyquist criterion were plotted. In section 4.1, the feedback formulism developed by Hoffmann and co-workers to derive a necessary condition for the onset of instability was presented. According to them, self-excited vibration, and consequently, instability, would happen if the in-plane and out-of-plane displacements were in phase and the magnitude of the frequency response function, defined as the ratio between the output and input of the closed loop, would exceed unit magnitude.

From figures 6.4a, 6.4b and 6.4c, it is possible to observe that, for subcritical configurations, the input and output are not in phase, because $F = F_x F_z$ and $F_x = -F_x$. For marginally critical, the input and output are in phase, but the closed loop transfer function F does not surround the critical point $(-1, i0)$, which means, that there is no displacement amplification. For supercritical configurations $\mu > \mu_c$, this point is surrounded by the transfer function, which means that at a particular frequency, which they called the zero phase shift frequency, there is an amplification of the in-plane displacement leading to an unstable behaviour, characterized by the increasing in-plane vibration.

Table 6.4: Operational parameters used in the analysis of the simplified brake system

Parameter	Symbol	Value	Units
Applied pressure	P	1	[MPa]
Rotational velocity	Ω	π	[rad/s]
Friction coefficient	μ	0.375	[/]

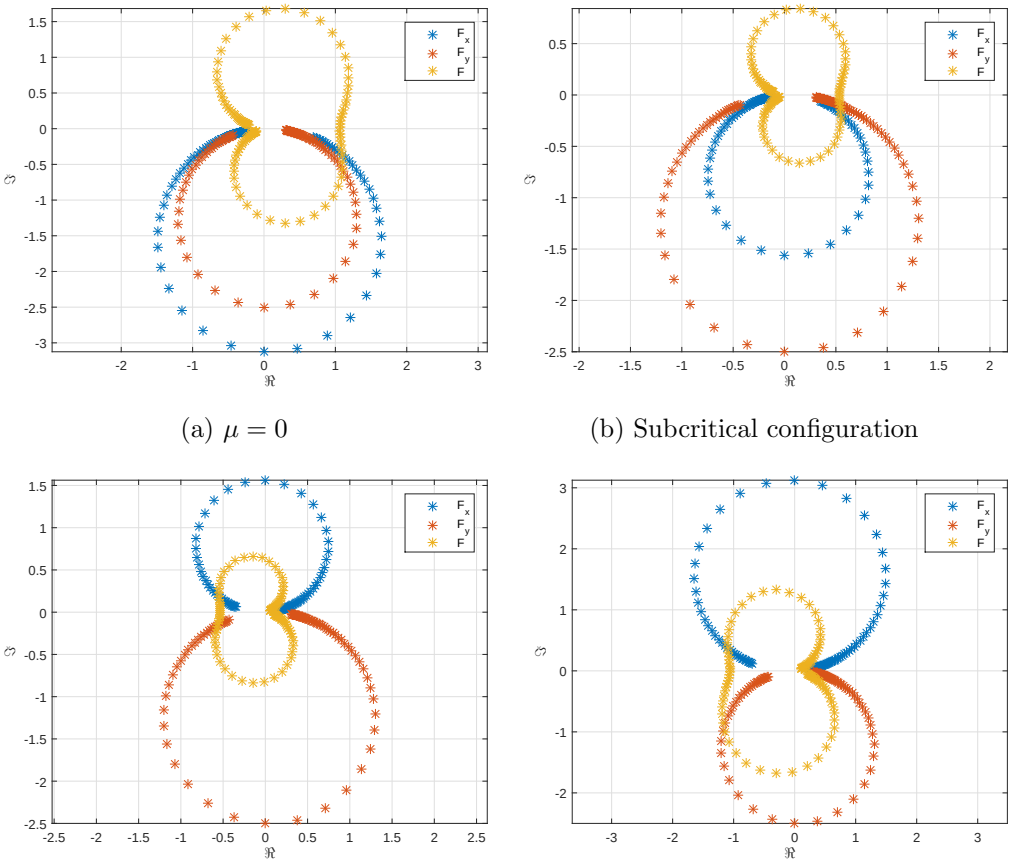

(a) $\mu = 0$

(b) Subcritical configuration

(c) Marginally critical configuration

(d) Supercritical configuration

Figure 6.4: Nyquist diagrams

6.4 Results and Discussion

6.4.1 Pin-on-disc system

As stated previously, the analysis started with the separate analysis of the components by extracting their vibration modes. Focusing on the disc, its natural frequencies and mode shapes are presented in table 6.5 and in fig. 6.5, respectively. From table 6.5 values from the 3 first columns were extracted to compare them with the analytical solutions of table 6.1 proposed in [Leissa, 1969]. In order to do so, after transforming frequency values into radians per second, they were introduced in equation 6.7 and error was calculated.

Examining table 6.6, values extracted from the FE software are in well accordance from the analytical results presented in [Leissa, 1969].

Natural vibration modes of the pin are presented in figure 6.6. Regarding the pin, it is noted the linearly dependent mode shapes of the transverse vibration due to the fact that

Table 6.5: Natural frequencies (Hz) of the flat disc

m,n	$0,0$	$0,\pm1$	$0,\pm2$	$0,\pm3$	$0,\pm4$	$0,\pm5$	$0,\pm6$	$0,\pm7$
ω_{mn}	1279.1	1165.7	1550.1	3055.5	5233.9	7887.8	10950	14374
		1165.7	1550.1	3055.5	5233.9	7887.9	10950	14374

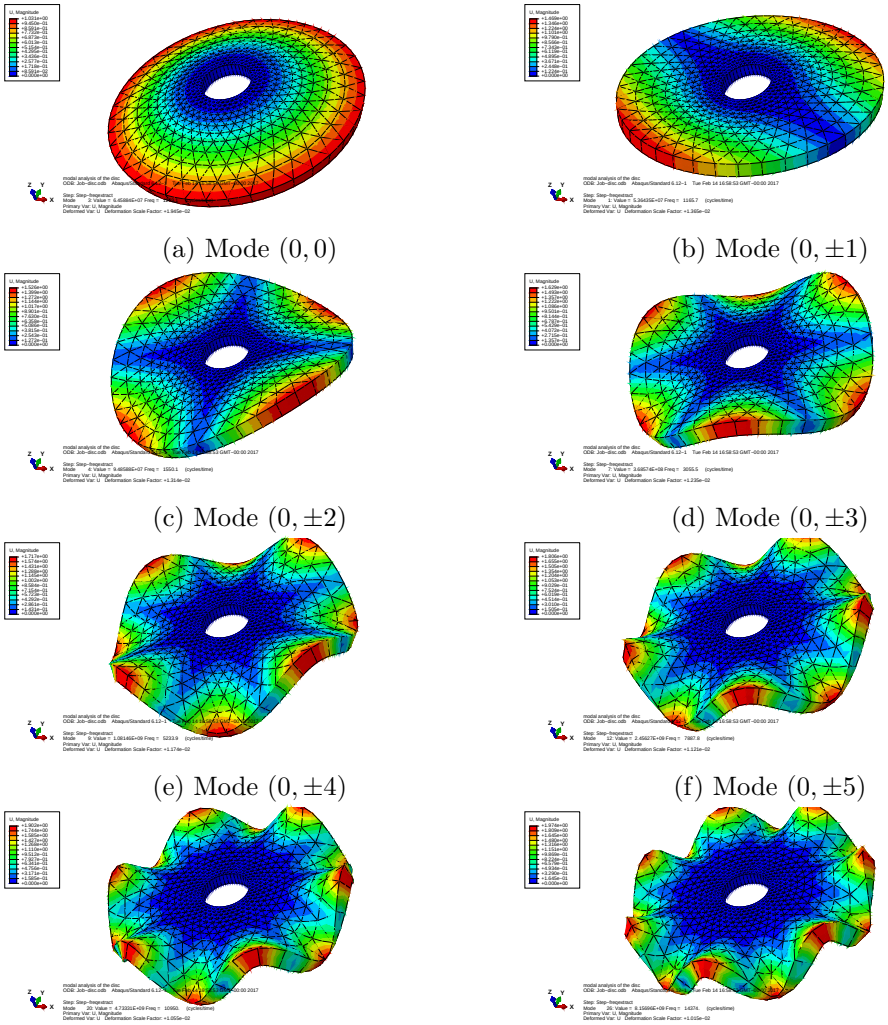

(a) Mode $(0, 0)$ (b) Mode $(0, \pm 1)$

(c) Mode $(0, \pm 2)$ (d) Mode $(0, \pm 3)$

(e) Mode $(0, \pm 4)$ (f) Mode $(0, \pm 5)$

(g) Mode $(0, \pm 6)$ (h) Mode $(0, \pm 7)$

Figure 6.5: Disc transverse vibration modes

Table 6.6: Comparison of natural frequencies extracted from Abaqus with analytical solutions from [Leissa, 1969]

Disc mode	Frequency (Hz)	Frequency (rad/s)	λ^2_{Leissa}	λ^2_{calc}	Error (%)
(0,0)	1279.1	8036.7	5.244	5.118	2.4
(0,±1)	1165.7	7324.2	4.814	4.665	3.1
(0,±2)	1550.1	9739.5	6.345	6.203	2.3

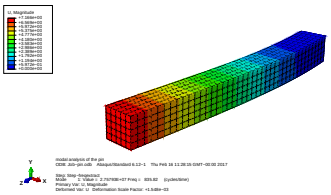

(a) 1^{st} mode at 835.82 Hz

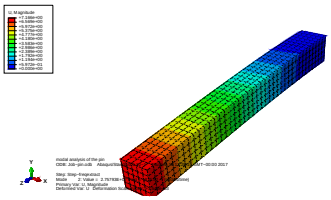

(b) 2^{nd} mode at 835.82 Hz

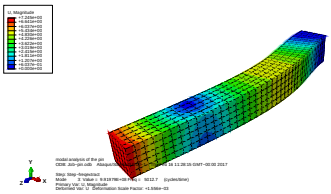

(c) 3^{rd} mode at 5012.7 Hz

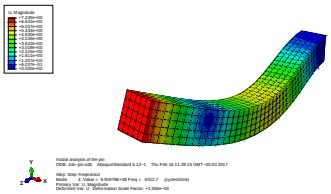

(d) 4^{th} mode at 5012.7 Hz

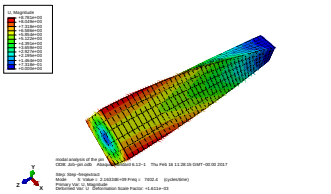

(e) 5^{th} mode at 7402.4 Hz

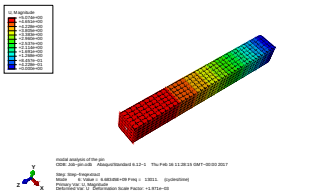

(f) 6^{th} mode at 13011 Hz

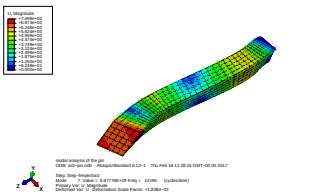

(g) 7^{th} mode at 13199 Hz

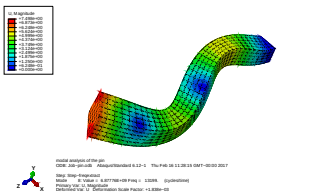

(h) 8^{th} mode at 13199 Hz

Figure 6.6: Pin vibration modes

the cross section of the pin is a perfect square.

After examining the components separately, they were assembled and the analysis procedure described in section 6.1 was undertaken. Considering that squeal noise happens for disc vibration modes whose frequencies lie in the range $[1 - 15]$ kHz, 32 complex modes were obtained. In that frequency range 16 complex modes involving transverse modes of the disc were identified and are presented in appendix 7.2. Also according to section 6.1, stability considerations are established by examining the modal damping ratio, which is directly related to the real part of the complex eigenvalues, for different operational parameters. The results achieved by performing the complex eigenvalue analysis are presented in the following.

Case A1: $P = 0.5$ **MPa,** $\mu = 0.4$

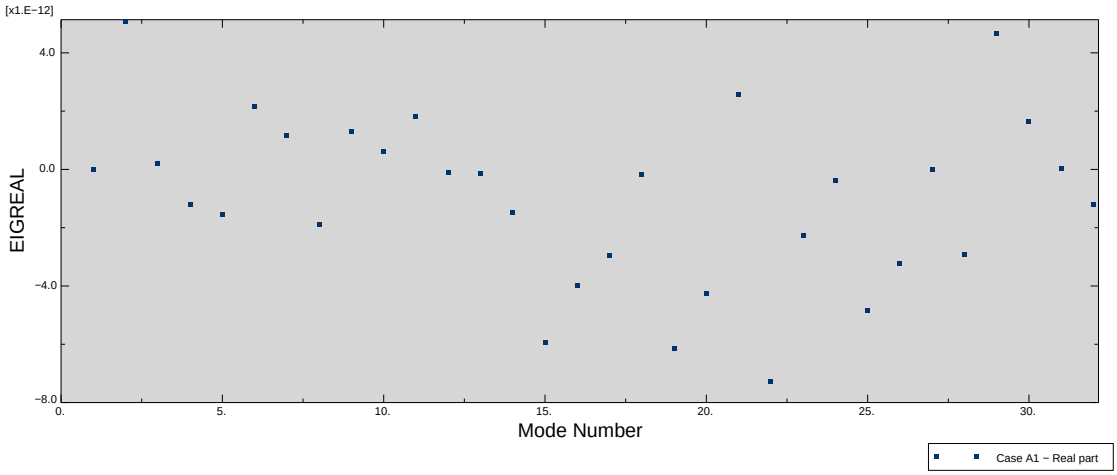

Figure 6.7: Real parts of the complex eigenvalues for mechanical case A1

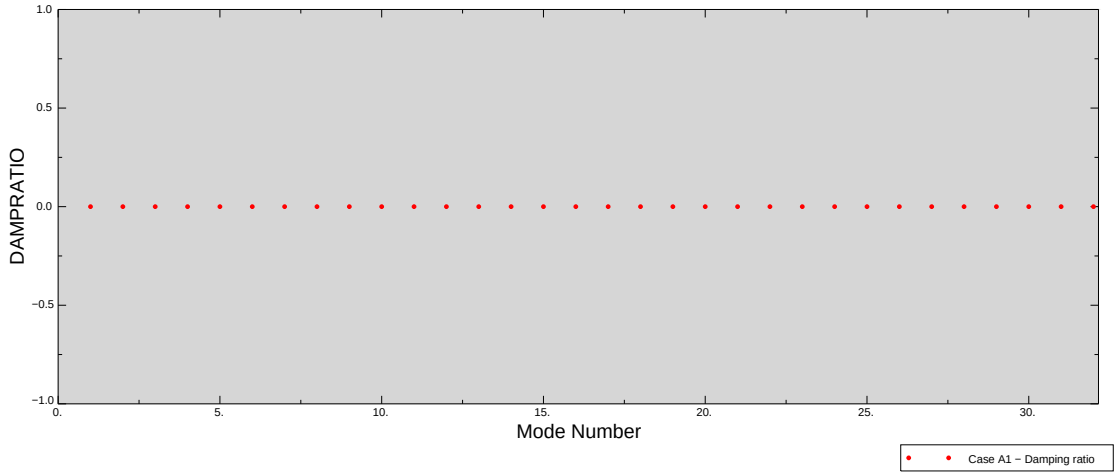

Figure 6.8: Modal damping ratios for mechanical case A1

According to the figure 6.8 the mechanical system analysed does not possess unstable modes. The friction coefficient used is lower than the static friction coefficient of steel-steel

contact and the pressure used is half of the usual applied. Regarding this, results are in accordance with the expectations.

Case A2: $P = 0.5$ **MPa,** $\mu = 0.5$

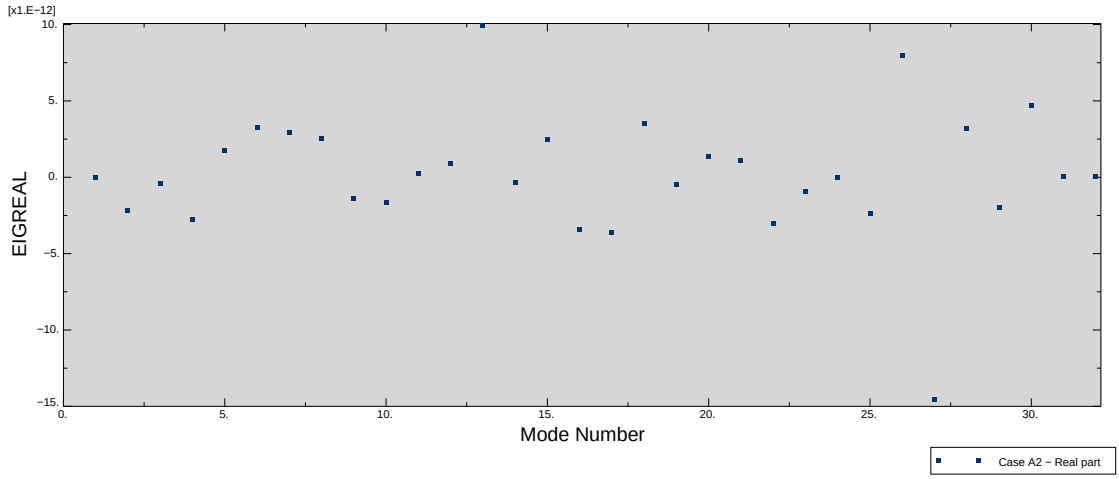

Figure 6.9: Real parts of the complex eigenvalues for mechanical case A2

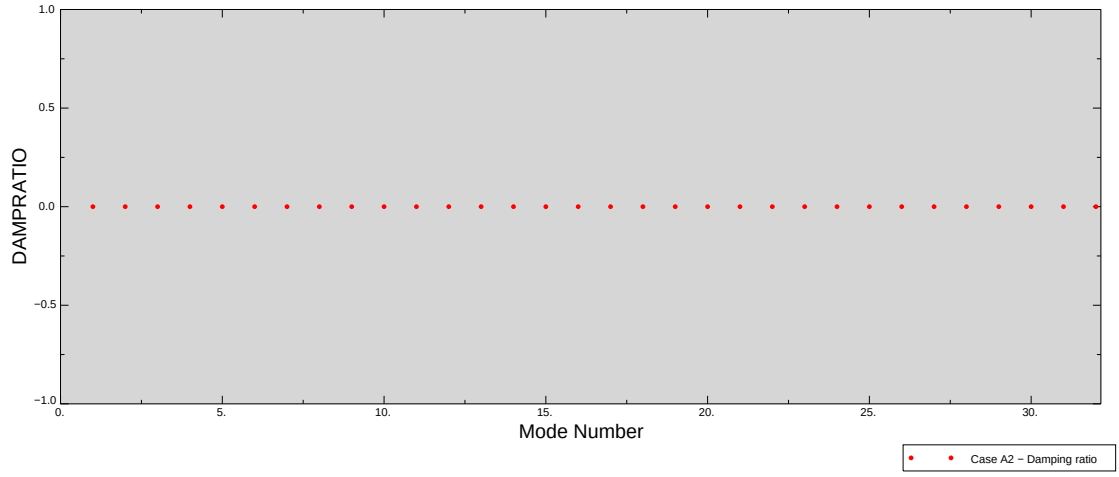

Figure 6.10: Modal damping ratios for mechanical case A2

In mechanical case A2, no unstable modes were identified (figure 6.10), although the friction coefficient was increased to a value in the range of the static friction coefficient of steel-steel contact.

Case A3: $P = 0.5$ **MPa,** $\mu = 0.9$

Results from case A3 were unexpected even considering the low braking pressure applied. The friction coefficient used should have produced unstable modes, however, from figure 6.12 those were not verified. The damping ratio is calculated from the magnitude of the complex eigenvalue real part. Looking at figure 6.11, magnitude of the real part of

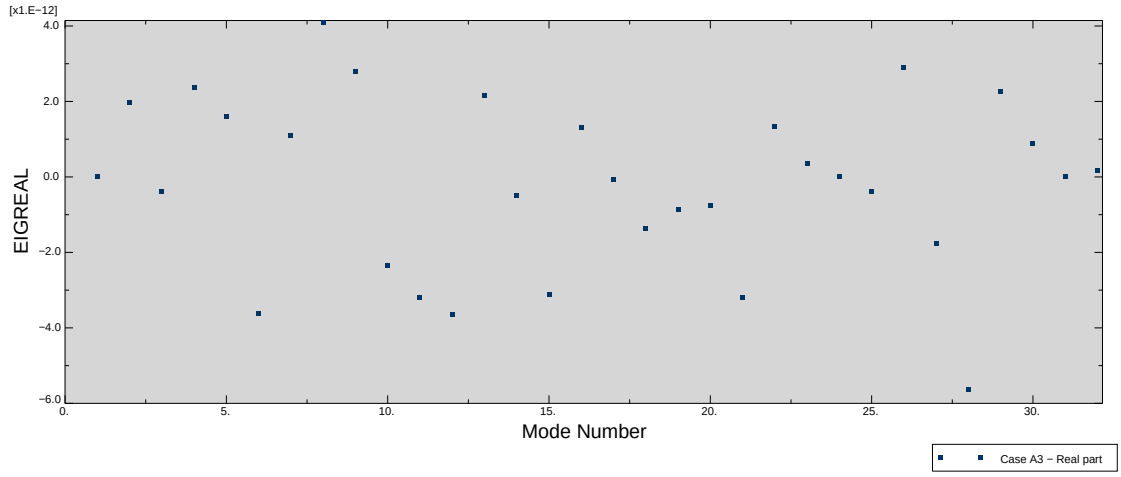

Figure 6.11: Real parts of the complex eigenvalues for mechanical case A3

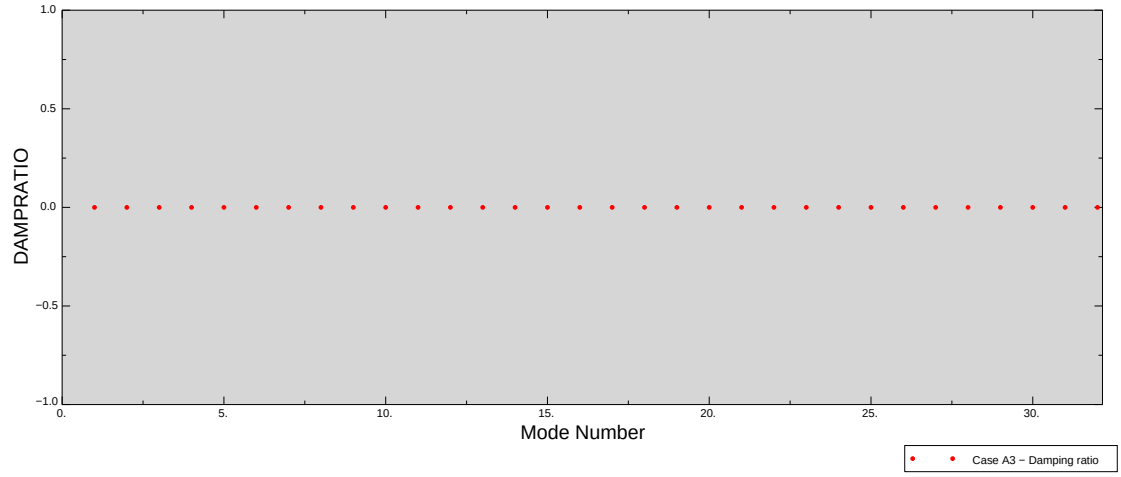

Figure 6.12: Modal damping ratios for mechanical case A3

all modes calculated are zero, when it should be expected values in the gross range of $[-1500;1500]$.

Case B1: $P = 0.9$ **MPa,** $\mu = 0.4$

Case B2: $P = 0.9$ **MPa,** $\mu = 0.5$

Case B3: $P = 0.9$ **MPa,** $\mu = 0.9$

Case C1: $P = 1.2$ **MPa,** $\mu = 0.4$

Case C2: $P = 1.2$ **MPa,** $\mu = 0.5$

Case C3: $P = 1.2$ **MPa,** $\mu = 0.9$

Cases B1 to C3 were developed to evaluate the influence of the applied pressure on the behaviour of complex eigenvalues and consequently, on the stability of the system. Such evaluation is made by examining the modal damping ratios in each case. For the cases mentioned above, the modal damping ratios are plotted in figure 6.13.

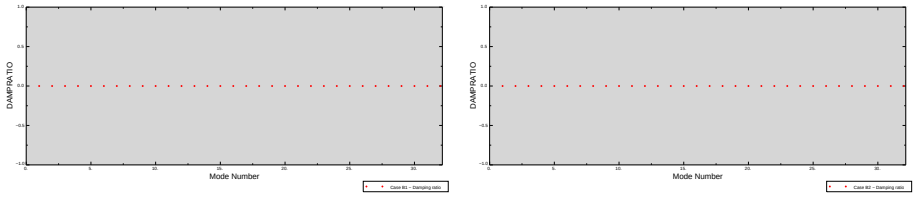

(a) Case B1: $P = 0.9$ MPa, $\mu = 0.4$

(b) Case B2: $P = 0.9$ MPa, $\mu = 0.5$

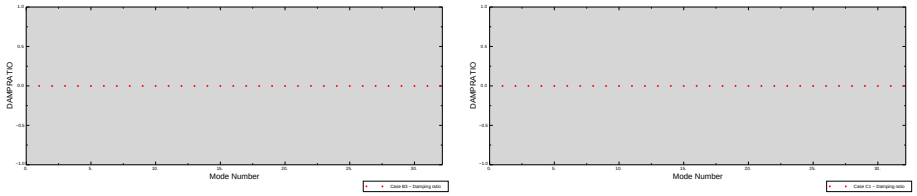

(c) Case B3: $P = 0.9$ MPa, $\mu = 0.9$

(d) Case C1: $P = 1.2$ MPa, $\mu = 0.4$

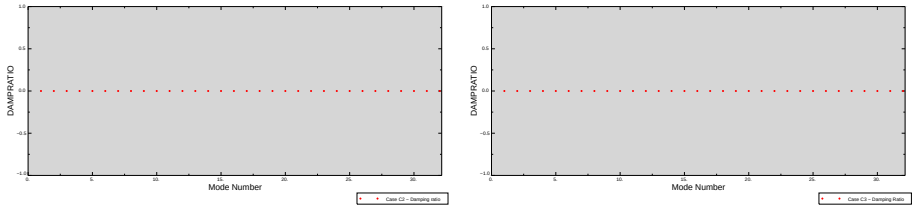

(e) Case C2: $P = 1.2$ MPa, $\mu = 0.5$

(f) Case C3: $P = 1.2$ MPa, $\mu = 0.9$

Figure 6.13: Modal damping ratios for the mechanical cases B1 to C3

From the results presented and regarding the objectives of the finite element analysis, one could conclude that, on one hand, the system investigated, in the conditions enunciated, does not possess unstable vibration modes and, considering disc brake squeal, noise would not be emitted by the sliding friction between the pin and the disc. On the other hand, pressure does not have influence in the stability of the system which is not true. Several papers previously referred had shown that an increase in braking pressure leads to an increase in the damping coefficient, though it has little influence.

Since that the friction coefficient used in cases B1 and C1 is low, regarding the steel on steel contact, no unstable modes are expected, even considering the increase on braking pressure. Increasing the braking pressure causes an increase in the contact stiffness which contributes to the appearance of complex eigenvalues with a positive real part. However, the friction coefficient is lower than the static and kinetic friction coefficient which means that it is lower than the first critical friction coefficient, the one which causes de lock-in.

Although the results presented in figures 6.13a and 6.13d are expected the damping ratios of the remaining cases were not. The value of the friction coefficients used would be enough to produce unstable modes, however those were not verified.

It is believed that the analysis undertaken did not produce reliable results, so any conclusion drawn would be counter-productive. It is believed that the error could be in the definition of the contact property model. As stated previously, in the analysis performed only the tangential behaviour was defined because it is in that direction that the sliding friction occurs. Several other options to complement the contact property model were available, such as the contact damping or the normal behaviour, but were not used.

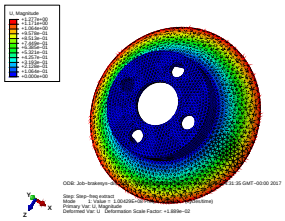

(a) Mode $(0, 0)$

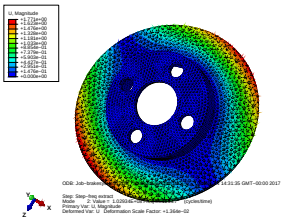

(b) Mode $(0, \pm 1)$

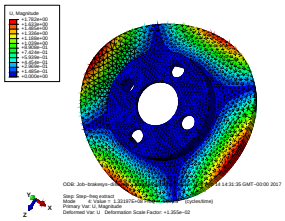

(c) Mode $(0, \pm 2)$

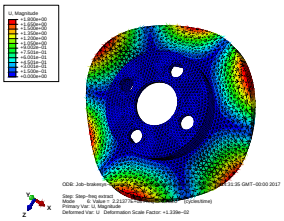

(d) Mode $(0, \pm 3)$

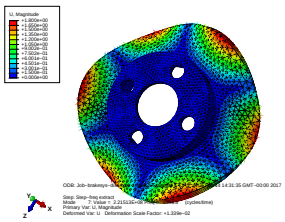

(e) Mode $(0, \pm 4)$

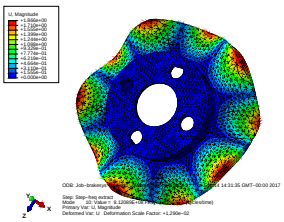

(f) Mode $(0, \pm 5)$

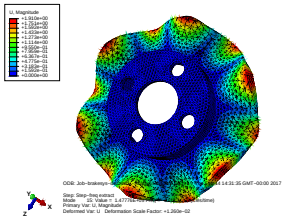

(g) Mode $(0, \pm 6)$

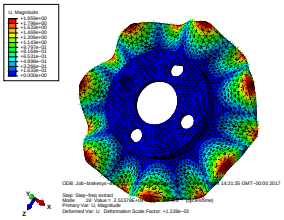

(h) Mode $(0, \pm 7)$

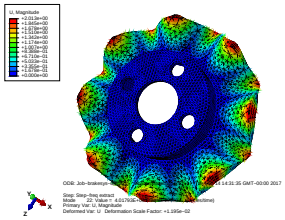

(i) Mode $(0, \pm 8)$

Figure 6.14: Top hat disc transverse vibration modes

Table 6.7: Numerical natural frequencies in Hz of the top hat disc

m,n	$0,0$	$0,\pm1$	$0,\pm2$	$0,\pm3$	$0,\pm4$	$0,\pm5$	$0,\pm6$	$0,\pm7$	$0,\pm8$
ω_{mn}	1595.0	1614.7	1836.8	2368.0	3270.7	4535.5	6118.2	7979.6	10088
		1615	1837	2368.8	3270.8	4535.7	6119.1	7980.6	10090

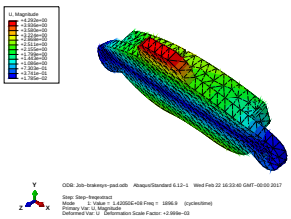

(a) Mode at 1896.9 Hz

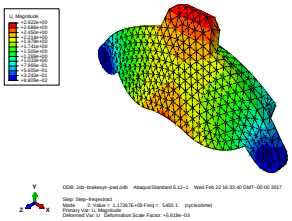

(b) Mode at 5450.1 Hz

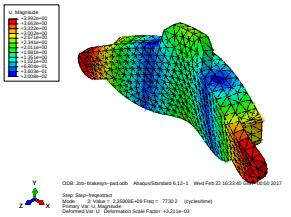

(c) Mode at 7730.2 Hz

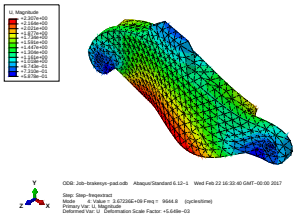

(d) Mode at 9644.8 Hz

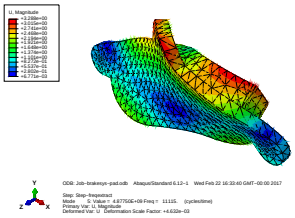

(e) Mode at 11115 Hz

Figure 6.15: Brake pad vibration modes

6.4.2 Simplified brake system

Regarding the simplified brake system, the same analysis procedure was undertaken. According to the exterior connections of the components, their vibration modes, whose frequency lie in the range [1 - 12] kHz, were obtained and are presented in table 6.7 and figure 6.14 for the transverse vibration of the disc, and in figure 6.15 for the pad.

As stated previously, the components were assembled and the contact was established between the components. The complex eigenvalue analysis was undertaken and for the operational parameters indicated previously, the modal damping ratios and the magnitude of the real part of the eigenvalues were extracted and are presented in figures 6.16 and 6.17, respectively.

The results achieved were not expected. The system modelled was from a real brake system and the operational parameters values used were in accordance with the values from the literature consulted, so, with the friction coefficient used, it should be expected that the system would possess some unstable modes.

As for the pin-on-disc system, it is also believed that the reason for these inconclusive results was due to the definition of the contact property model.

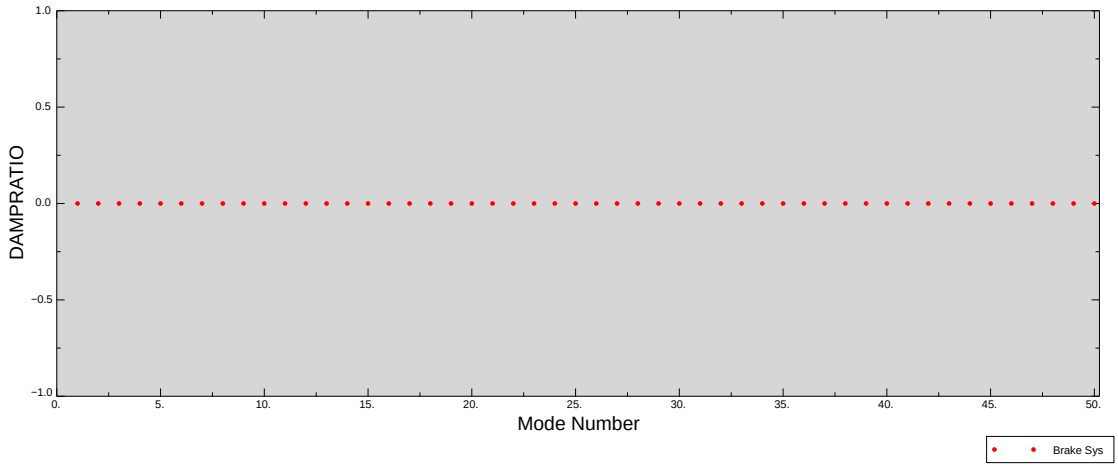

Figure 6.16: Modal damping ratios extracted from the CEA of the simplified brake system

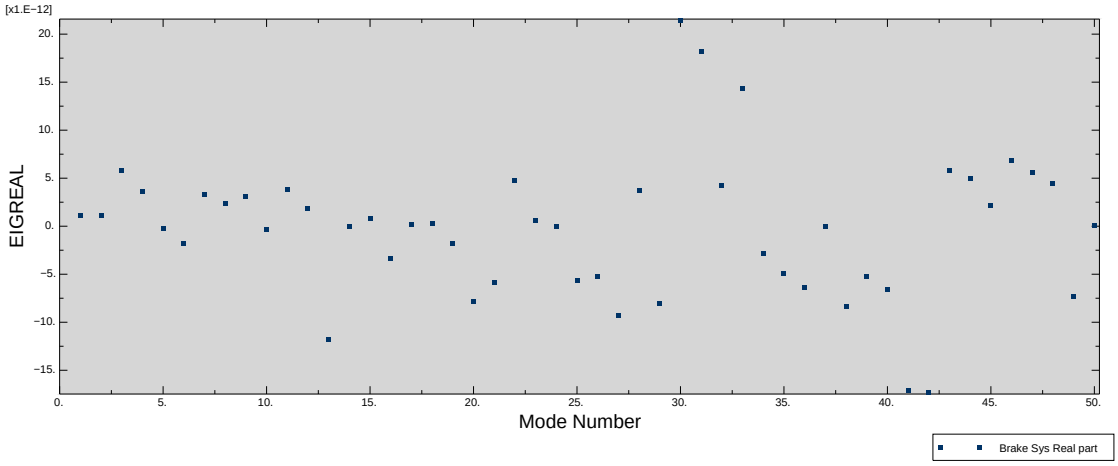

Figure 6.17: Magnitude of the real part of the complex eigenvalues

6.5 Summary and outlook

Having collected a wealth of information concerning mode-coupling instability type regarding disc brake squeal, finite element models of a pin-on-disc system and of a simplified brake system were developed. The objective was to study the stability of such systems by the complex eigenvalue analysis, a feature available in the commercial software ABAQUS, to discuss the results obtained in light of mode-coupling instability type and to assess about the influence of operational parameters in the stability of the systems, namely the applied braking pressure. So, the dynamic behaviour of components of both systems was obtained, and it would be expected that, if there was natural frequencies in close range, their respective vibration modes would couple, once a critical friction coefficient was achieved, and, eventually, would produce unstable vibrations.

To infer about the stability of the system, the sign and magnitude of the real part of the complex eigenvalues was took as a measure of squeal propensity, since it was directly related to the damping ratio, which, if it was negative, would be interpreted as an absorption of energy.

To conduct a complex eigenvalue analysis, contact between the components would have to be defined, by specifying the type of contact, the areas involved and the contact property model. So, for both systems, a general contact was chosen and the contact model was defined by specifying the tangential behaviour of the bodies in contact. It was used Coulomb's friction law.

The results obtained from the finite element models were not satisfactory. Modal damping ratios obtained from the mechanical cases proposed were all zero, and magnitude of the real parts was insignificant. This leads to believe that the contact model lacked property definition, thus preventing from drawing any significant conclusion.

Besides conducting the finite element analysis mentioned above, numerical work about the influence of structural damping in mode coupling instability type from [Hoffmann and Gaul, 2003] was complemented by plotting the Nyquist diagrams. The graphics allowed to see that for friction coefficients higher than the critical one, the in-plane and out-of-plane displacements would be in phase and the motion would be amplified leading to a dynamic motion of increasing amplitude.

Chapter 7

Conclusion

7.1 Conclusions

From the beginning of this investigation on disc brake squeal, it was seen that this was not a classical problem. In this thesis, we tried to provide a concise and yet broad perspective on mode-coupling instability type as a disc brake squeal mechanism, causing low to high frequency noises due to the presence of unstable, self-excited vibrations.

Research on disc brake squeal has increased over the years, but the phenomena is far from being completely understood and knowledge obtained is yet to be incorporated in the industry to design quieter brakes without affecting braking performance.

Due to the geometric complexity of the components and the sliding friction phenomena, first early approaches have been made trying to identify the sources for squeal events, or in other words, mechanisms that would lead to instability.

Several mechanisms were identified. In early years it was thought that squeal would be caused by stick-slip motion. This phenomena would arise due to a higher static friction coefficient relative to the kinetic one. It was seen that, by considering a negative friction coefficient-sliding velocity gradient, the system would possess negative damping. Later, squeal was observed even assuming a constant friction coefficient leading to believe that instability would be caused by a geometric constraint. This fits in the sprag-slip theory. Instability induced by friction was also thought to arise from the follower force nature of friction forces. In this context, experimental evidences were provided where it was observed dynamic motions of increasing amplitude.

Experimental investigation is of crucial importance and is a current practice in the automotive industry to face NVH issues, allowing to capture both the dynamic behaviour of the brake system and squeal occurrence. Experimental approaches have used either simplified brake systems such as the pin-on-disc systems or full brake systems. As squeal mechanisms were identified, this systems have gained popularity because they account for the coupling and elasticity of the components. Consequently, the multi-natural frequency nature of elastic bodies is considered, allowing to see how different transverse modes of the pin couple with the diametral modes of the disc.

In this frame, we enhance the TriboBrake, an experimental test rig that allowed to correlate the geometrical coupling of the modes of vibration of the substructures with squeal occurrence. By using it, it was seen that different substructures were allowed to couple, not only the disc and the pad vibration modes, but also, the calliper and the pad.

Although there are several mechanisms that could lead to squeal, regarded as a consequence of dynamic instability, it is generally accepted that mode-coupling, leading to the appearance of an unstable mode, is the responsible for the majority of the events.

Mode-coupling occurs when the vibration modes of two components lock together giving rise to an unstable mode.

In order to analyse and understand vibration phenomena and modal interaction in friction-induced vibrations, minimal models are used.

Although they do not represent the brake system, they are useful to capture the physical aspects and characteristics of the phenomena. General approach to investigate mode-coupling instability type consists on a stability analysis and then, on parametric studies.

Regarding the stability analysis, the Routh-Hurwitz criterion is often used, allowing to describe regions of instability and to define critical parameters, such as the critical friction coefficient, identified in [Sinou and Jézéquel, 2007] as the bifurcation point. The stability criterion mentioned above allows to address the stability of the mechanical system without solving the equations of motion. We also noticed the use of the simplified Nyquist criterion, to infer on the conditions for the onset of instability.

Parametric studies are performed to evaluate how the system dynamic motion and stability are affected, by changing operational parameters. Applied pressure, rotational velocity, friction material, stiffness of the components, determined either by their geometry or their mechanical properties, and structural damping were found to have a strong influence in disc brake squeal propensity.

Our objective was to provide an insight about mode-coupling instability in disc brake squeal. The non-conservative work produced by friction forces produces a non-symmetric stiffness matrix (due to the frictional coupling term) which is necessary for the appearance of complex eigenvalues with a positive real part. It was seen that by increasing the friction coefficient, the frequencies of real modes approach each other until they merge at the critical friction coefficient. At this point, two complex conjugate modes, in which one of them is unstable arise. It was shown that when two modes lock, an energy flow is established, and its direction depends on the relative phase between excitation and response. In some cases, by further increasing the friction coefficient, a second critical value is achieved, where the modes uncouple.

Insight about the effect of damping on modal interaction has been gained. However it is not fully understood. It was seen that a proportional damping scheme constitutes a stabilizing effect and a non-proportional damping scheme may destabilize the system. For a certain combination of parameters an optimal damping ratio, that provides the most stable system, may exist. In this frame, we notice the existence of a robust damping factor, developed to assist engineers in avoiding design errors.

Rotation effects are found to influence the stability of the system. Although the majority of papers assume a velocity such that gyroscopic and radial dissipative effects cancel out, influence of these effects on the stability of the system was also investigated.

Gyroscopic mechanism provides a smoothing effect on the growth rate curves, similar to the damping effect, thus meaning that it constitutes a destabilizing feature. Radial dissipative terms have a stabilizing effect. Considering rotation effects and non-proportional damping, it was seen that the locus plot would rotate around the pivot point ($\mu = 0$). This consists on the tilting effect.

Some analytical formulations to address the stability of disc brake systems was then presented.

Regarding disc brake squeal problem as a moving-load problem, it was seen that instabilities would be speed-dependent.

It was found that, under determined conditions, stick-slip motion caused by the in-plane flexibility of the pads, that were modelled as lumped systems, would excite the transverse vibration of the disc and eventually the two motions would couple. This fits in

the feedback frame provided by using the minimal models.

The analytical model provided by Kang and co-workers seem to be the most similar model to a real brake system. They assumed an annular plate in contact with two annular sector plates over a finite contact area. Transverse displacements of the disc and the pads were expressed by modal expansion, and mode shapes were calculated from the Assumed Modes method for the disc and from the Rayleigh-Ritz method for the pads.

Equations of motion were developed by the Lagrange equations, considering the kinetic energy of the three bodies, the contact strain energy and the non-conservative work produced either by the friction couple and the frictional follower forces.

Lastly, a finite element analysis of a pin-on-disc system and a simplified brake system was conducted to study their stability in light of mode-coupling instability type by a complex eigenvalue analysis and to evaluate the influence of the braking pressure. Several mechanical cases were simulated, however the results obtained were inconclusive, since that for all of them no unstable modes were identified and it was not possible to infer about the influence of the braking pressure in the stability of the mechanical systems. This lead to believe that the finite element models proposed were in fault, namely in the contact property model.

7.2 Future Work

Disc brake squeal is far from being completely understood and still presents challenges in the dynamics and tribology fields of investigation. There is still no model that accounts for all squeal mechanisms.

In this dissertation, a finite element analysis was undertaken to evaluate the dynamic stability of the studied systems in light of mode coupling. However the inconclusive results achieved have not permitted to draw any concrete conclusion, so a continuous improvement of the finite element models developed are in order, particularly in the contact definition between the components. Further improvement would be the development of finite element models of the complete brake system, since that it comprehends more contact interfaces that could influence the dynamic behaviour of the whole system.

The development of a test rig with well known and changeable dynamics is also suggested because, in one hand, complex eigenvalue analysis is a conservative approach since it underestimates unstable modes and, on the other, disc brake squeal was shown to have a random nature. The experimental approach is very useful because it is possible to establish a correlation between the CEA prediction and the actual dynamical behaviour of the mechanical system. By having a changeable dynamics, the test rig can be manipulated to induce mode coupling instability type by tuning the mode frequencies of the subsystems.

References

N.M. Kinkaid, O.M. O'Reilly, and P. Papadopoulos. Automotive disc brake squeal. *Journal of Sound and Vibration*, 267(1):105 – 166, 2003. ISSN 0022-460X.

A. Akay. Acoustics of friction. *J. Acoust. Soc. Am.*, 111(4):1525–1548, 2002.

A. Papinniemi, J. C. S. Lai, J. Zhao, and L. Loader. Brake squeal: a literature review. *Applied Acoustics*, 63:391 – 400, 2002.

M. Nouby, M. El-Sharkawi, and I. Ahmed. A review of automotive brake squeal mechanisms. *Journal of Mechanical Design and Vibration*, 1(1):5–9, 2014.

Laurent Baillet Francesco Massi, Oliviero Giannini. Brake squeal as dynamic instability: An experimental investigation. *Journal of the Acoustical Society of America*, 120(3): 1388–1398, 2006. ISSN 0001-4966.

S. Yang and R.F. Gibson. Brake vibration and noise: reviews, comments, and proposals. *International Journal of Materials and Product Technology*, 12:496–513, 1997.

H. Ouyang, W. Nack, Y. Yuan, and F. Chen. Numerical analysis of automotive disc brake squeal: a review. *Int. J. Vehicle Noise and Vibration*, 1(3/4):207–231, 2005.

A. R. AbuBakar and H. Ouyang. Complex eigenvalue analysis and dynamic transient analysis in predicting disc brake squeal. *International Journal of Vehicle Noise and Vibration*, 2(2):143 – 155, 2006.

D.J. Inman G. Lallement. A tutorial on complex eigenvalues. IMAC-XIII - 13^{th} International Modal Analysis Conference, 1995. Society for Experimental Mechanics.

H.R. Mills. Brake squeal. Technical Report 9000 B, Institution of Automobile Engineers, 1938.

Graduate R. P. Jarvis and Associate Member B. Mills. Vibrations induced by dry friction. *Proceedings of the Institution of Mechanical Engineers*, 178(1):847–857, 1963.

L. Gaul N. Hoffmann. A sufficient criterion for the onset of sprag-slip oscillations. *Archive of Applied Mechanics*, 73(9):650–660, 2004. ISSN 1432-0681.

M. R. North and Institution of Mechanical Engineers. Disc brake squeal. Technical report, Mechanical Engineering Publications, 1977.

Huajiang Ouyang. Moving loads and car disc brake squeal. *Noise & Vibration Worldwide*, December 2003.

H. Ouyang and J. E. Mottershead. Dynamic instability of an elastic disk under the action of a rotating friction couple. *Journal of Applied Mechanics*, 71:753 – 758, November 2004.

D. Bigoni and G. Noselli. Experimental evidence of flutter and divergence instabilities induced by dry friction. *Journal of Mechanics Physics of Solids*, 59:2208–2226, October 2011.

P. Liu, H. Zheng, C. Cai, Y.Y. Wang, C. Lu, K.H. Ang, and G.R. Liu. Analysis of disc brake squeal using the complex eigenvalue method. *Applied Acoustics*, 68(6):603 – 615, 2007. ISSN 0003-682X.

M. Nouby and K. Srinivasan. Parametric studies of disc brake squeal using finite element approach. *Jurnal Mekanikal*, (29):52–66, December 2009.

M. Nouby, D. Mathivanan, and K. Srinivasan. A combined approach of complex eigenvalue analysis and design of experiments to study disc brake squeal. *International Journal of Engineering, Science and Technology*, 1(1):254–271, January 2009.

M. Nouby, C. Sujatha, and K. Srinivasan. Modelling of automotive disc brake squeal and its reduction using rotor design modifications. *International Journal of Vehicle Noise and Vibration*, 7(2):129 – 148, 2011.

C.J. Talbot J.D. Fieldhouse, W.P. Steel and M.A. Siddiqui. Brake noise reduction using rotor asymmetric. In *Proceedings of IMechE International Conference-Braking 2004*, 2004.

Ibrahim Ahmed. Analysis of disc brake squeal using a ten-degree-of-freedom model. *International Journal of Engineering, Science and Technology*, 3(8):142–155, 2011.

F. Cantone and F. Massi. A numerical investigation into the squeal instability: Effect of damping. *Mechanical Systems and Signal Processing*, 25(5):1727 – 1737, 2011. ISSN 0888-3270.

Francesco Massi, Aurélien Saulot, Mathieu Renouf, and Guillaume Messager. Simulation of dynamic instabilities induced by sliding contacts. DINAME 2013, Feb. 2013.

R. Allgaier, L. Gaul, W. Keiper, and K. Willner. Mode lock-in and friction modelling. In WIT Press, editor, *Transactions on Engineering Sciences*, volume 24, 1999.

A Tuchinda, NP Hoffmann, DJ Ewins, and W Keiper. Mode lock-in characteristics and instability study of the pin-on-disc system. In *IMAC-XIX: A Conference on Structural Dynamics,*, volume 1, pages 71–77, 2001.

Anantawit Tuchinda. *Development of validated models for brake squeal prediction.* PhD thesis, Imperial College London, 2003.

Oliviero Giannini Francesco Massi. Effect of damping on the propensity of squeal instability: An experimental investigation. *Journal of the Acoustical Society of America*, 123 (4):2017–2023, 2008.

Utz von Wagner, Daniel Hochlenert, and Peter Hagedorn. Minimal models for disk brake squeal. *Journal of Sound and Vibration*, 302:527–539, 2007.

K. Shin, M.J. Brennan, J.-E. Oh, and C.J. Harris. Analysis of disc brake noise using a two-degree-of freedom model. *Journal of Sound and Vibration*, 254(5):837 – 848, 2002. ISSN 0022-460X.

Norbert Hoffmann, Michael Fischer, Ralph Allgaier, and Lothar Gaul. A minimal model for studying properties of the mode-coupling type instability in friction induced oscillations. *Mechanics Research Communications*, 29(4):197 – 205, 2002. ISSN 0093-6413.

N. Hoffmann and L. Gaul. Effects of damping on mode-coupling instability in friction induced oscillations. *ZAMM - Journal of Applied Mathematics and Mechanics / Zeitschrift für Angewandte Mathematik und Mechanik*, 83(8):524–534, 2003. ISSN 1521-4001.

Jean-Jacques Sinou and Louis Jézéquel. Mode coupling instability in friction-induced vibrations and its dependency on system parameters including damping. *European Journal of Mechanics - A/Solids*, 26(1):106 – 122, 2007. ISSN 0997-7538.

L. Jézéquel J-J. Sinou, G. Fritz. The role of damping and definition of the robust damping factor for a self-exciting mechanism with constant friction. *Journal of Vibration and Acoustics*, 129(3):297–306, 2007.

Johan Hultén. Brake squeal - a self-exciting mechanism with constant friction. In *SAE Technical Paper*. SAE International, November 1993.

Jaeyoung Kang, Charles M. Krousgrill, and Farshid Sadeghi. Dynamic instability of a thin circular plate with friction interface and its application to disc brake squeal. *Journal of Sound and Vibration*, 316(1–5):164 – 179, 2008. ISSN 0022-460X.

Jaeyoung Kang, Charles M. Krousgrill, and Farshid Sadeghi. Comprehensive stability analysis of disc brake vibrations including gyroscopic, negative friction slope and mode-coupling mechanisms. *Journal of Sound and Vibration*, 324(1–2):387 – 407, 2009a. ISSN 0022-460X.

Jaeyoung Kang, Charles M. Krousgrill, and Farshid Sadeghi. Analytical formulation of mode-coupling instability in disc–pad coupled system. *International Journal of Mechanical Sciences*, 51(1):52 – 63, 2009b. ISSN 0020-7403.

Huajiang Ouyang. Moving-load dynamic problems: A tutorial (with a brief overview). *Mechanical Systems and Signal Processing*, 25(6):2039 – 2060, 2011. ISSN 0888-3270. Interdisciplinary Aspects of Vehicle Dynamics.

H. Ouyang, J. E. Mottershead, M. P. Cartmell, and M. I. Friswell. Friction-induced parametric resonances in discs: Effect of a negative friction-velocity relationship. *Journal of Sound and Vibration*, 209(2):251–264, 1998.

H. Ouyang, J.E. Mottershead, M.P. Cartmell, and D.J. Brookfield. Friction-induced vibration of an elastic slider on a vibrating disc. *International Journal of Mechanical Sciences*, 41(3):325 – 336, 1999. ISSN 0020-7403.

Q. Cao, H. Ouyang, M. I. Friswell, and J. E. Mottershead. Linear eigenvalue analysis of the disc-brake squeal problema. *International Journal for NUmerical Methods in Engineering*, (61):1546–1563, November 2004.

D.N. Vanderlugt. *Analytical and Experimental Study of Automotive Disc Brake Squeal Vibration*. Master thesis, Purdue University, 2004.

H. Ouyang, J. E. Mottershead, D. J. Brookfield, S. James, and M. P. Cartmell. A methodology for the determination of dynamic instabilities in a car disc brake. *International Journal of Vehicle Design*, 23:241 – 262, October 2000.

Arthur W. Leissa. Vibration of plates. Technical report NASA-SP-160, NASA, 1969.

H. Ouyang, J. E. Mottershead, M. P. Cartmell, and M. I. Friswell. In-plane stick-slip vibration on the surface of a flexible disc. In *Transactions of the American Society of Mechanical Engineers, 16ht Biennial Conference on Vibration and Noise*, 1997.

J. Dias Rodrigues. *Apontamentos de Vibrações de Sistemas Mecânicos*. Faculdade de Engenharia da U.PORTO, PORTO, 2016 edition, 2016.

H. Mahé L. Jézéquel B. Hervé, J.-J. Sinou. Analysis of squeal noise and mode coupling instabilities including damping and gyroscopic effects. *European Journal of Mechanics - A/Solids*, 27(2):141–160, 2008.

H. Ouyang and J.E. Mottershead. Unstable travel waves in the friction-induced vibration of discs. *Journal of Sound and Vibration*, 248(4):768 – 779, 2001. ISSN 0022-460X.

Appendix A

Pin-on-disc vibration modes

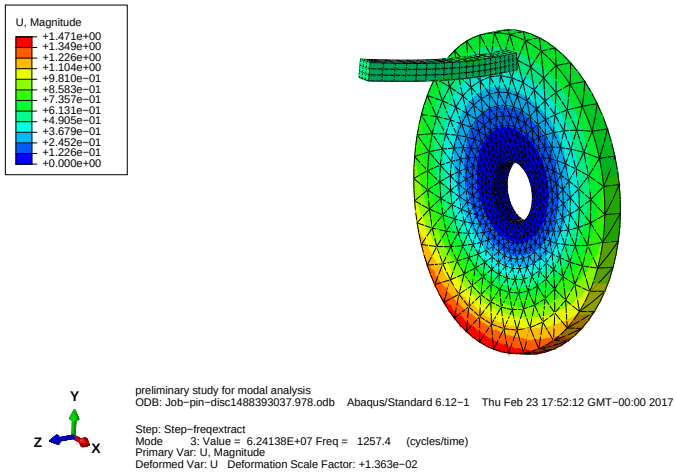

Figure A.1: Vibration mode of the system involving the (0,0) mode of the disc at 1257.4 Hz

(a) 1113.6 Hz (b) 1170.6 Hz

Figure A.2: Vibration modes of the system involving the (0,±1) modes of the disc

(a) 1502.0 Hz (b) 1574.3 Hz

Figure A.3: Vibration modes of the system involving the (0,±2) modes of the disc

(a) 2886.1 Hz (b) 3343.4 Hz

Figure A.4: Vibration modes of the system involving the (0,±3) modes of the disc

(a) 5083.6 (b) 5391.3

Figure A.5: Vibration modes of the system involving the (0,±4) modes of the disc

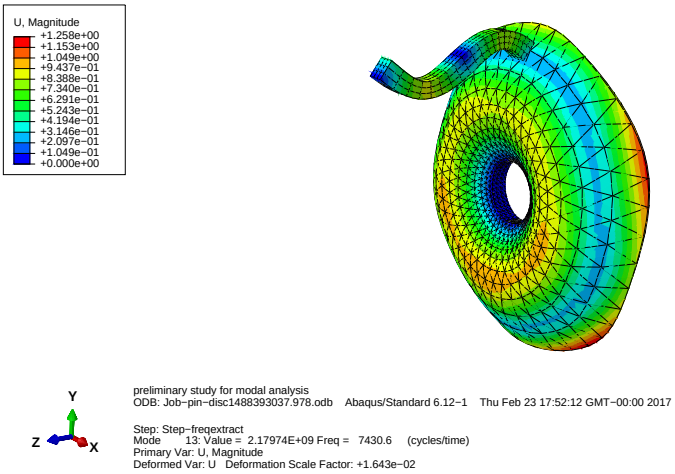

Figure A.6: Vibration modes of the system involving the (1,0) mode of the disc at 7430.6 Hz

(a) 7627.9 Hz (b) 7999.9 Hz

Figure A.7: Vibration modes of the system involving the (0,±5) modes of the disc

(a) 7894.7 Hz (b) 7894.9 Hz

Figure A.8: Vibration modes of the system involving the (1,±1) modes of the disc

(a) 9365.0 Hz (b) 9573.2 Hz

Figure A.9: Vibration modes of the system involving the (2,±2) modes of the disc

Appendix B

Simplified brake system vibration modes

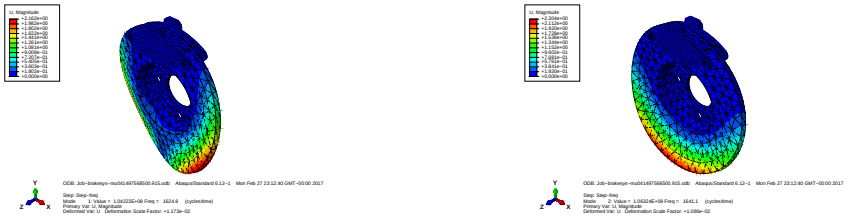

(a) 1624.8 Hz (b) 1641.1 Hz

Figure B.1: Vibration modes of the system involving the (0,±1) modes of the rotor

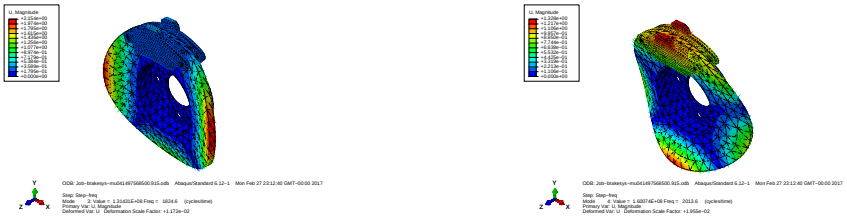

(a) 1824.6 Hz (b) 2013.6 Hz

Figure B.2: Vibration modes of the system involving the (0,±2) modes of the rotor

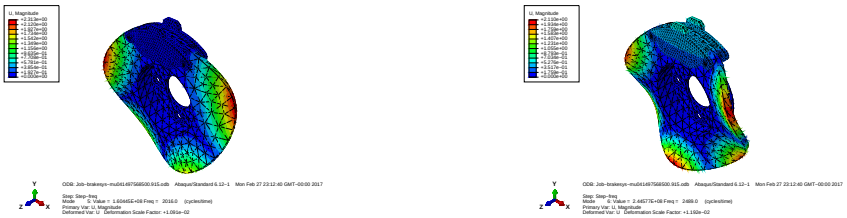

(a) 2016.0 Hz (b) 2489.0 Hz

Figure B.3: Vibration modes of the system involving the (0,±3) modes of the rotor

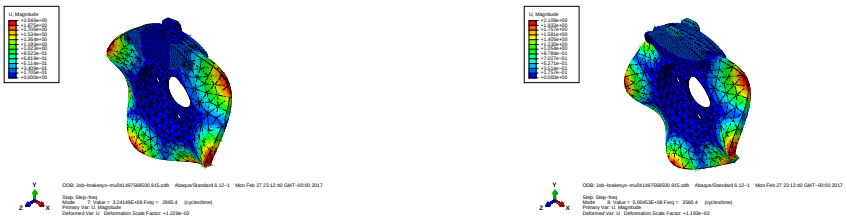

(a) 2865.4 Hz (b) 3560.4 Hz

Figure B.4: Vibration modes of the system involving the (0,±4) modes of the rotor

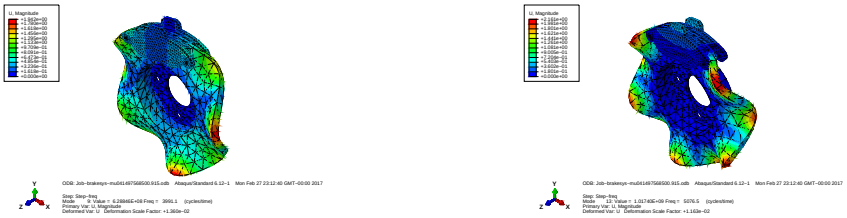

(a) 3991.1 Hz (b) 5076.5 Hz

Figure B.5: Vibration modes of the system involving the (0,±5) modes of the rotor

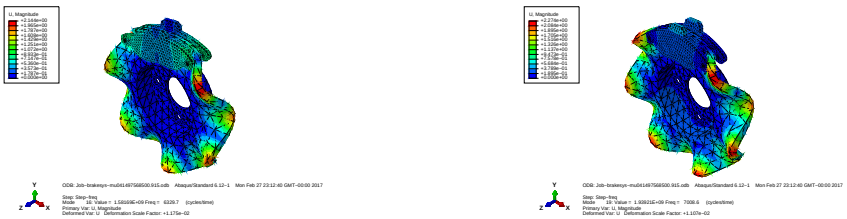

(a) 6329.7 Hz (b) 7008.6 Hz

Figure B.6: Vibration modes of the system involving the (0,±6) modes of the rotor

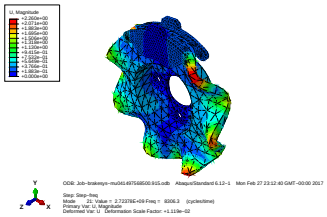

(a) 8306.3 Hz

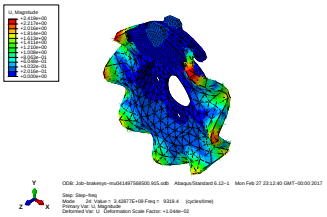

(b) 9319.4 Hz

Figure B.7: Vibration modes of the system involving the (0,±7) modes of the rotor

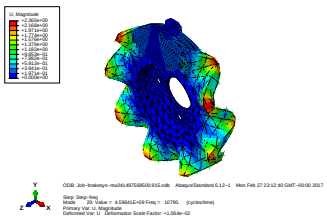

(a) 10790 Hz

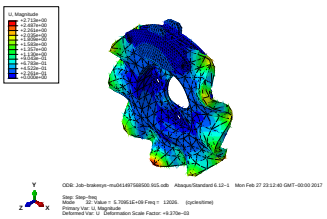

(b) 12026 Hz

Figure B.8: Vibration modes of the system involving the (0,±8) modes of the rotor